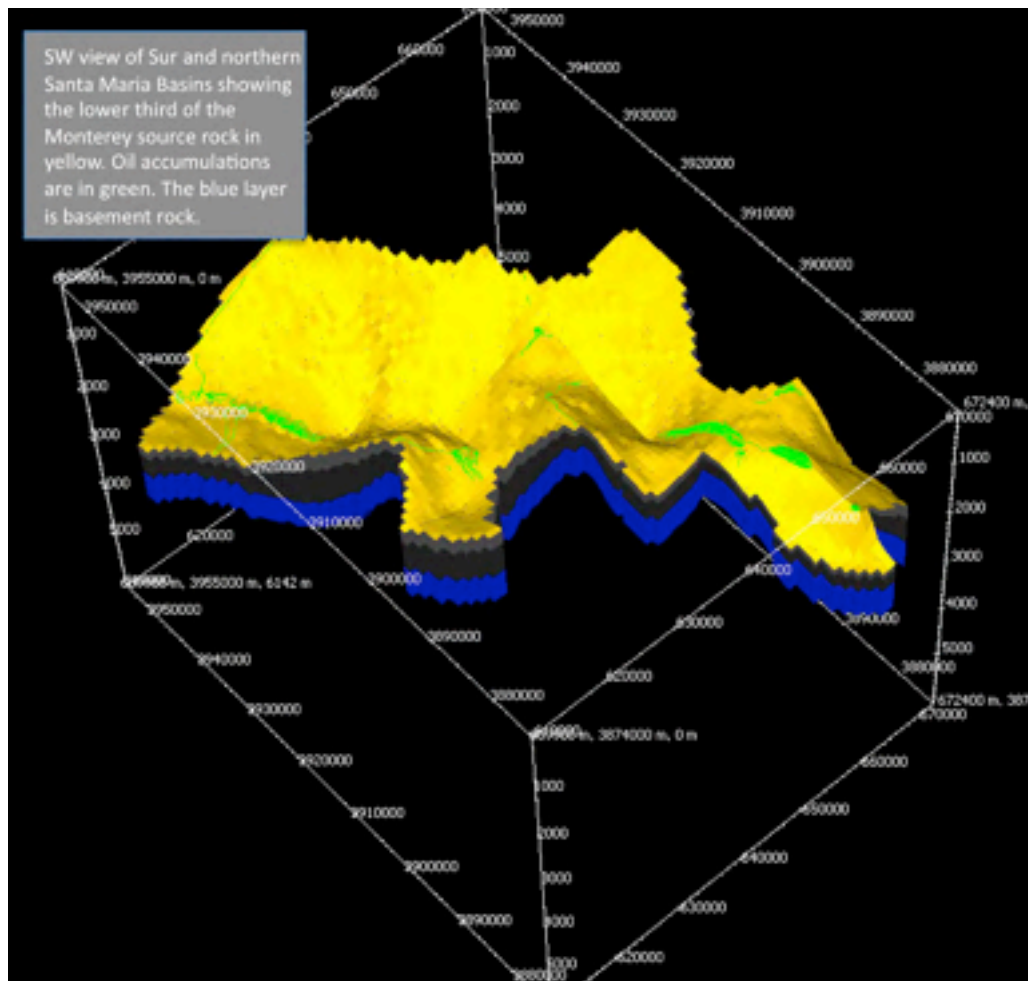


**Stanford University 4th Annual
Basin & Petroleum System Modeling
Industrial Affiliates Meeting
November 3-5, 2011**

<http://bpsm.stanford.edu>



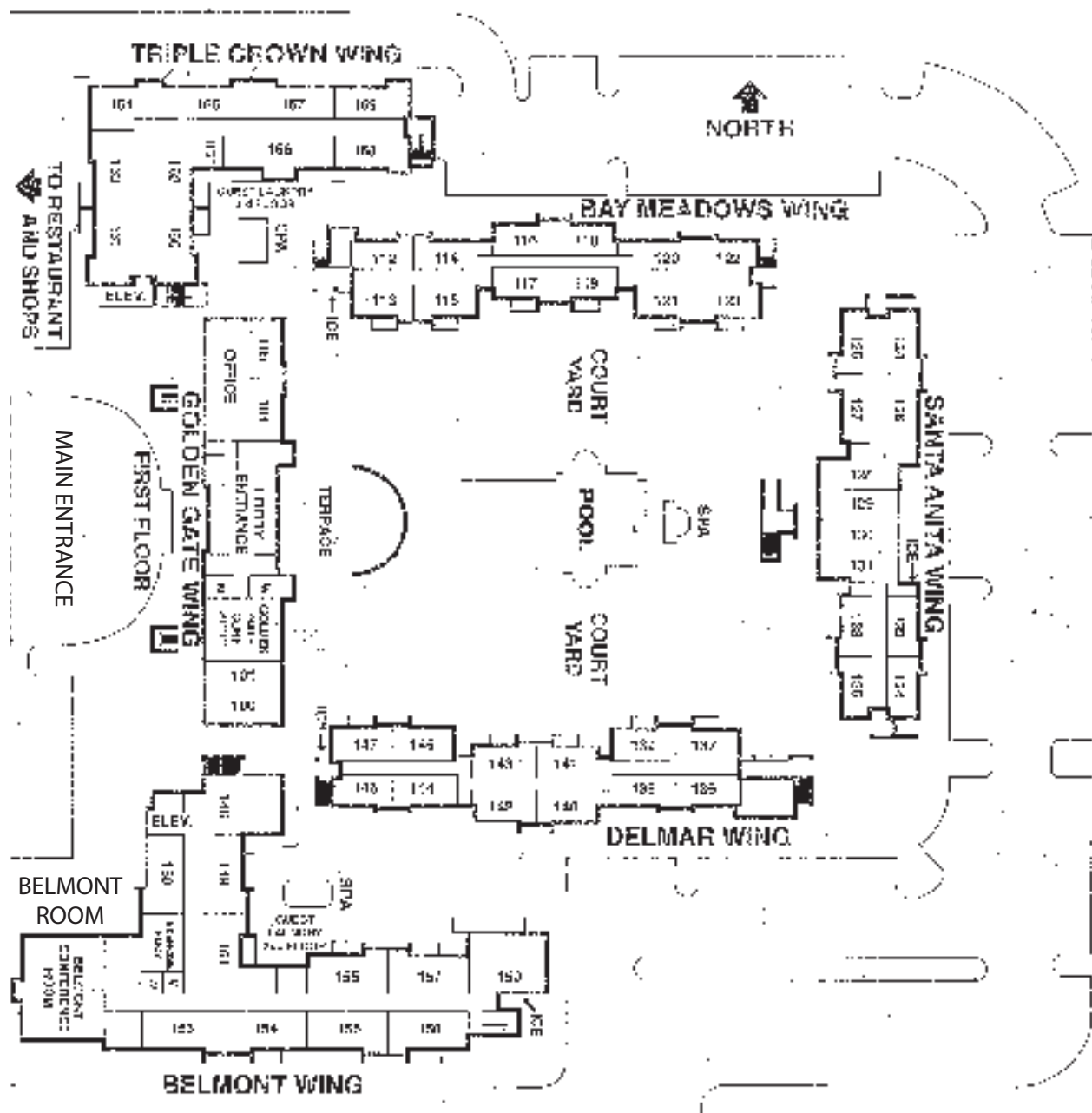
**Western San Joaquin Basin Field Trip
& BPSM Oral Session**

Compiled by: S.A. Graham, L.B. Magoon, A.H. Scheirer

*Harris Ranch Inn & Restaurant
Coalinga, California*



The fourth annual Stanford University Basin and Petroleum System Modeling Industrial Affiliates Meeting is scheduled for Thursday, Friday and Saturday, November 3, 4 and 5, 2011. The conference will be held at Harris Ranch Inn and Restaurant in Coalinga, CA. The first evening (Thursday) will be a hosted bar and hors d'oeuvres from 5:30 to 7:30 PM. The second day (Friday) features a field trip to investigate the Kreyenhagen-Temblor(!) and essential elements of other petroleum systems in the western San Joaquin Basin, California. During the course of the day, we will be able to see all elements of that petroleum system, exposed due to geologically recent uplift/erosion. Saturday features an oral session by Stanford graduate students, who will present talks and be available for questions on their basin and petroleum system modeling research, including a new strike-slip faulting model in the Salinas Basin, a new 2-D petroleum system model of the Vallecitos Syncline of the San Joaquin Basin, a new 2-D petroleum system model of the East Coast Basin of New Zealand, and a new 3-D petroleum system model of the Sur Basin offshore of California, as well as lab experiments on the kinetics of the opal-CT to quartz transition as a function of temperature and pore fluid chemistry. Many of the principal advisors in the program will be available for discussions.



HARRIS
RANCH
 INN & RESTAURANT

Stanford BPSM Industrial Affiliate Members in 2011



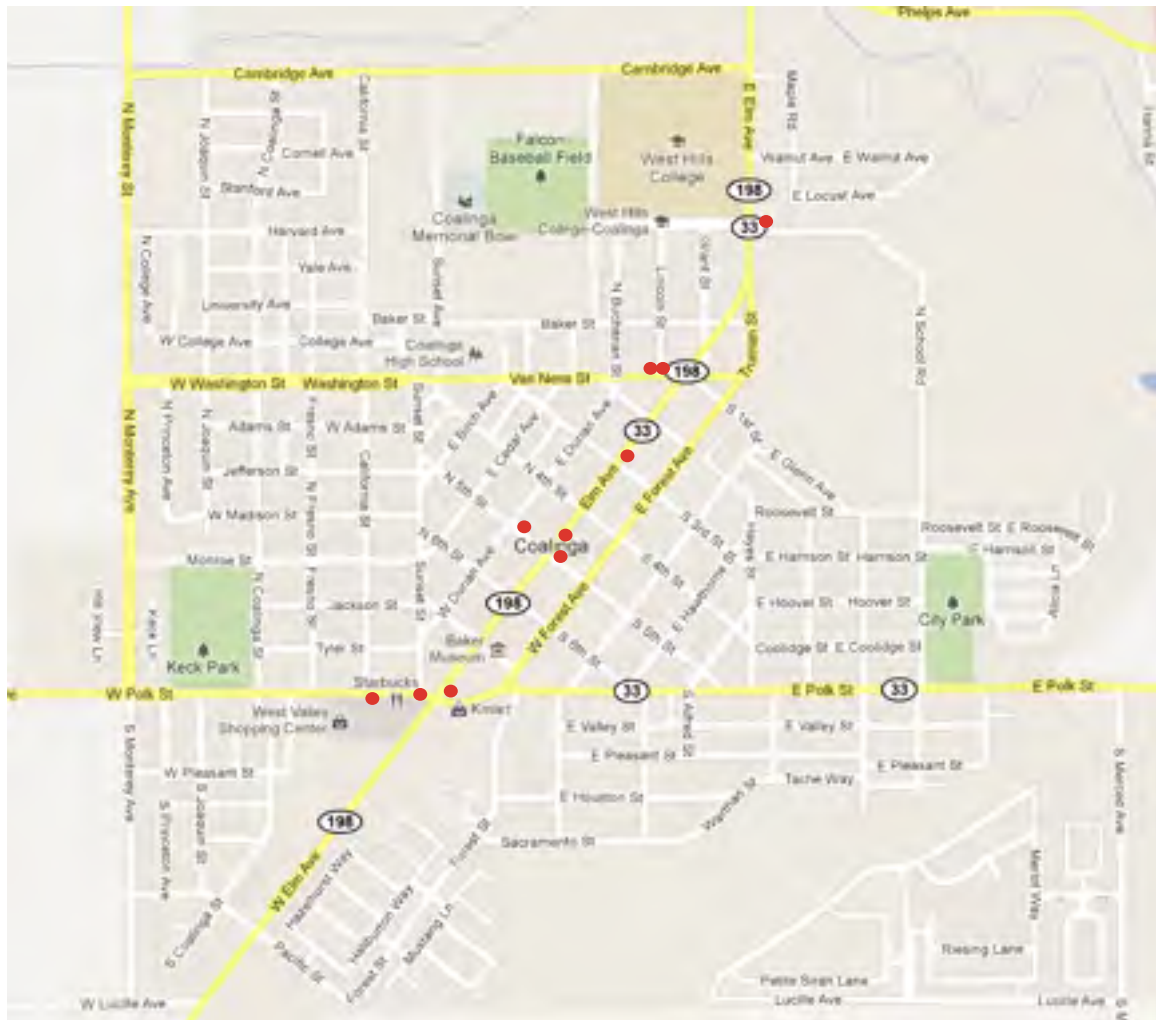
New Members for 2011



Meeting Attendees:

First Name	Last Name	Affiliation	First Name	Last Name	Affiliation
Linji	An	Aera Energy LLC	Randolph	Pepper	Schlumberger
Plamen	Ganev	Aera Energy LLC	Ken	Peters	Schlumberger
Terence	OSullivan	Aera Energy LLC	Oliver	Schenk	Schlumberger
Noel	Velasco	Aera Energy LLC	Blair	Burgreen	Stanford University
Veit	Matt	British Petroleum	Danica	Dralus	Stanford University
Sami	Riahi	British Petroleum	Keisha	Durant	Stanford University
Chris	Crescini	Chevron	Steve	Graham	Stanford University
Noelle	Schoellkopf	Chevron - retired	Meng	He	Stanford University
John	Guthrie	Hess Corporation	Carolyn	Lampe	Stanford University /Ucon
Hilario	Camacho Fernandez	Occidental Oil & Gas	Les	Magoon	Stanford University
Gregg	Pyke	Occidental Oil & Gas	Tess	Menotti	Stanford University
Luiz Felipe	Carvalho Coutinho	Petrobras	Tapan	Mukerji	Stanford University
Guilherme	Moreira	Petrobras	Yao	Tong	Stanford University
Thomas	Lorenson	US Geological Survey	David	Zinniker	Stanford University

Coalinga Restaurants



The Mountain Oyster Steak House & Saloon
260-270 Van Ness Street
Coalinga, CA 93210
559 935-3908
4/5 stars

New China Restaurant
186 N. 5th St.
Coalinga, CA 93210
559 935-0779
4/5 stars

China 1 Express
179 W. Polk St.
Coalinga, CA 93210
559 935-8781
5/5 stars

Campus Drive In
660 E. Elm Ave
Coalinga, CA 93210
559 935-1127
5/5 stars

Fat Jack's
276 N. 5th St.
Coalinga, CA 93210
559 935-5216
4/5 stars

Taqueria Y Mariscos El 2000
320 E. Elm Ave.
Coalinga, CA 93210
559 935-5841
3.5/5 stars

Fatte Albert's Pizza
235 N. 5th St.
Coalinga, CA 93210
559 935-0841
3/5 stars

Imperial Palace Chinese Restaurant
280 Van Ness St.
Coalinga, CA 93210
559 935-2450
3/5 stars

Perko's Cafe
101 W. Polk St.
Coalinga, CA 93210
559 935-3531
2/5 stars

Kmart Little Caesars Pizza Station
25 W. Polk St.
Coalinga, CA 93210
559 935-3393
1/5 stars

Western San Joaquin Basin Field Trip

Time		Miles	Stop	Stop Description / Activity	Special Note / Hazards
Arrival	Departure	to:	No.		
7:45 AM	8:00 AM	0.0	0	Meet outside main entrance of Harris Ranch Inn	Leave on time
8:15 AM	9:00 AM	5.1	1	Aera oil field office for mandatory safety orientation	Last restrooms until lunch
9:15 AM	9:45	5.6	2	Stop at NW edge of Coalinga field for overview	Overview of Coalinga field
9:50	10:15 AM	0.9	3	New development at Oil City pool; UK Moreno shale	Porcellanite facies
10:20 AM	11:00 AM	0.3	4	Road cut in Kreyenhagen Formation	Opal A-CT transition facies
11:05 AM	11:45 AM	0.3	5	Temblor Formation to see breccia or tar sand	Updip seal of Coalinga field
Noon	12:45 PM	1.6	6	Cartwheel Ridge	Kreyenhagen Temblor contact
1:15 PM	2:00 PM	10.6	7	Lunch	Restrooms
2:40 PM	3:15 PM	23.5	8	Oil seeping from Kreyenhagen; Monterey; Temblor	Walk along road to see outcrop
3:30 PM	4:00 PM	2.8	9	View point from Tar Peak or Roundtop	Regional geology
3:45 PM	4:15 PM	9.8	9A	View point from abandoned drill pad	Regional geology
5:00 PM		17.8	0	Return to Harris Ranch Inn & Restaurant	

*Sunrise 7:37 AM; Sunset 6:09 PM

Driving directions for the western San Joaquin basin field trip

Stop 0 to Stop 1. Drive from Harris Ranch Inn & Restaurant main entrance onto Hwy 198. Turn left or west onto Hwy 198 (W. Dorris Ave.) for 4.7 miles to intersection with Hwy 33. Continue across intersection to Aera Field Office for 0.4 miles on Shell Road.

Stop 1 to Stop 2. From Aera Field Office drive southwest for 2.9 miles to Oil Creek Road. Make a hard right turn onto Oil Creek Road to travel due North for 2.7 miles for overview of Coalinga field.

Stop 2 to Stop 3. Drive 0.9 miles further on Oil Creek Road to next stop to Oil City, a pool that produces out of the Moreno Formation, and to look at the porcellanite facies of the Moreno shale.

Stop 3 to Stop 4. Drive 0.3 miles back or south on Oil Creek Road to look at road cut of Kreyenhagen Formation in the Opal A-CT transition facies.

Stop 4 to Stop 5. Drive another 0.3 miles south on Oil Creek Road to where we walk up a side canyon to see the Temblor Formation breccia or tar sand (asphalt) that is the updip seal for the Coalinga field.

Stop 5 to Stop 6. Drive back north to stop 3 for 0.6 miles, then through a gate and turn at northern edge of Coalinga field onto an oil field road. Field trip leader will guide us for about one mile through the maze of oil field roads upgrade to Cartwheel Ridge. Stop consists of exposures of uppermost Kreyenhagen Formation, its contact with the overlying Temblor Formation, and oil saturated fluvial and estuarine sands of the lower Temblor Formation. Return down hill to intersection with Oil Canyon Road.

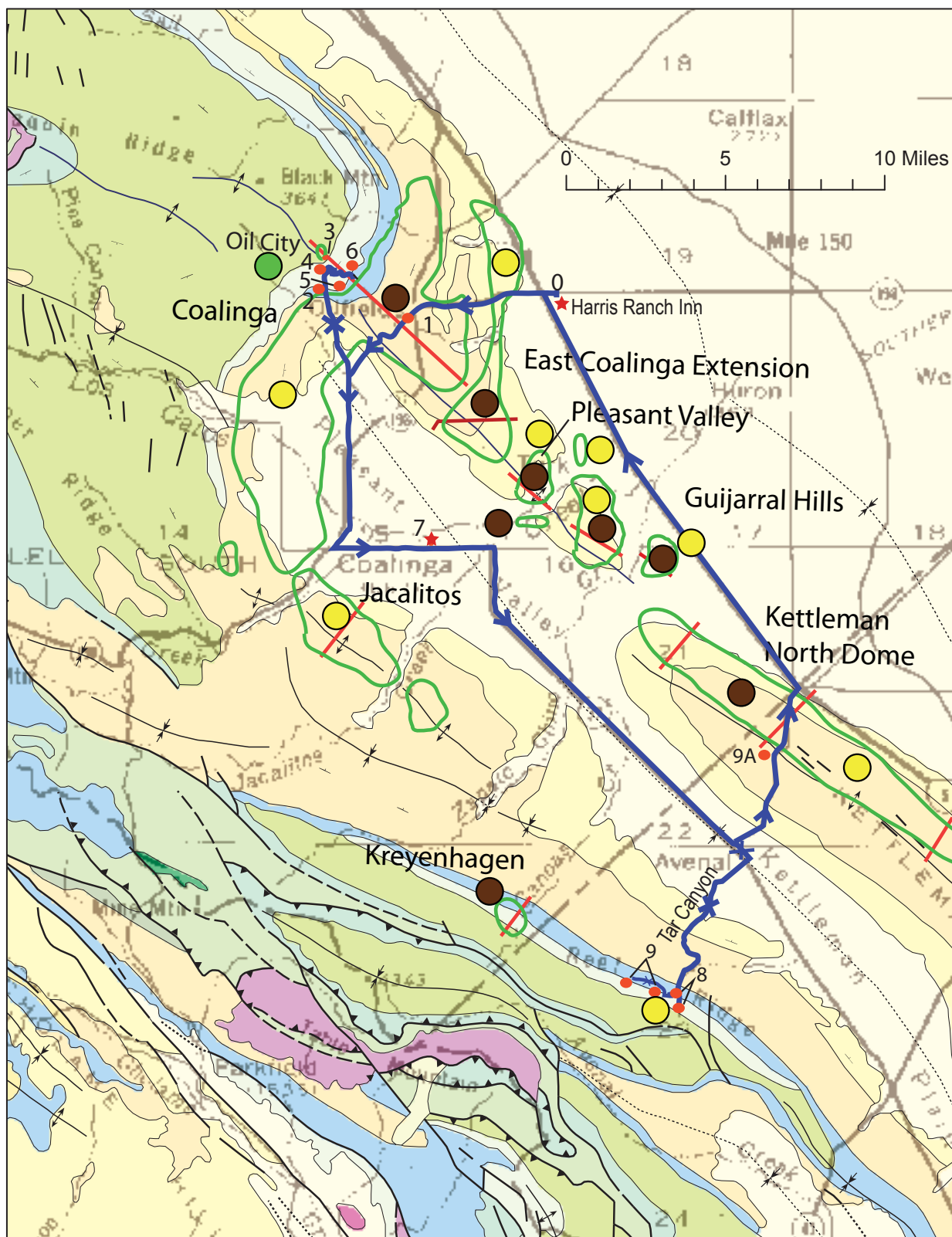
Stop 6 to Stop 7. Drive south on Oil Creek Road 5.6 miles to Three Corners where you intersect Hwys 198/33. Continue driving south for 3.0 miles into Coalinga until the road continues as Elm Ave in town. Turn left at East Polk St. (Hwy 33) and continue east until you see the City Park on the left where we will have lunch. The distance from Stop 6 is about 9.0 miles.

Stop 7 to Stop 8. After lunch, drive east on Hwy 33 to just past Avenal for 17.7 miles to Tar Canyon Road. Turn right on Tar Canyon Road and drive for 5.8 miles to Big Tar Canyon where oil is seeping out of the Kreyenhagen Formation. Walk along this road to examine the Monterey, Temblor and Kreyenhagen formations.

Stop 8 to Stop 9. If weather permits we will proceed south on Tar Canyon Road for another 0.4 mile to a road that goes off to the right. Proceed on this dirt road for 1.6 miles to Tar Peak (elevation 2442 ft) or 0.8 miles further on to Roundtop (elevation 2581 ft) for an overview of the San Joaquin basin.

Stop 8 to Stop 9A (alternate). If weather wet, proceed back down Tar Canyon Road for 5.8 miles to Hwy 33 and turn left and drive for a 0.5 mile, then right onto Skyline Blvd in Avenal. Continue on Skyline Blvd for 3.2 miles to Skyline Road. Continue on Skyline Blvd for another 0.2 mile to a fork where Skyline Road goes left so stay right on Skyline Blvd for 0.1 mile and take a slight left off the road to a lookout.

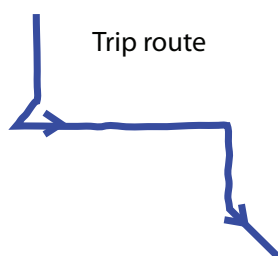
Stop 9 or 9A to Stop 0. Proceed from either Stop 9 or Stop 9A along Skyline Blvd another 2.8 miles to Hwy 5. Turn north onto Hwy 5 and drive for 15 miles back to the Harris Ranch Inn & Restaurant.



Field Trip Map & Route

Geologic Map Explanation

Petroleum System		Oil from source rock
Tumey-Temblor(.)		Tumey Formation
Kreyenhagen-Temblor(!)		Kreyenhagen Fm
Moreno-Nortonville(.)		Moreno Formation



Trip route

6

Geologic stop

7

Start/end or lunch stop

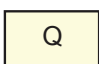
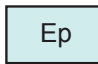
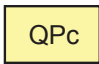

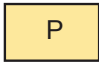
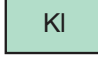


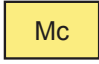
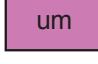


Field outline



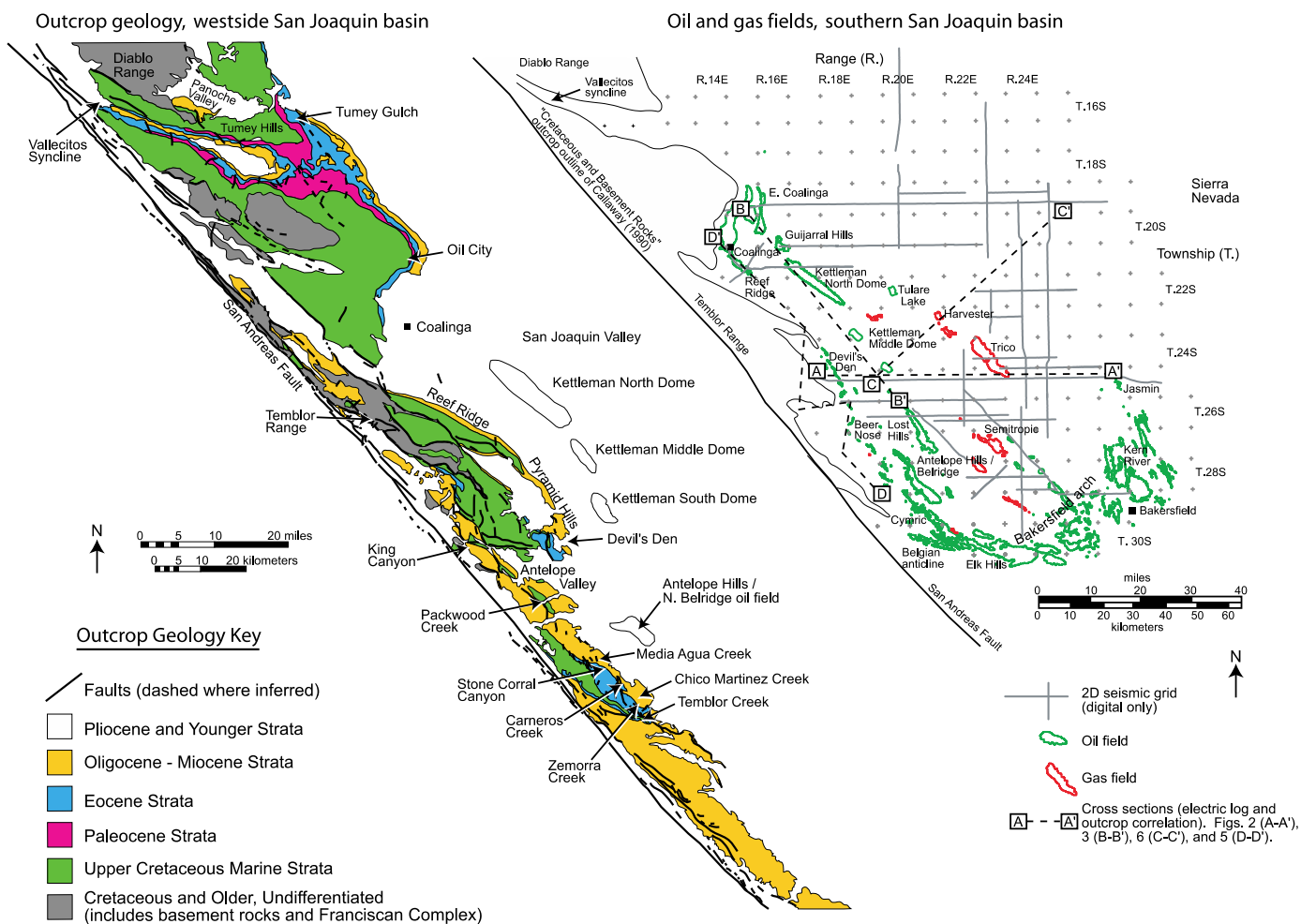
Field cross section

Qls

Selected large landslides, such as Blackhawk Slide on north side of San Gabriel Mountains; early to late Quaternary.

	Alluvium, lake, playa, and terrace deposits; unconsolidated and semi-consolidated. Mostly nonmarine, but includes marine deposits near the coast. Quaternary		Sandstone, shale, and conglomerate; mostly well consolidated. Paleocene.
	Pliocene and/or Pleistocene sandstone, shale, and gravel deposits; mostly loosely consolidated.		Upper Cretaceous sandstone, shale, and conglomerate.
	Sandstone, siltstone, shale, and conglomerate; mostly moderately consolidated. Pliocene.		Lower Cretaceous sandstone, shale, and conglomerate.
	Sandstone, shale, siltstone, conglomerate, and breccia; moderately to well consolidated. Miocene.		Franciscan Complex: Cretaceous and Jurassic sandstone with smaller amounts of shale, chert, limestone, and conglomerate.
	Sandstone, shale, conglomerate, and fanglomerate; moderately to well consolidated. Miocene.		Ultramafic rocks, mostly serpentine. Minor peridotite, gabbro, and diabase. Chiefly Mesozoic.
	Shale, sandstone, conglomerate, minor limestone; mostly well consolidated. Eocene.		Gabbro and dark dioritic rocks; chiefly Mesozoic.

Background information



Johnson and Graham, 2006

SAN JOAQUIN BASIN PROVINCE

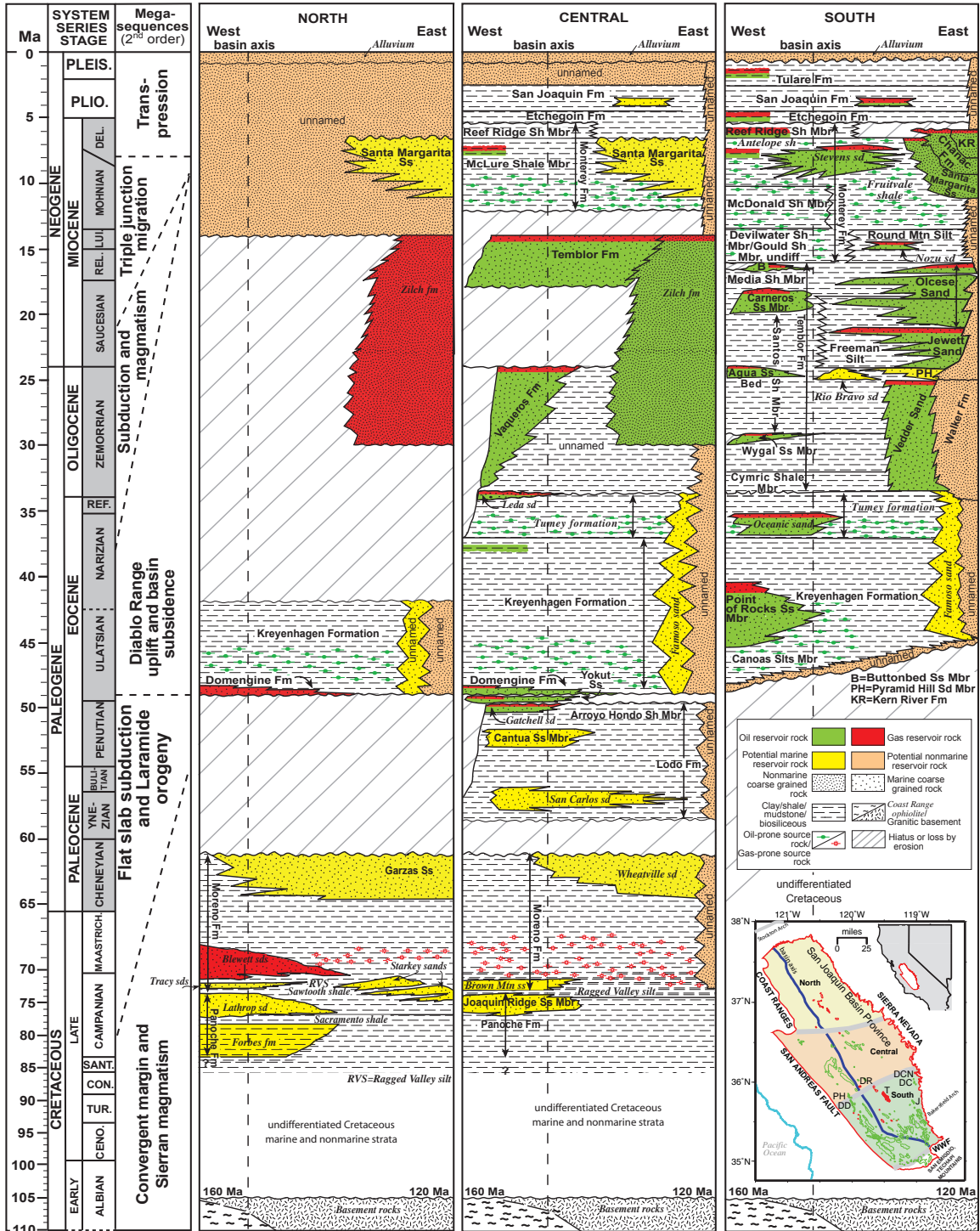
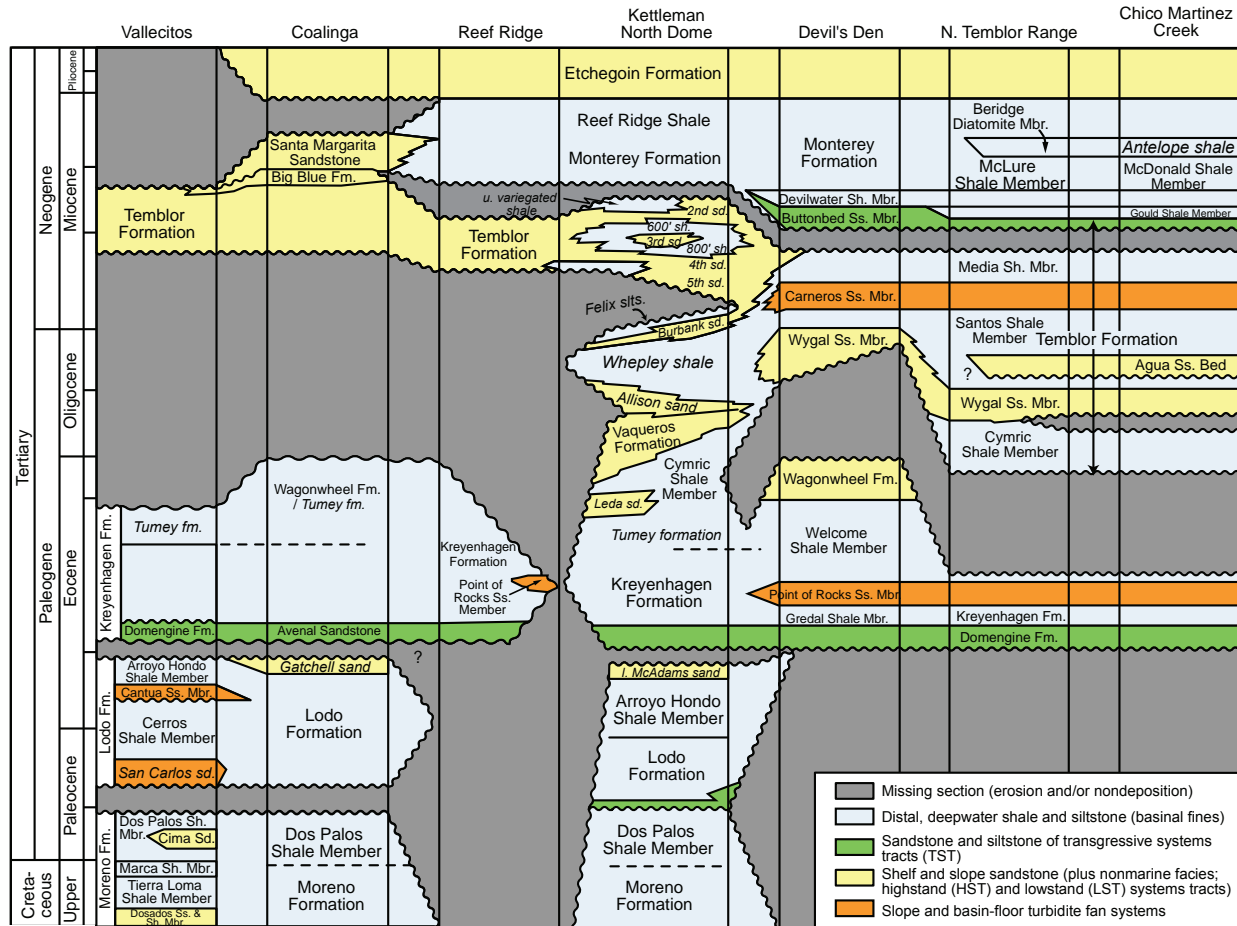


Figure 5.1a

Scheirer and Magoon, 2006

Northwest

Southeast



Johnson & Graham, 2006

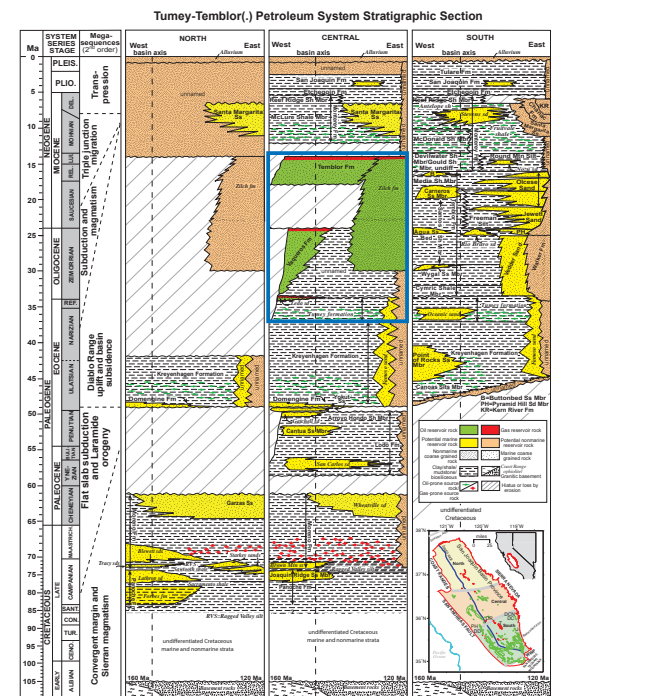
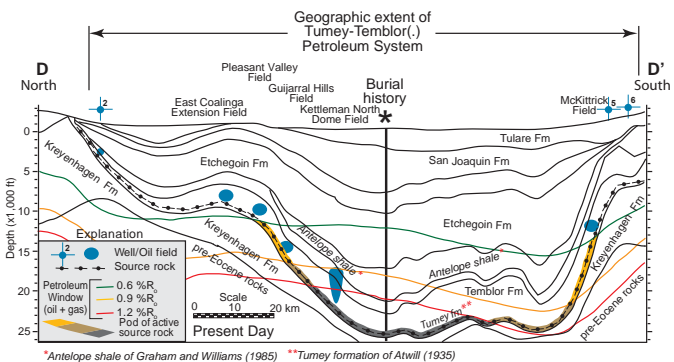
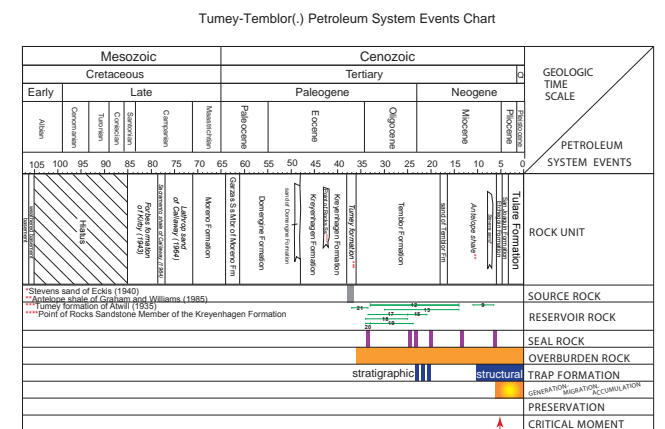
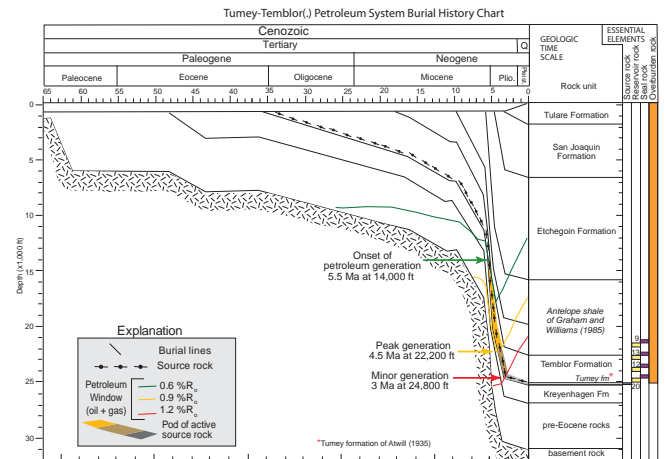
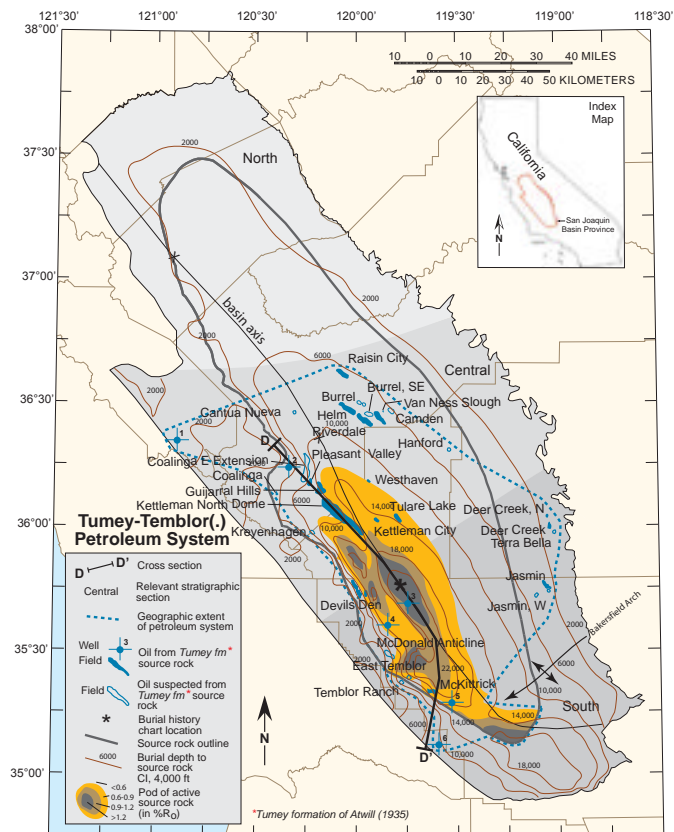


Table 8.8. Tumey-Temblor(.) petroleum system petroleum volumes by reservoir rock. (Data from appendix 8.1 and appendix 8.2. Res No., Reservoir Number corresponding to column 8 in appendix 8.1; Ma, million years ago; EUR Oil, Estimated ultimate recovery of oil; Mbo, thousands of barrels of oil; EUR Gas, Estimated ultimate recovery of gas; MMcf, millions of cubic feet of gas; GOR, gas-to-oil ratio; cftg/bo, cubic feet of gas per barrel of oil; Boe, Barrel of oil equivalent; NA, Not Applicable; zz-undesignated, unknown reservoir rock. ** and yellow shading highlight the major reservoir rock for the petroleum system; * and green shading highlight source rock interval for the petroleum system)

Res No.	Reservoir Rock Unit	Age Range (Ma)	Number of Pools	EUR Oil (Mbo)	EUR Gas (MMcf)	GOR (cftg/bo)	Oil (%)	Gas (%)	EUR Boe (Mbo)	Boe (%)
9	Santa Margarita Sandstone	11-6.5	3	3,352	7	2	0.5	0.0	3,353	0.3
10	Stevens sand of Eckis (1940)	9.5-7	1	0	0	0	0.0	0.0	0	0.0
12	Temblor Formation*	38-14	32	485,214	1,976,597	4,074	75.2	93.3	814,647	84.3
13	Zich formation of Loken (1959)	30-14	9	76,989	62,500	791	12.9	3.0	89,406	9.3
15	Jewett Sand	25-21	1	2	0	0	0.0	0.0	2	0.0
17	Vedder Sand	33.5-25	1	4,005	5	1	0.7	0.0	4,006	0.4
18	Walker Formation	25-34	1	71	0	0	0.0	0.0	71	0.0
19	Vaqueros Formation	33-24	3	27,339	49,114	1,796	4.5	2.3	35,525	3.7
20	Leda sand of Sullivan (1962)	34-33	2	10,240	22,758	2,222	1.7	1.1	14,033	1.5
21	Tumey formation of Atwill (1935)*	37-33.5	4	173	889	5,139	0.0	0.0	321	0.0
34	zz-undesignated	NA	1	3,617	5,998	1,658	0.6	0.3	4,617	0.5
	Total		58	613,002	2,117,868	3,455	100.0	100.0	965,980	100.0

Tumey-Temblor(.) Folio Sheet

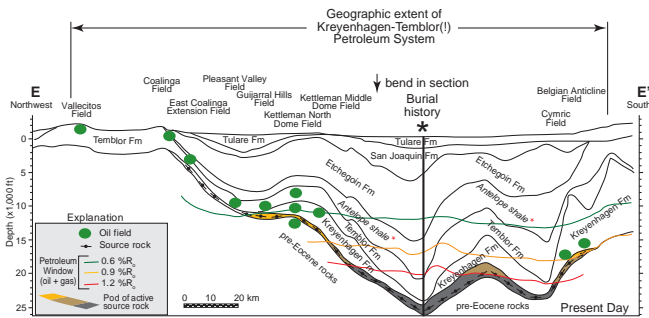
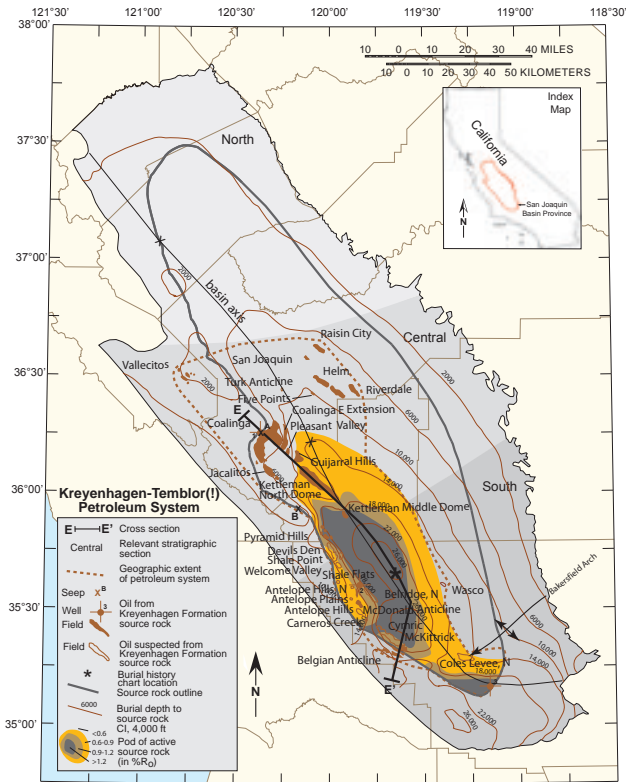
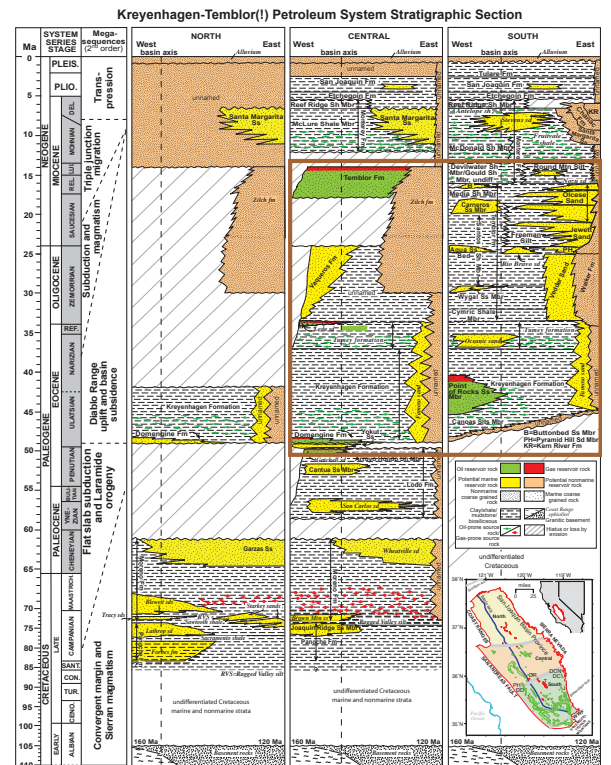
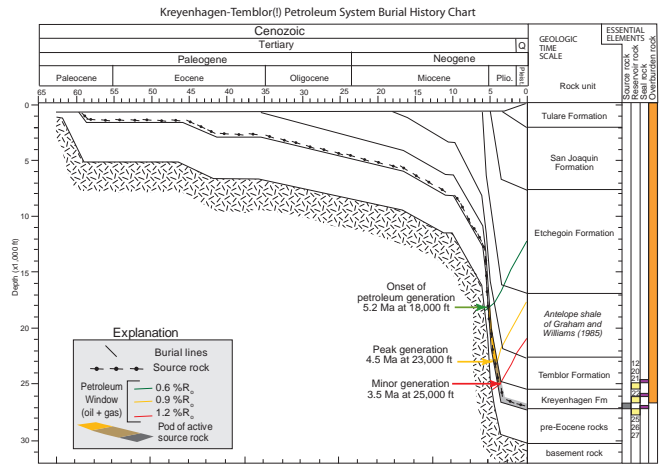
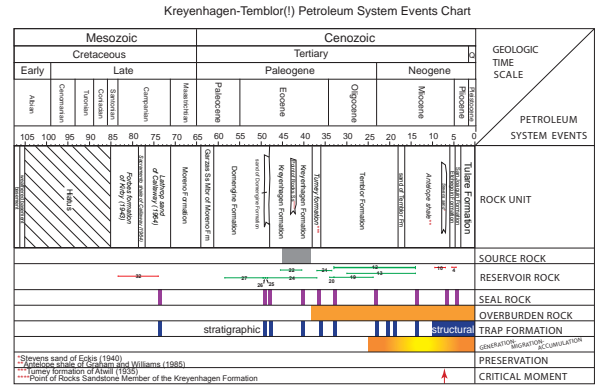


Table 8.9. Kreyenhagen-Temblo(!!) petroleum system petroleum volumes by reservoir rock.

[Data from appendix 8.1 and appendix 8.2. Res No., Reservoir Number corresponding to column 8 in appendix 8.1; Ma, million years ago; EUR Oil, Estimated ultimate recovery of oil; Mbo, thousands of barrels of oil; EUR Gas, Estimated ultimate recovery of gas; MMcf, millions of cubic feet of gas; GOR, gas-to-oil ratio; cftg/b, cubic feet of gas per barrel of oil; Boe, Barrel of oil equivalent; Ss, Sandstone; Mbr, Member; Fm, Formation; NA, Not Applicable; zz-undesignated, unknown reservoir rock. ** and yellow shading highlight the major reservoir rock for the petroleum system; * and green shading highlight source rock interval for the petroleum system]

Res No.	Reservoir Rock Unit	Age Range (Ma)	Number of Pools	EUR Oil (Mbo)	EUR Gas (MMcf)	GOR (cftg/b)	Oil (%)	Gas (%)	EUR Boe (Mbo)	Boe (%)
4	Etchegoin Formation	5.5-4.5	2	3	403	134,333	0.0	0.0	70	0.0
10	Stevens sand of Ecks (1940)	9.5-7	2	0	586	NA	0.0	0.0	98	0.0
12	Temblo Formation**	33-14	23	1,069,169	906,423	848	60.2	30.0	1,220,240	53.5
13	Zilch formation of Loken (1959)	30-14	2	784	1,247	1,591	0.0	0.0	992	0.0
19	Vaqueros Formation	33-24	1	2	12	6,000	0.0	0.0	4	0.0
20	Leda sand of Sullivan (1962)	34-33	2	23,702	32,704	1,380	1.3	1.1	29,153	1.3
21	Tumey formation of Atwill (1935)	37-33.5	8	31,886	94,172	2,953	1.8	3.1	47,581	2.1
22	Point of Rocks Ss Mbr, Kreyenhagen Fm	45.5-40.5	26	15,069	82,994	5,508	0.8	2.7	28,901	1.3
24	Kreyenhagen Formation*	48.5-37	4	761	848	1,114	0.0	0.0	902	0.0
25	Domengine Formation	49-48.5	6	23,555	74,105	3,146	1.3	2.5	35,906	1.6
26	Yokut Sandstone	49.5-49.3	3	5,351	5,622	1,051	0.3	0.2	6,288	0.3
27	Lodo Formation	58.5-49.5	16	556,719	1,661,893	2,985	31.3	55.0	833,701	36.6
30	Moreno Formation	71-61	1	0	0	0.0	0.0	0.0	0	0.0
32	Panoche Formation	83.5-74	1	0	8	NA	0.0	0.0	1	0.0
34	zz-undesignated	NA	2	49,710	159,610	3,211	2.8	5.3	76,312	3.3
	Total		99	1,776,710	3,020,627	1,700	100.0	100.0	2,280,149	100.0

Kreyenhagen-Temblo(!!) Folio Sheet



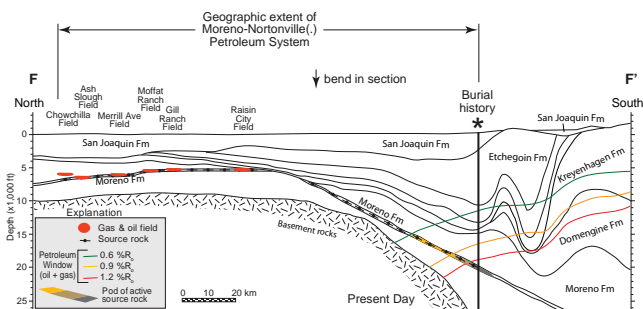
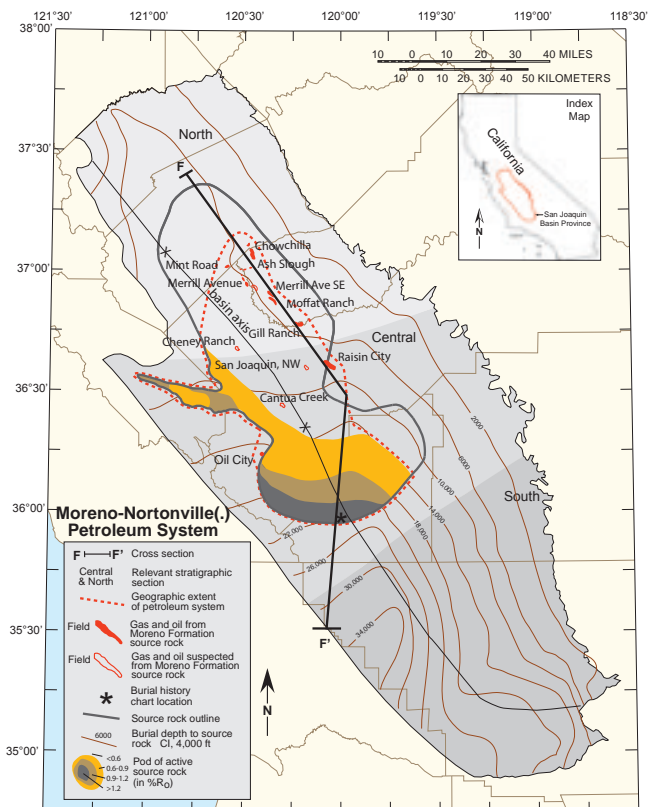


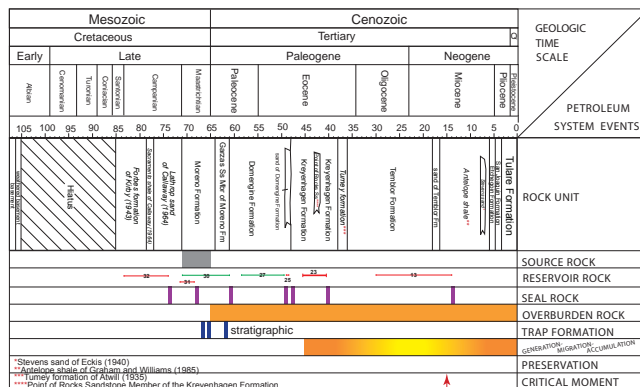
Table 8.10. Moreno-Nortonville(.) petroleum system gas and oil volumes by reservoir rock.

(Data from appendix 8.1 and appendix 8.2. Res No., Reservoir Number corresponding to column 8 in appendix 8.1; Ma, million years ago; EUR Oil, Estimated ultimate recovery of oil; Mbo, thousands of barrels of oil; EUR Gas, Estimated ultimate recovery of gas; MMcf, millions of cubic feet of gas; GOR, gas-to-oil ratio; cftg/bo, cubic feet of gas per barrel of oil; Boe, Barrel of oil equivalent; NA, Not Applicable. ** and yellow shading highlight the major reservoir rock for the petroleum system; * and pink shading highlight source rock interval for the petroleum system)

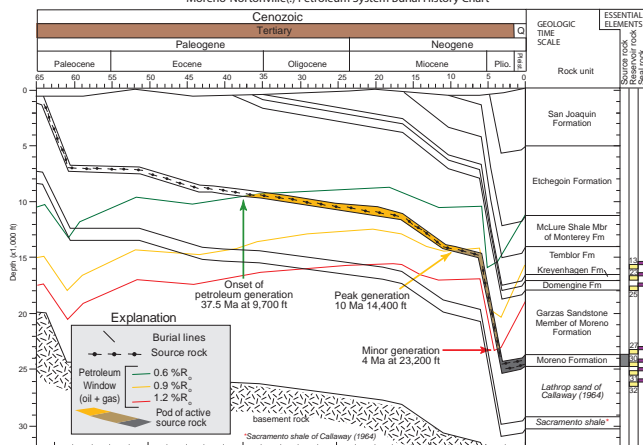
Res No.	Reservoir Rock Unit	Age Range (Ma)	Number of Pools	EUR Oil (Mbo)	EUR Gas (MMcf)	GOR (cftg/bo)	Oil (%)	Gas (%)	EUR Boe (Mbo)	Boe (%)
13	Zlich formation of Loken (1959)	30-14	3	0	5,968	NA	0.0	3.3	995	3.2
23	Nortonville sand of Frame (1950)**	45.5-40.5	4	0	74,067	NA	0.0	40.5	12,345	40.3
25	Domengne Formation	49-45.5	2	0	2,435	NA	0.0	1.3	406	1.3
27	Lodo Formation	58.5-49.5	1	40	801	20,025	25.3	0.4	174	0.6
30	Moreno Formation*	71-61	4	118	4742	40,186	74.7	2.6	908	3.0
31	Blewett sands of Hoffman (1964)	71.5-68.5	4	0	34905	NA	0.0	19.1	5,818	19.0
32	Panoche Formation	83.5-74	3	0	59,856	NA	0.0	32.7	9,976	32.6
	Total		21	158	182,774	1,156,797	100.0	100.0	30620	100.0

Moreno-Nortonville(.) Folio Sheet

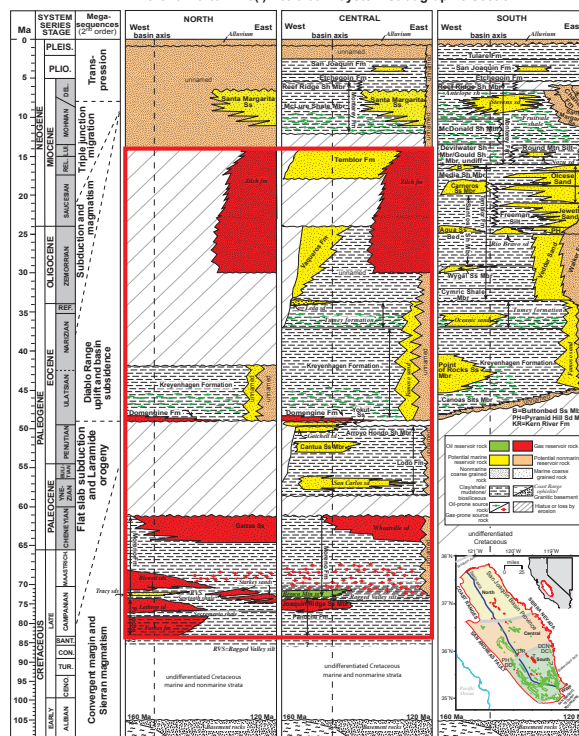
Moreno-Nortonville(.) Petroleum System Events Chart

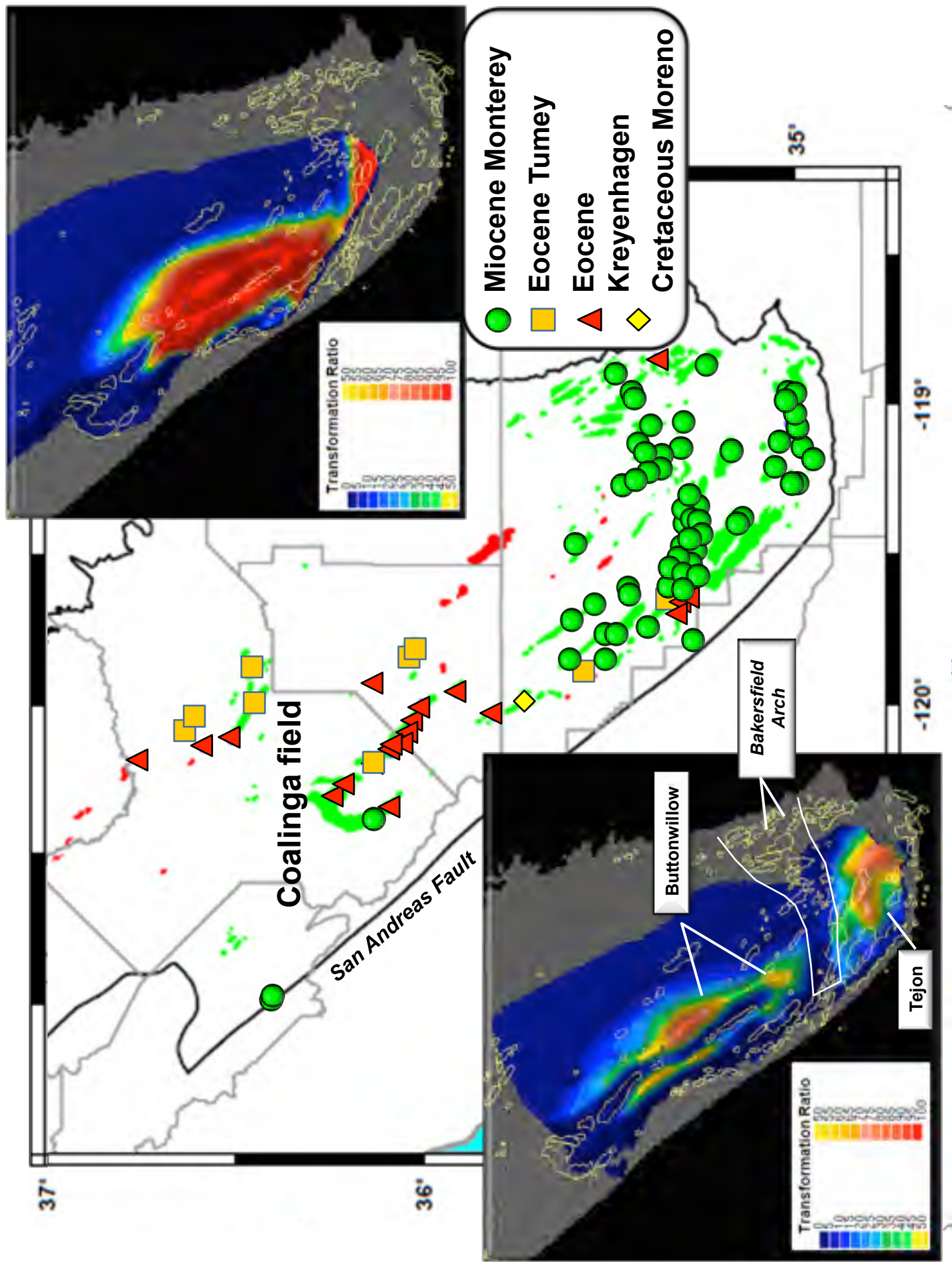


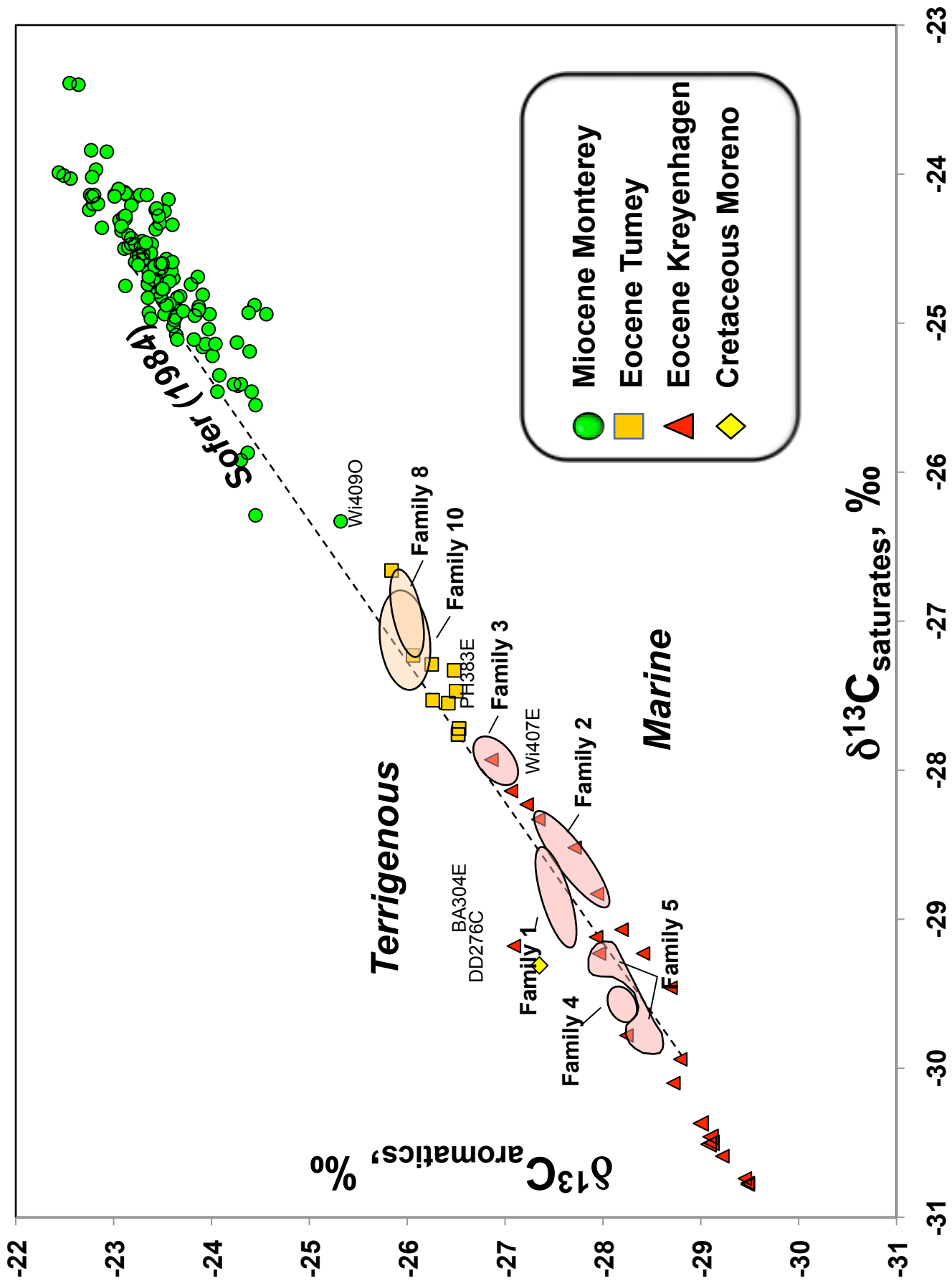
Moreno-Nortonville(.) Petroleum System Burial History Chart



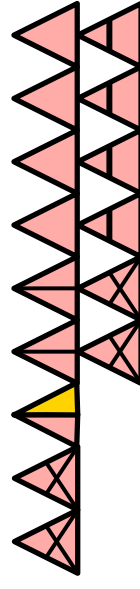
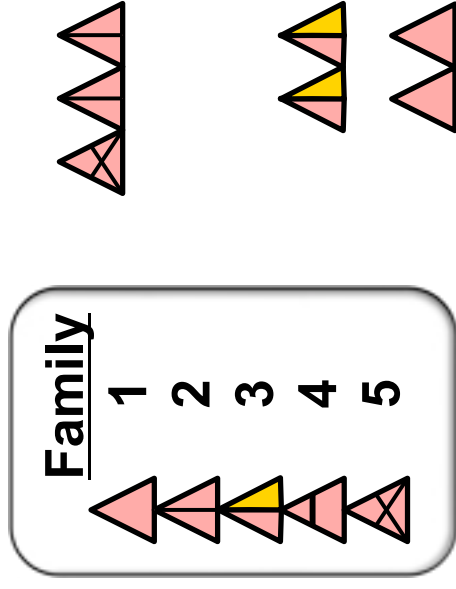
Moreno-Nortonville(.) Petroleum System Stratigraphic Section



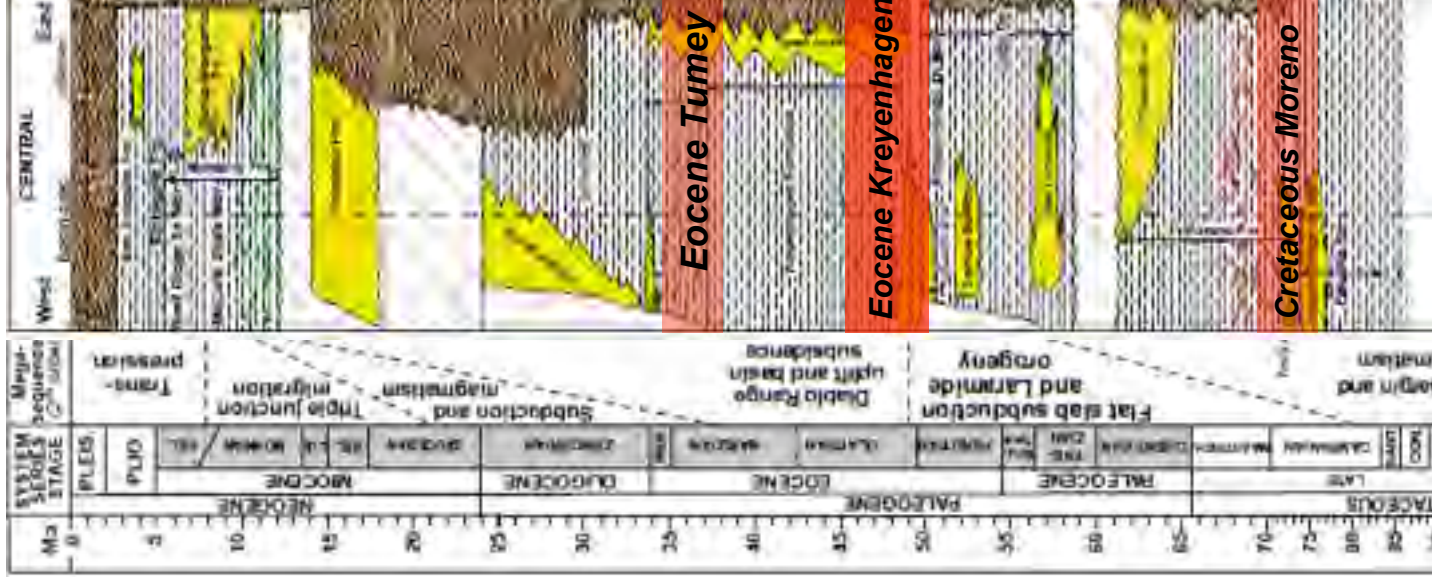
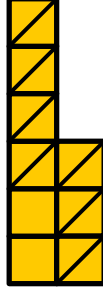




Families 1-5: Kreyenhagen Source, Mostly Eocene Pools



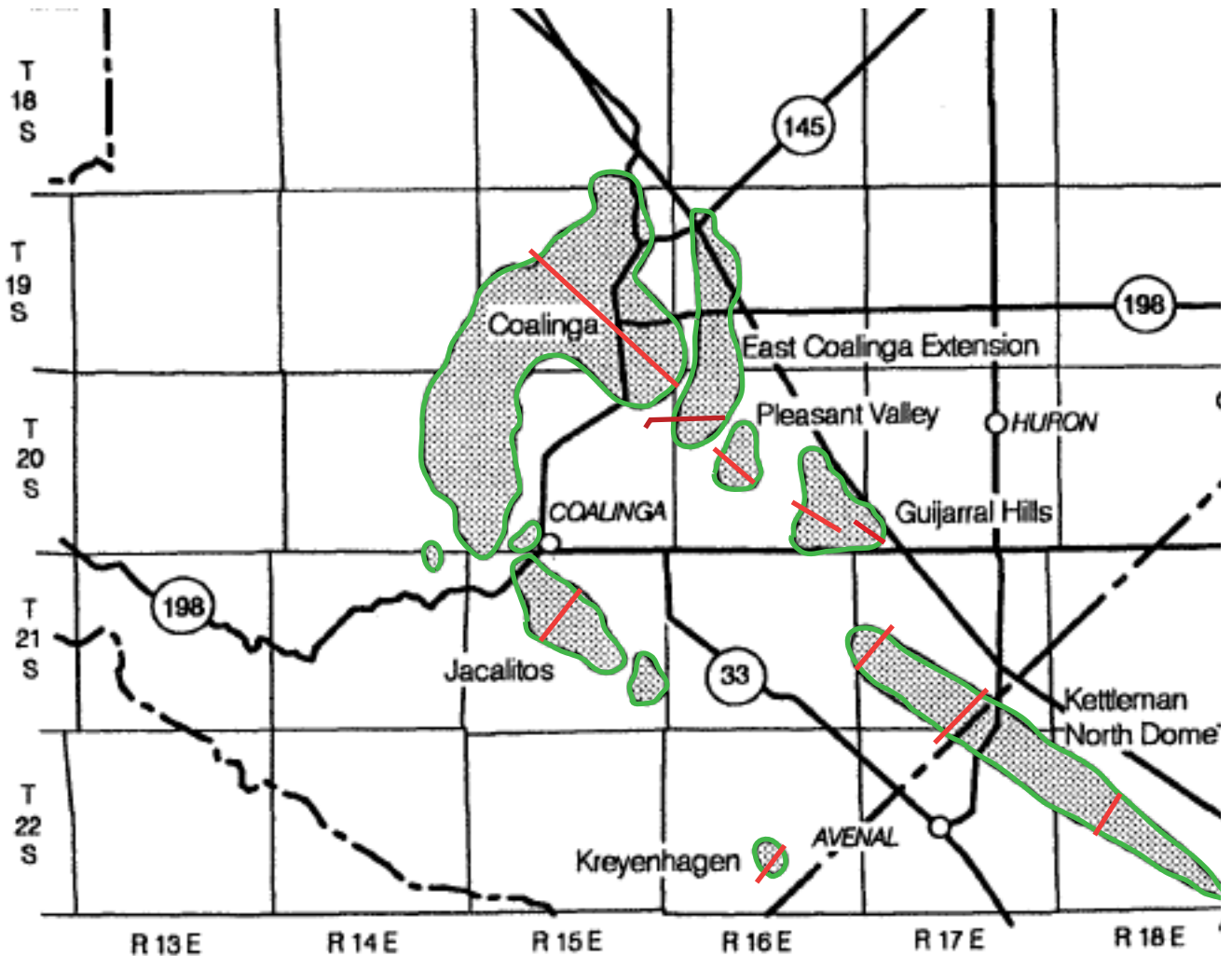
Families 8 and 10: Tumey Source, Mostly Miocene Pools



**Family 9: Moreno Source,
Upper Cretaceous Pool**



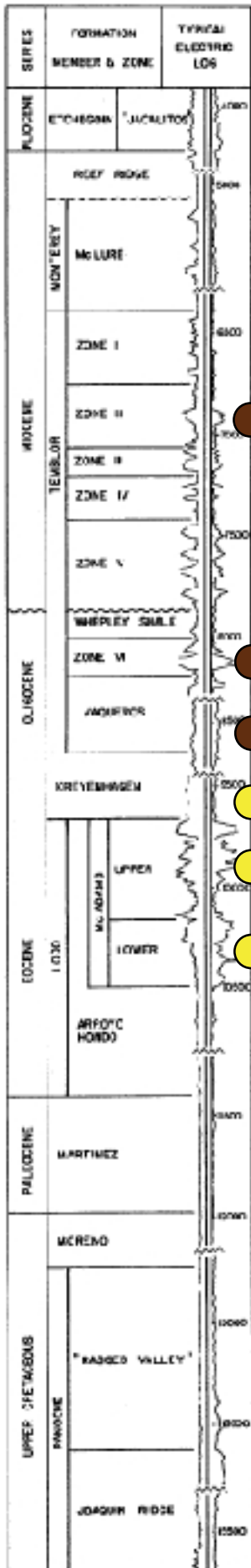
Oil Types on Oil Field Maps and Cross Sections



Three oil types are shown on the field maps and cross sections above to demonstrate the migration route of the petroleum from the Buttonwillow deep to the Coalinga field. The farthest south field, Kettleman North Dome is first followed by Gujarral Hills, Pleasant Valley, East Coalinga Extension and ends with the Coalinga field. Jacalitos and Kreyenhagen fields are on this migration path to Coalinga.

The three oil types area as follows. The Moreno oil type is interpreted to come from the Moreno source rock and is part of the gas prone petroleum system the Moreno-Nortonville(.). The Kreyenhagen oil type originates from the basal portion of the Kreyenhagen Formation and is the source rock in the Kreyenhagen-Temblor(!). The last oil type is the Tumey which is the source rock in the Tumey-Temblor(.). The notation on the maps and cross sections show a solid colored circle because the geochemistry of an oil sample was used to type the oil, whereas an open colored circle indicates that the oil type is interpreted based on stratigraphy.

KETTLEMAN NORTH DOME OIL FIELD



Oil from source rock

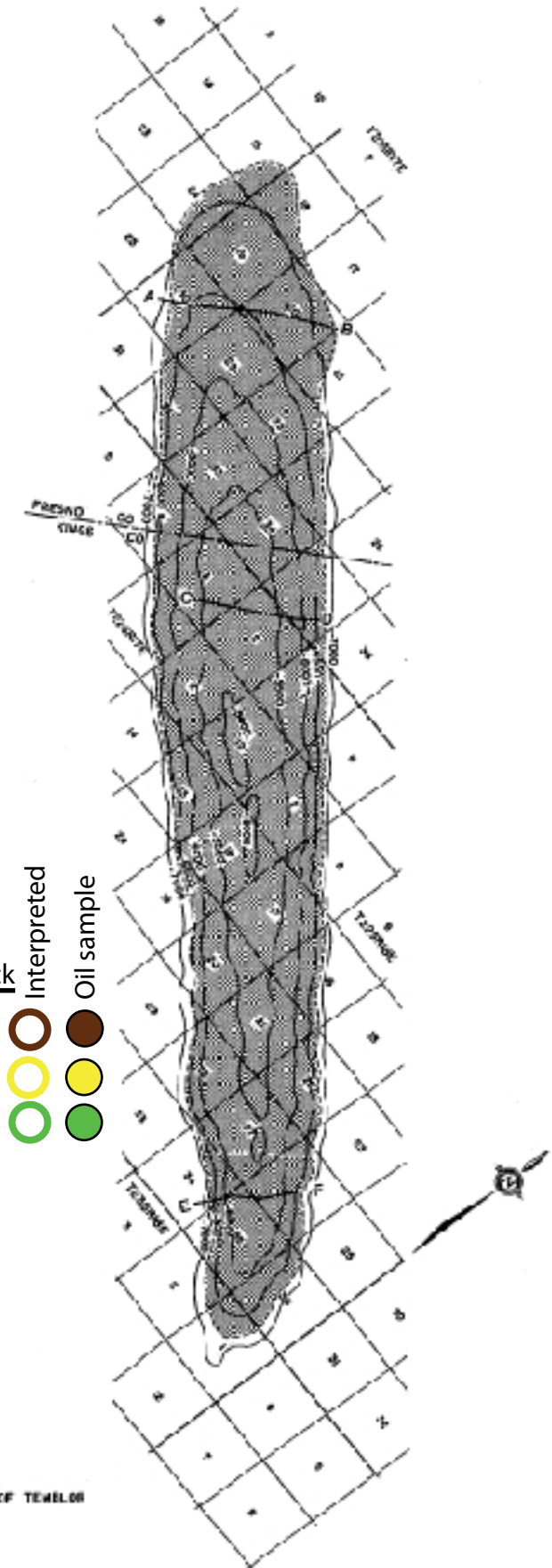
Tumey Formation

Kreyenhagen Fm

Moreno Formation

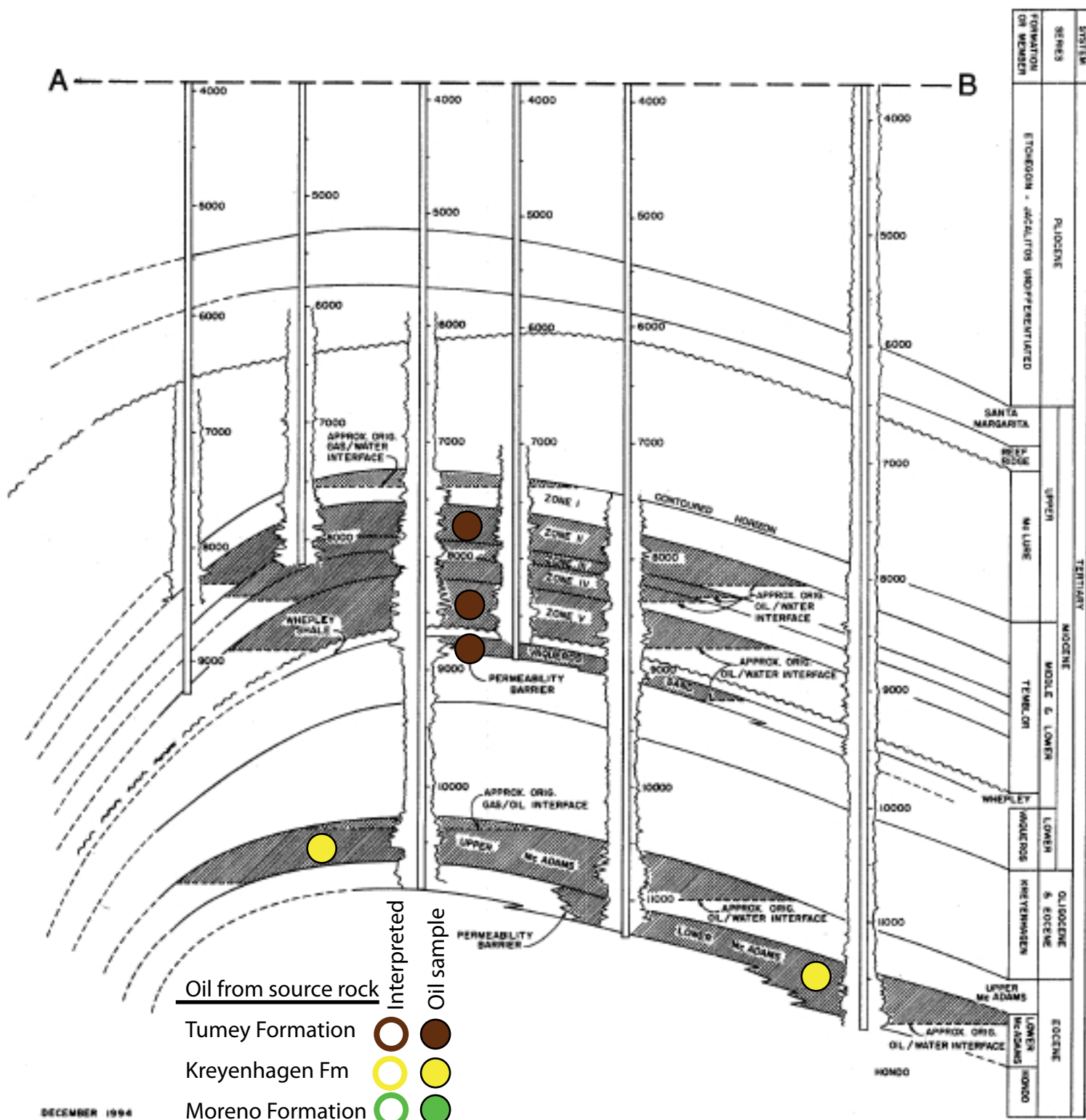
Interpreted

Oil sample

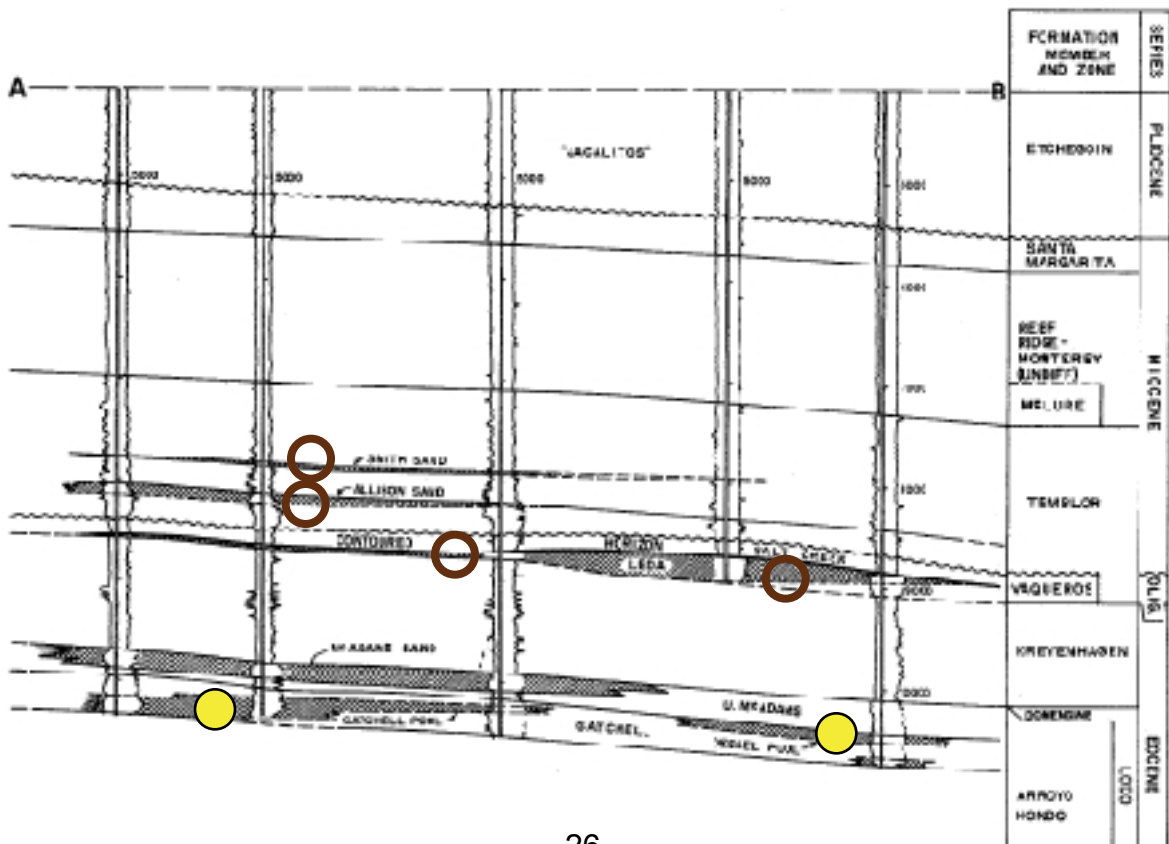
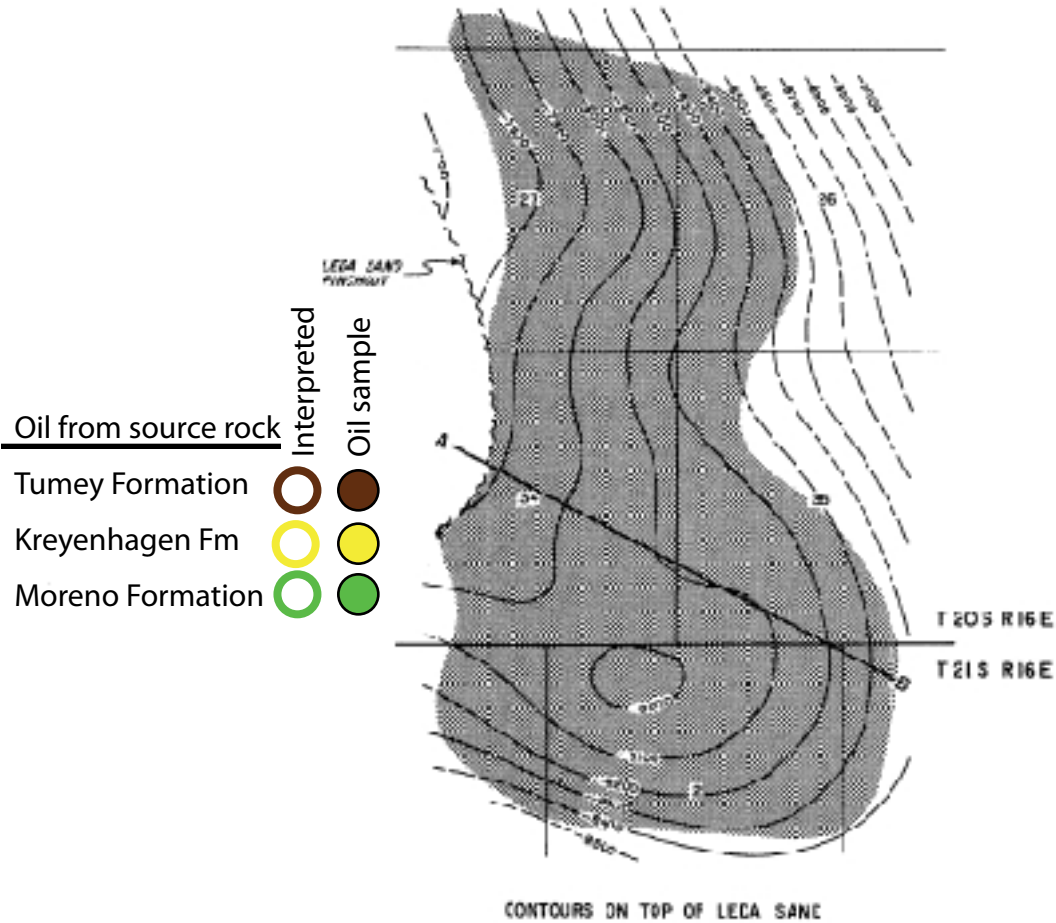


CONTOURS ON TOP OF TEMBLOR

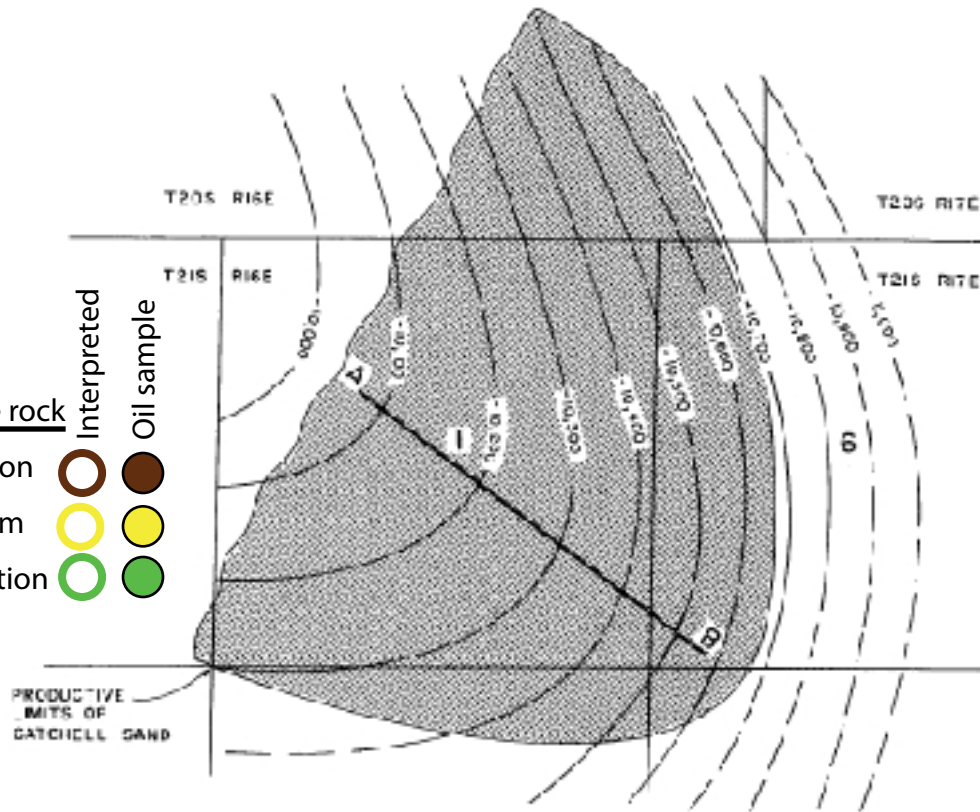
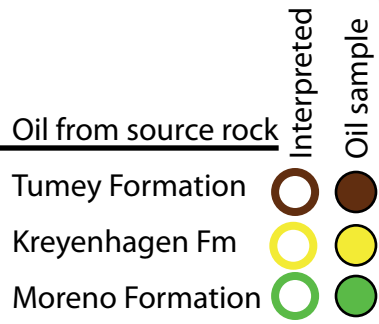
KETTLEMAN NORTH DOME OIL FIELD



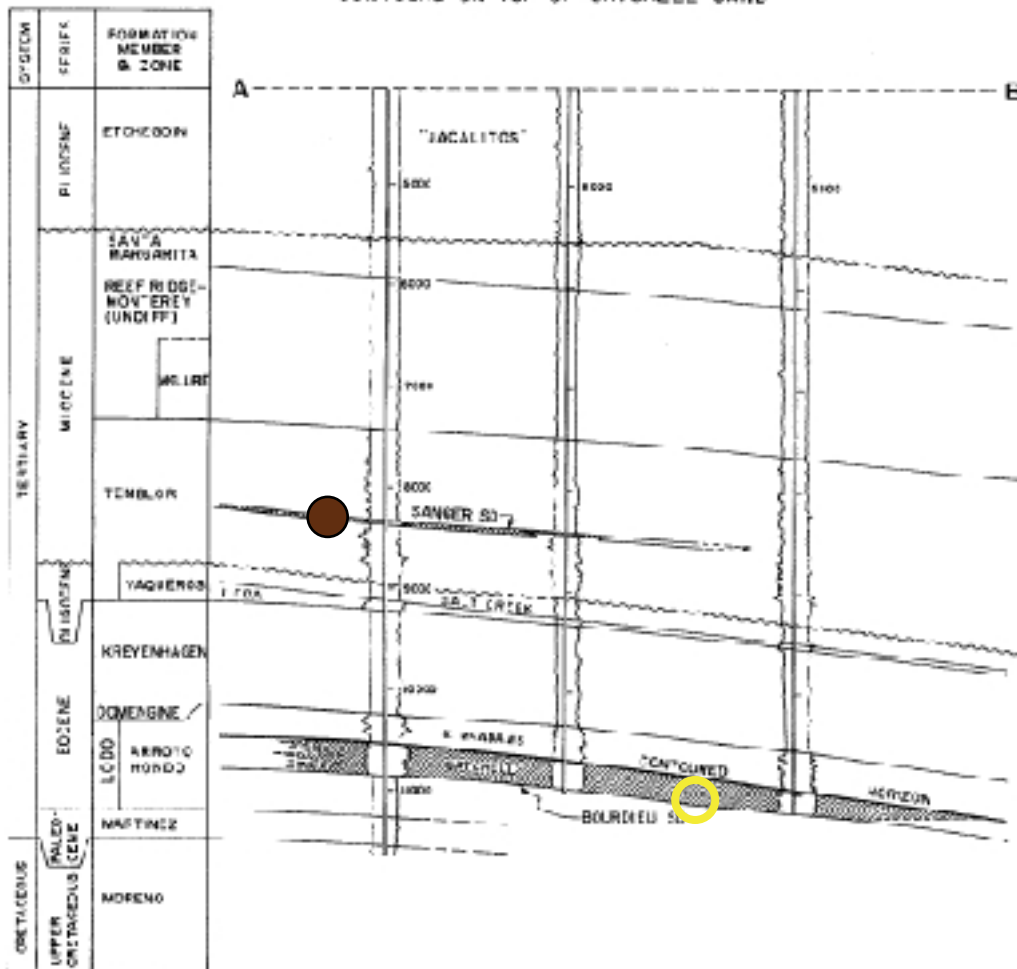
GUIJARRAL HILLS OIL FIELD Main Area



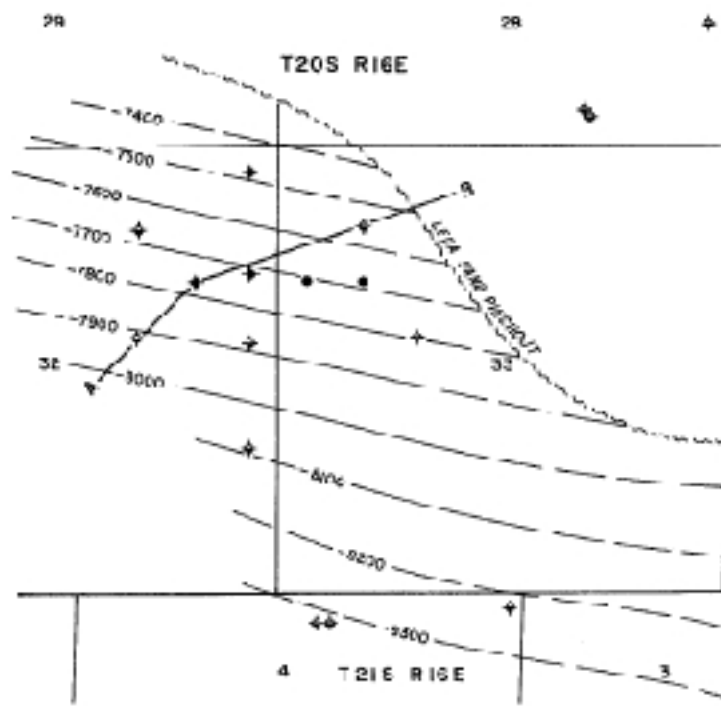
GUIJARRAL HILLS OIL FIELD **Polvadero Area**



CONTROLS ON TCP OF GATCHELL SAND



GUIJARRAL HILLS OIL FIELD West Area



CONTOURS ON TOP OF LEJA SAND

Oil from source rock

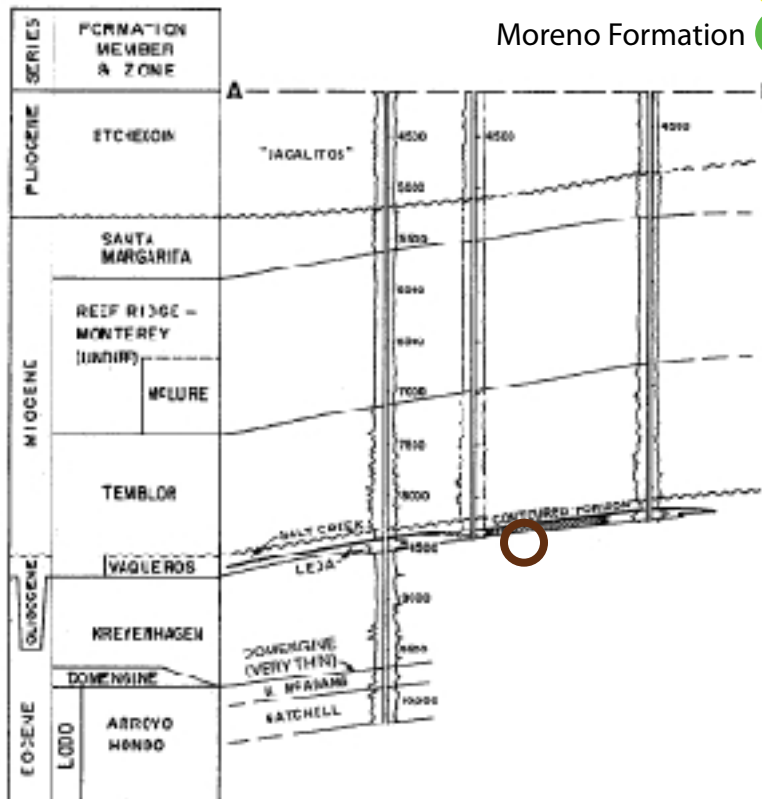
Tumey Formation

Kreyenhagen Fm

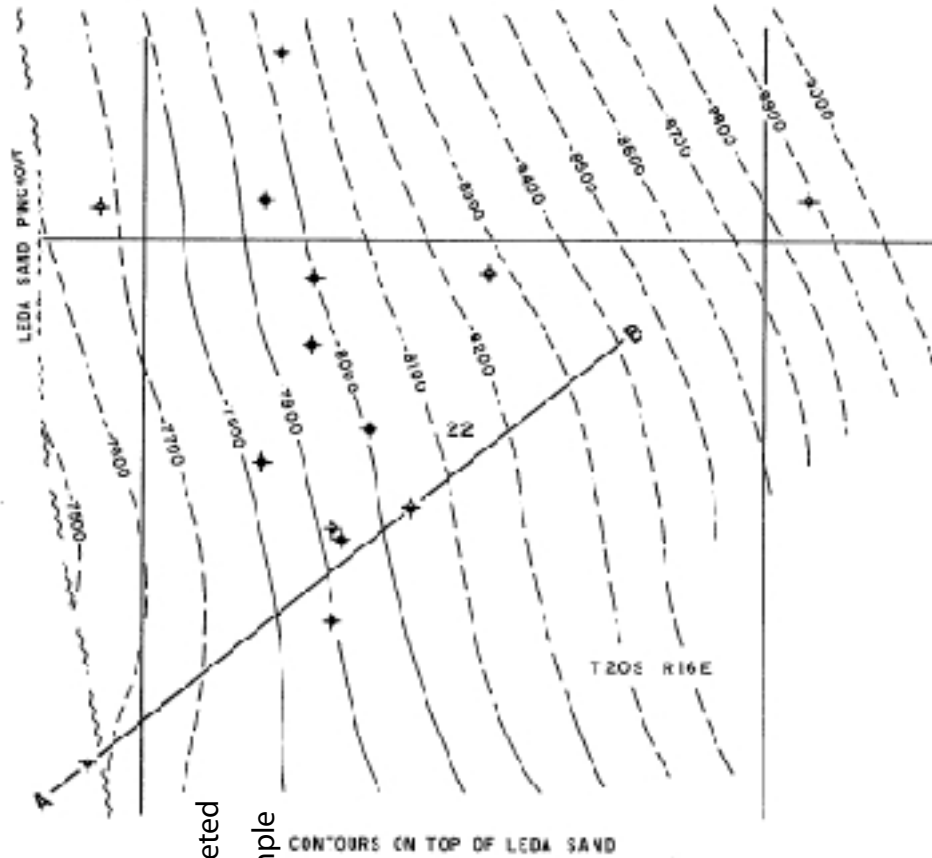
Moreno Formation

Interpreted

Oil sample



GUIJARRAL HILLS OIL FIELD Northwest Area (Abandoned)



Oil from source rock

Interpreted

Oil sample

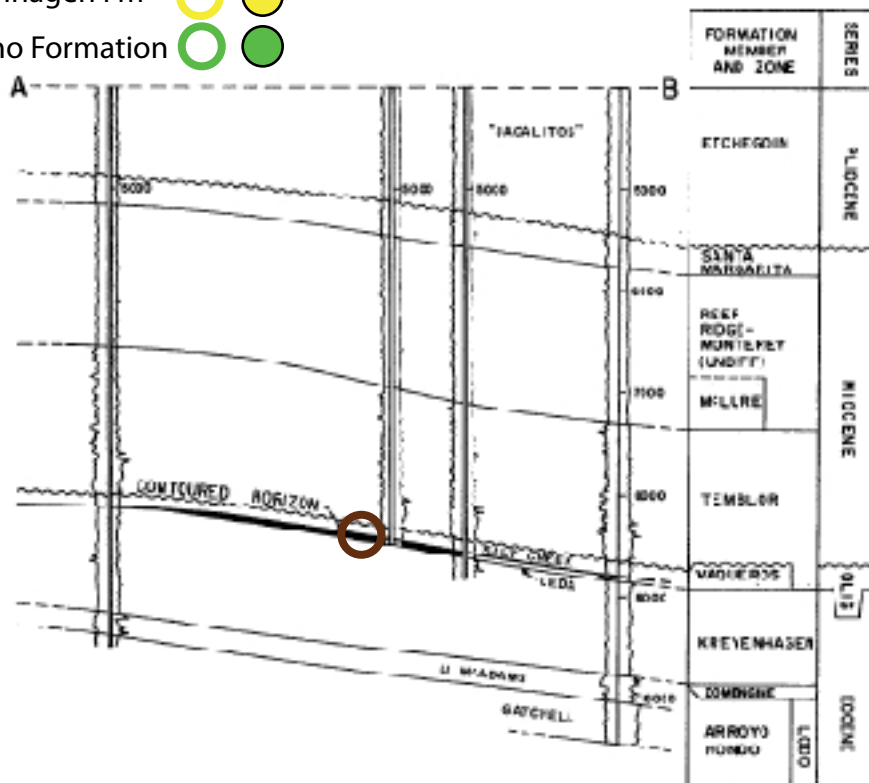
Tumey Formation



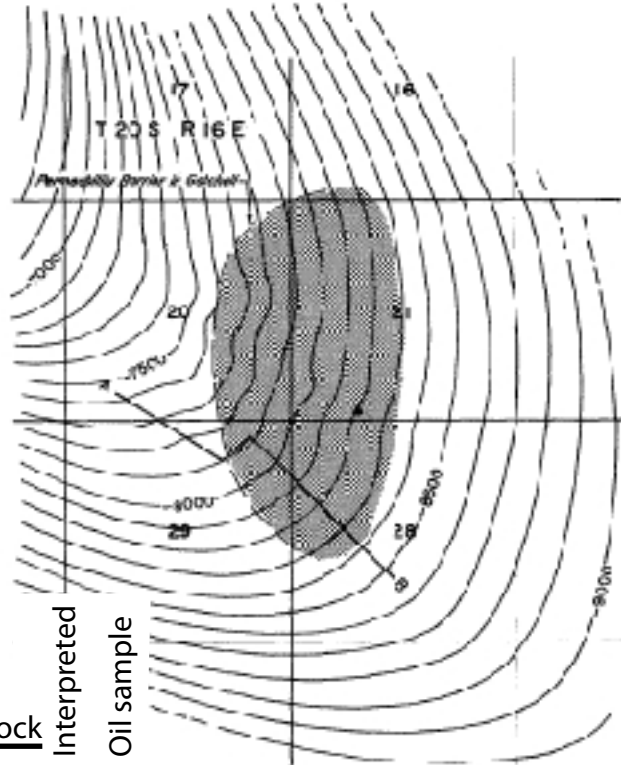
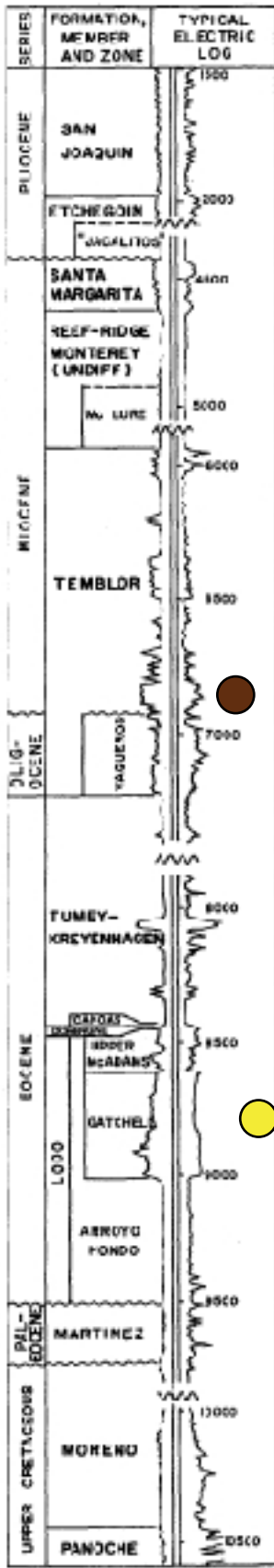
Kreyenhagen Fm



Moreno Formation



PLEASANT VALLEY OIL FIELD

Oil from source rock

Tumey Formation

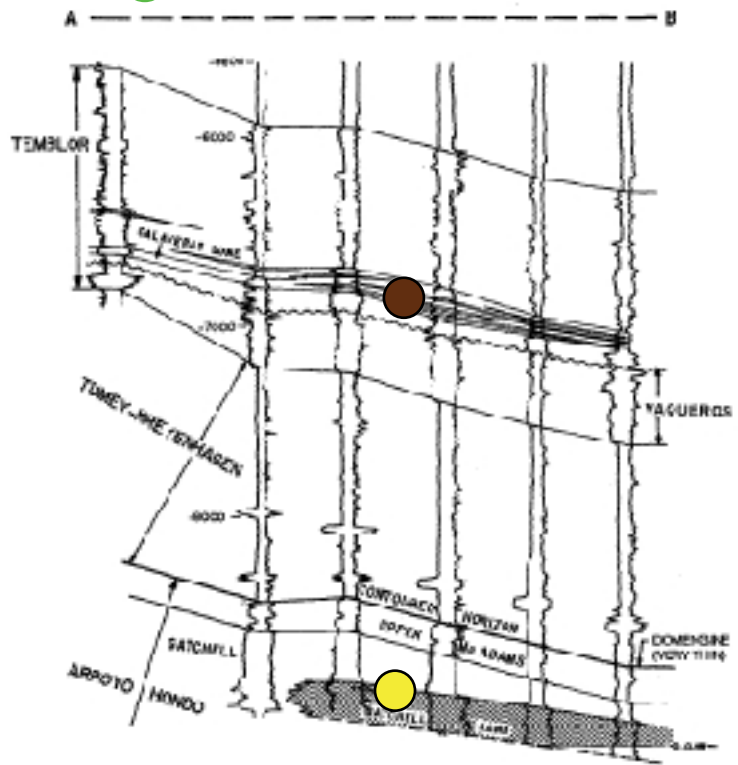
Kreyenhagen Fm

Moreno Formation

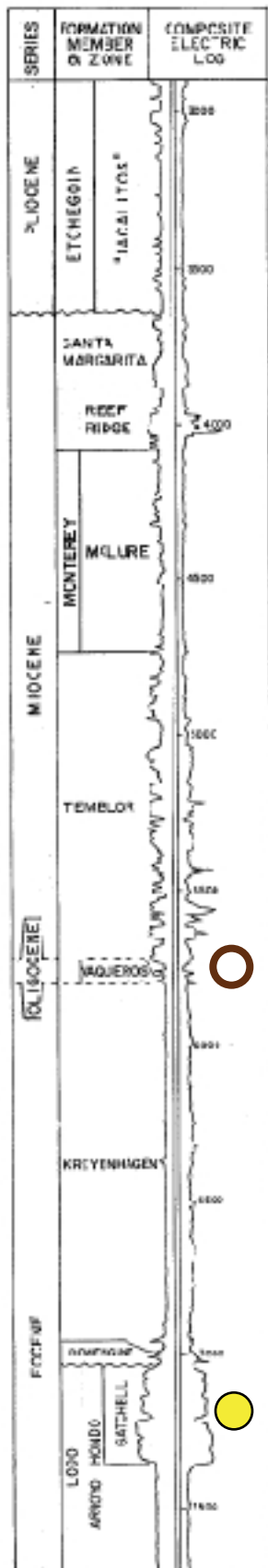
interpreted

Oil sample

INTOURS ON TOP OF COMENGINE



EAST COALINGA EXTENSION OIL FIELD



Oil from source rock

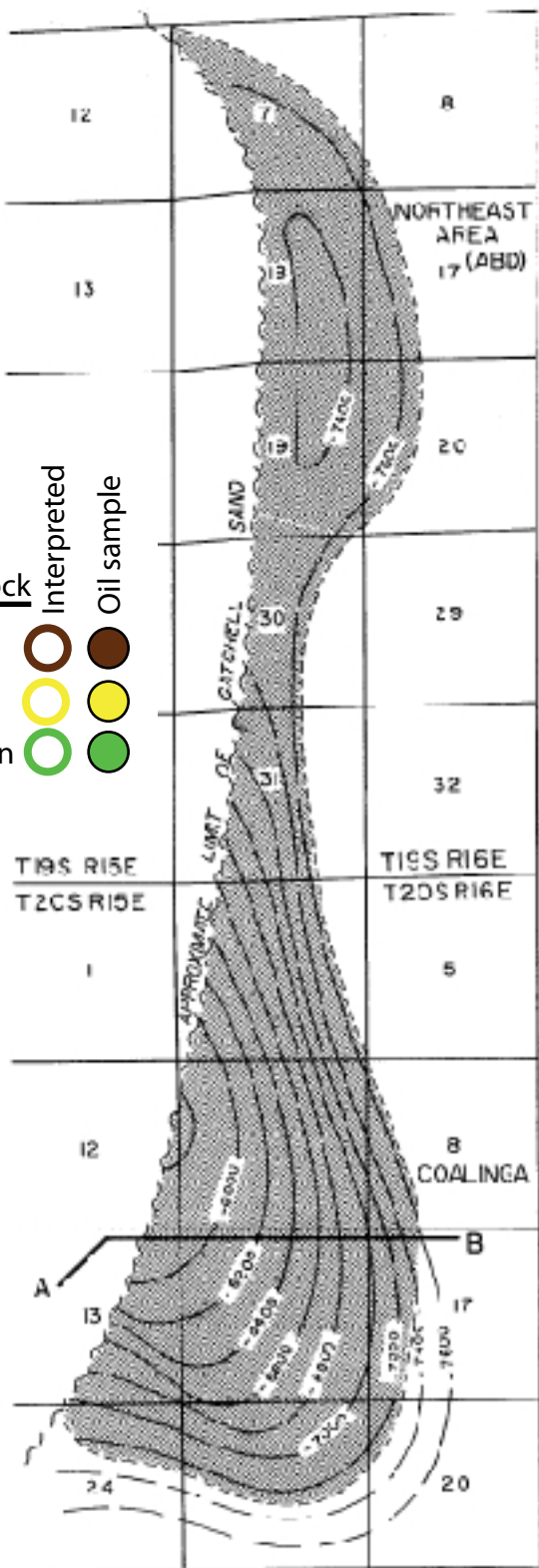
Tumey Formation

Kreyenhagen Fm

Moreno Formation

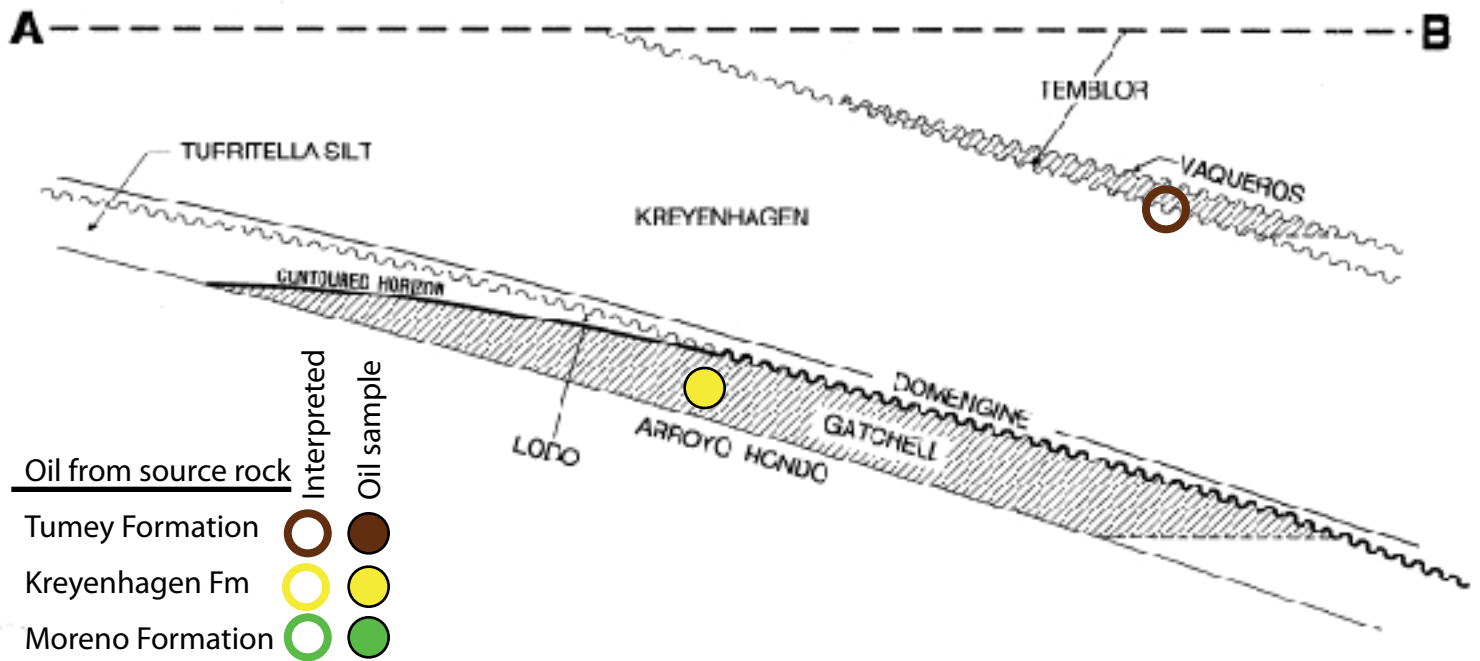
Interpreted

Oil sample

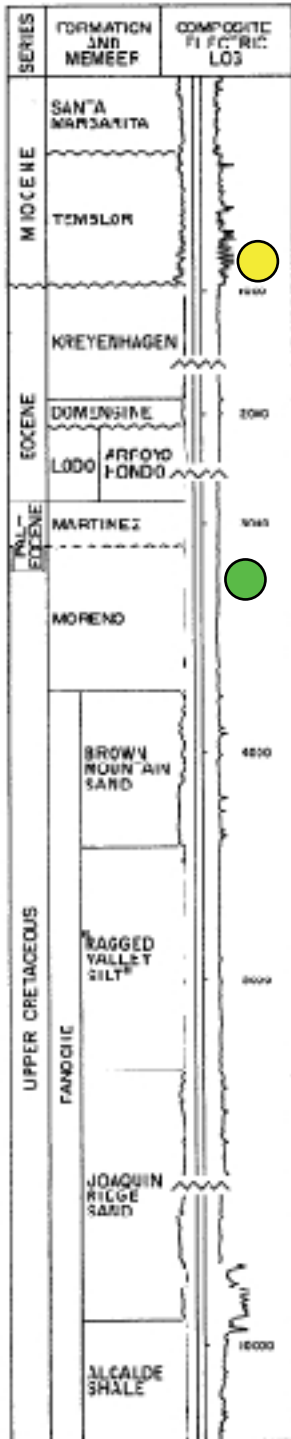


CONTOURS ON TOP OF GATCHELL SAND

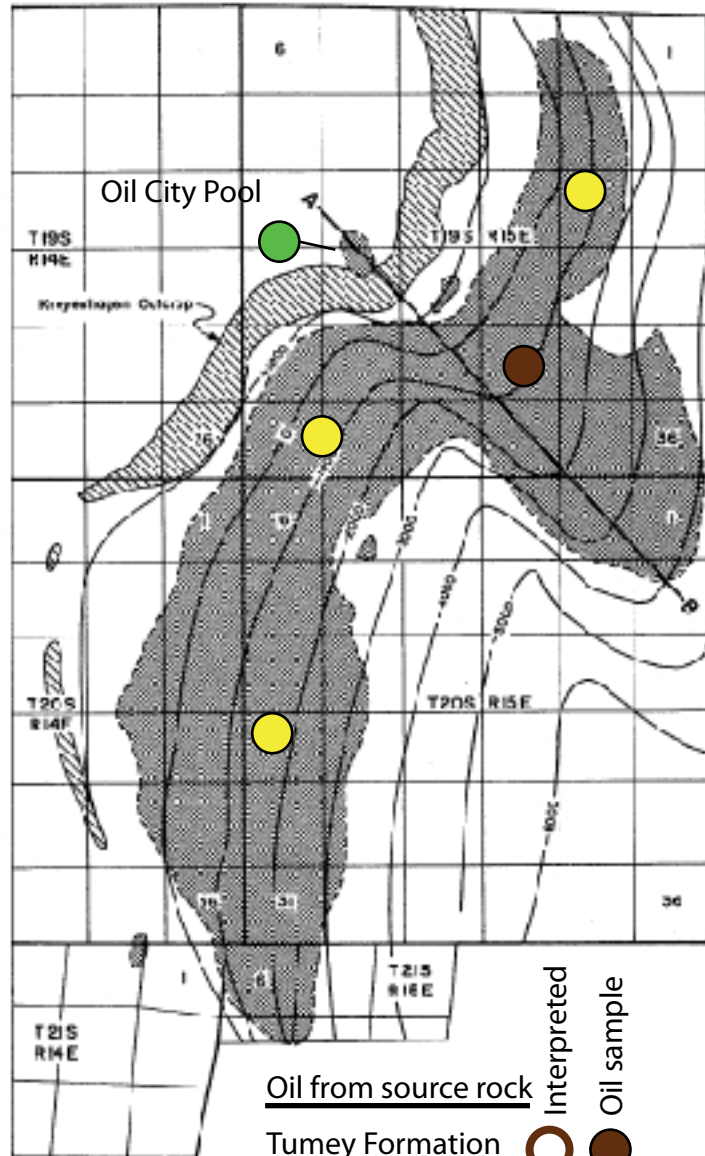
EAST COALINGA EXTENSION OIL FIELD



COALINGA OIL FIELD



Contours on top of Kreyenhagen Fm



Oil from source rock

Tumey Formation

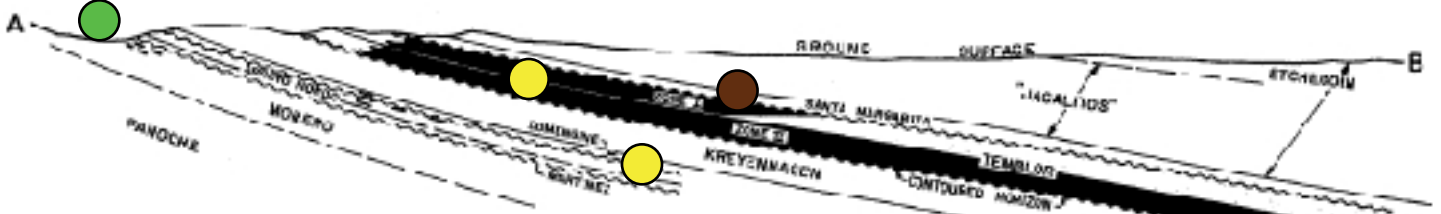
Kreyenhagen Fm

Moreno Formation

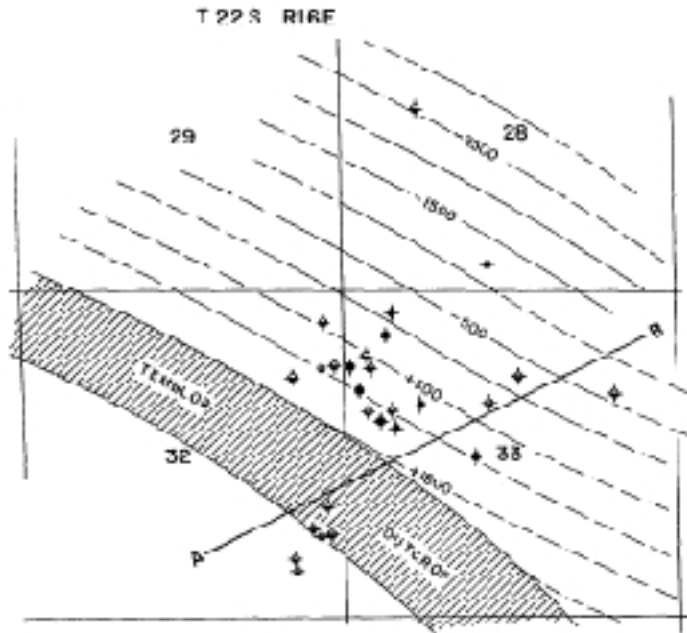
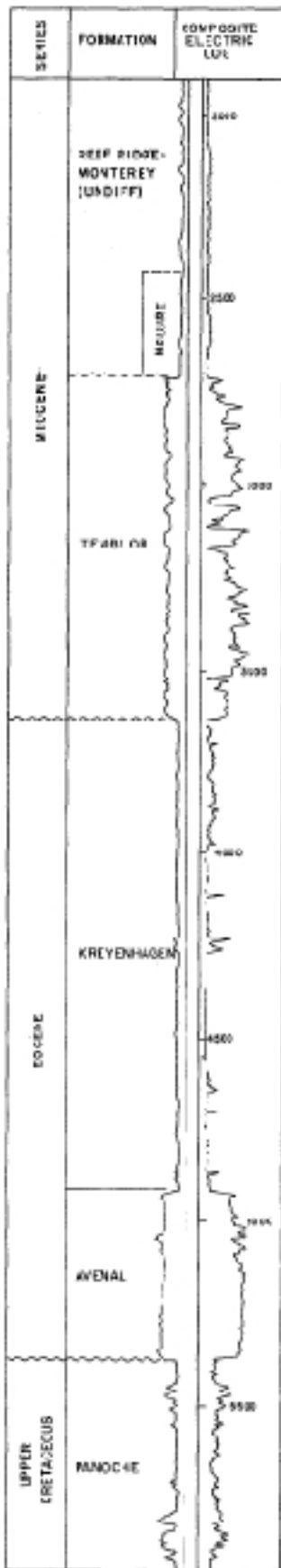
Interpreted

Oil sample

Oil City Pool



KREYENHAGEN OIL FIELD



CONTOURS ON TOP OF TEMBLOR

Oil from source rock

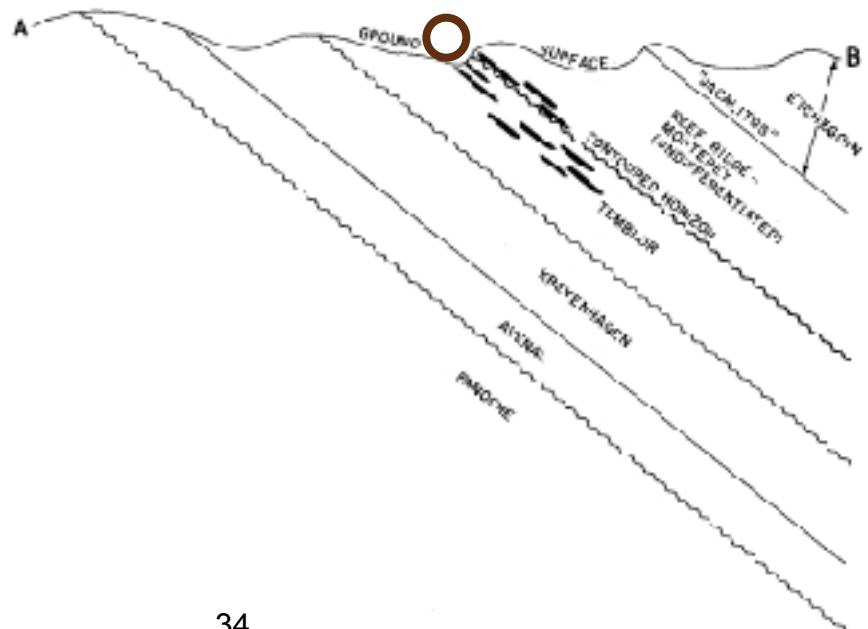
Tumey Formation

Kreyenhagen Fm

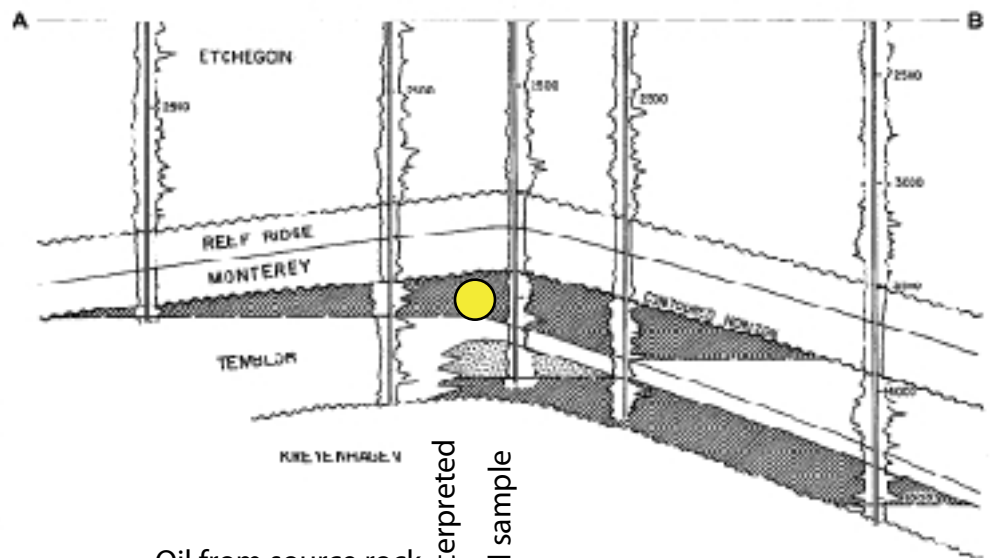
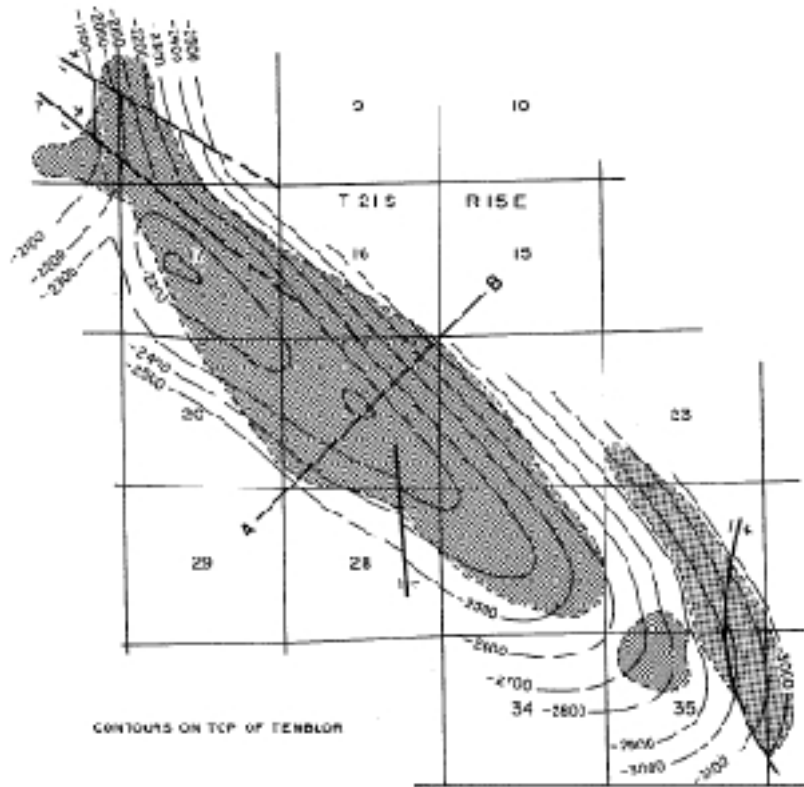
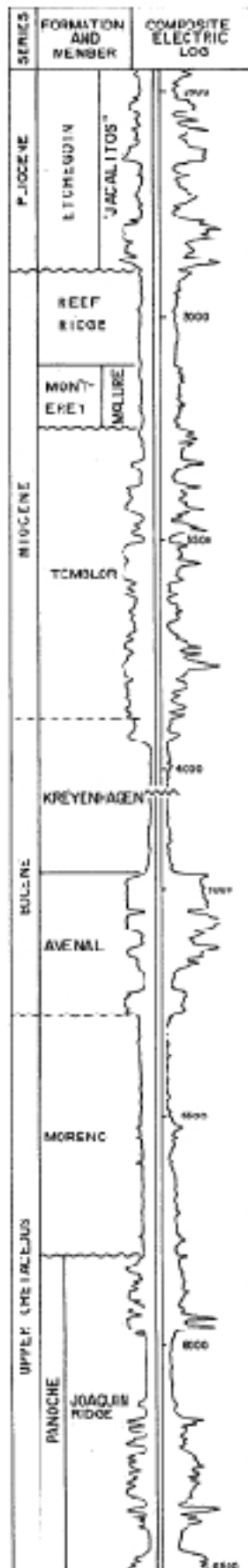
Moreno Formation

Interpreted

Oil sample



JACALITOS OIL FIELD



Oil from source rock

Tumey Formation

Kreyenhagen Fm

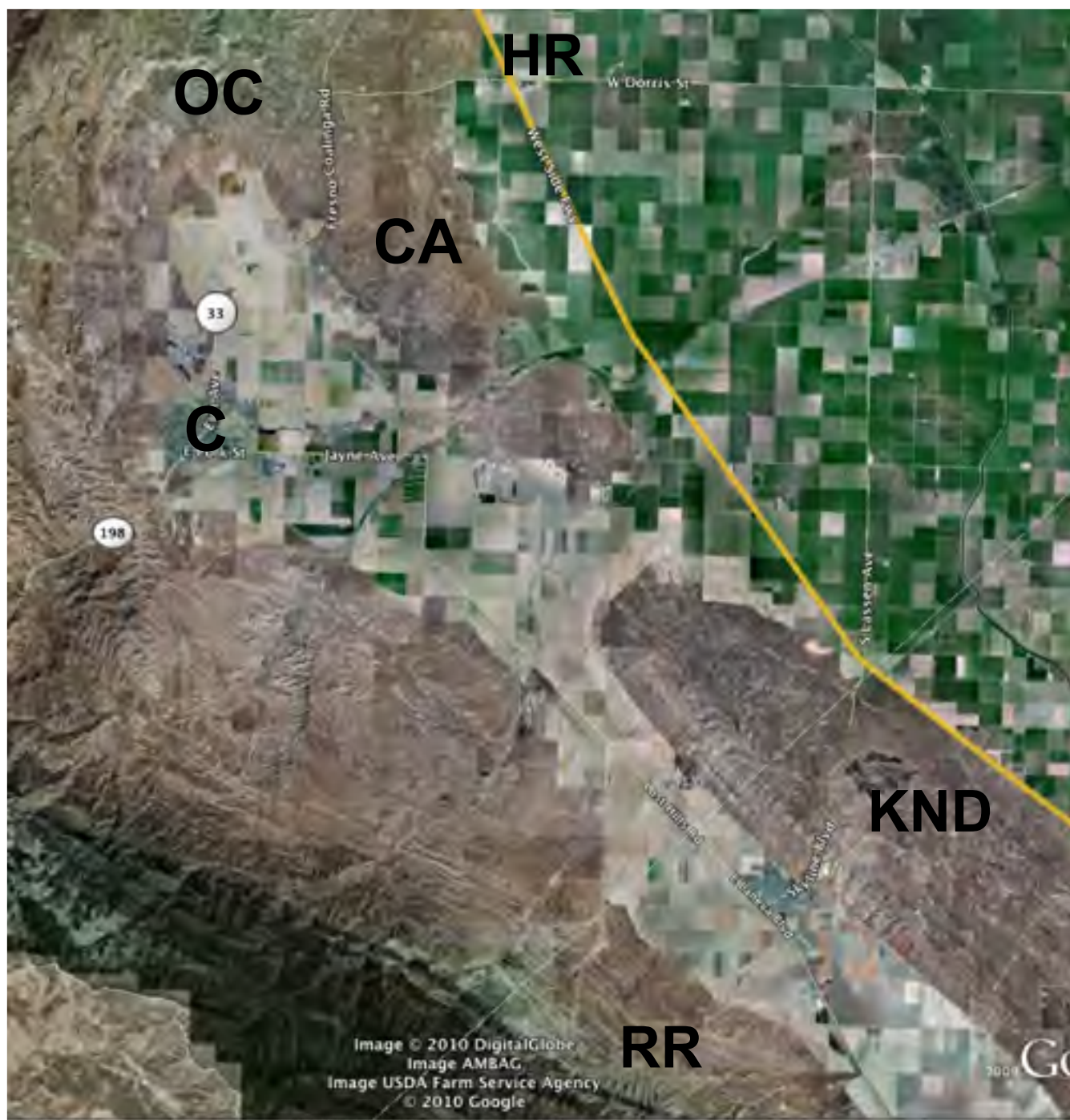
Moreno Formation

Interpreted

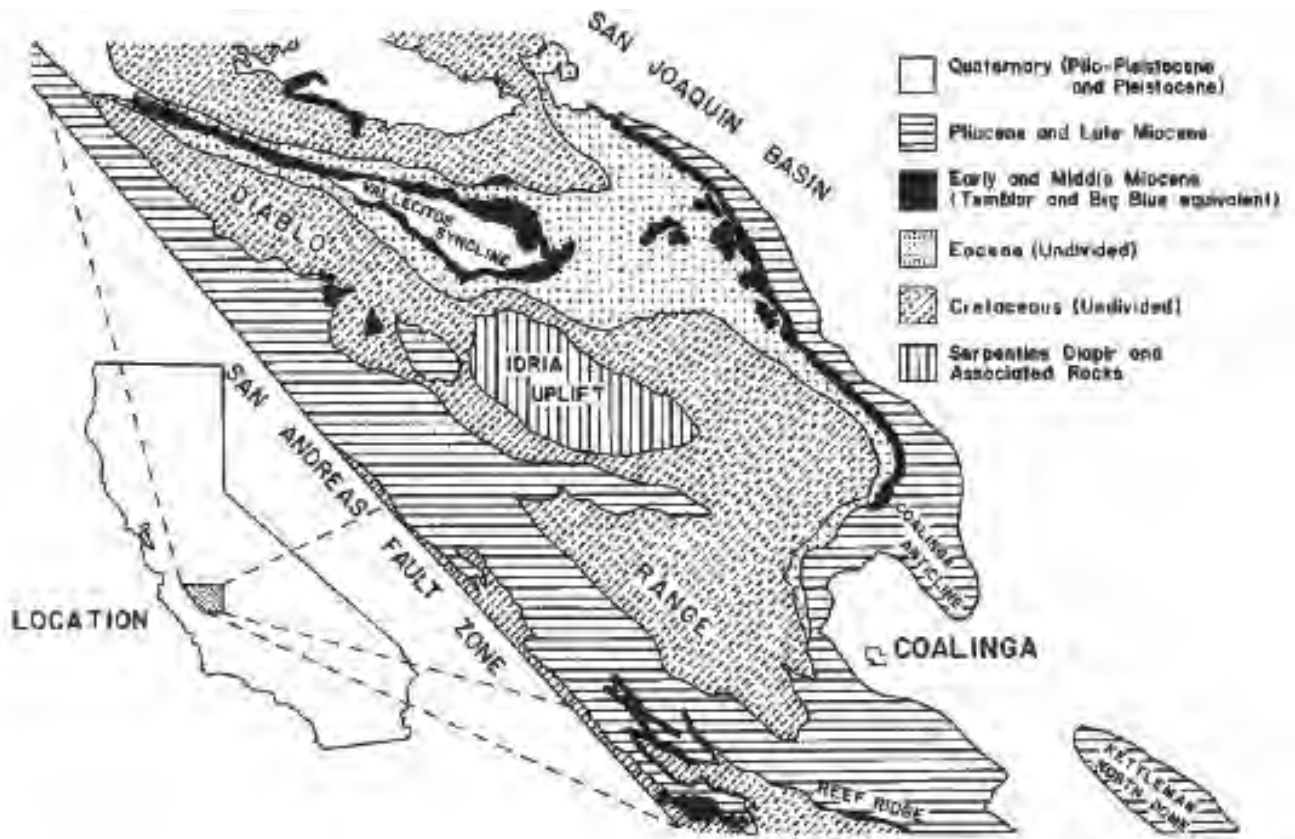
Oil sample



Stop 2: Coalinga Anticline



CA = Coalinga anticline
 OC = Oil Canyon
 KND = Kettleman North Dome
 RR = Reef Ridge
 C = Coalinga
 HR = Harris Ranch



Bate, 1985

ANDERSON AND PACK, 1915		PAYNE, 1941 AND GOUDKOFF, 1945		PAYNE, 1951, 1962		MARTIN, 1964		THIS REPORT				
UPPER CRETACEOUS	PALEOCENE	UPPER CRETACEOUS	PALEOCENE	UPPER CRETACEOUS	UPPER CRETACEOUS	UPPER CRETACEOUS	MAASTRICHTIAN	CRETACEOUS	PALEOCENE	EO.	LOCO FORMATION (AND EQUIVALENTS)	
	MARTINEZ(?) FORMATION		"MARTINEZ"		PAL.				EO.	DAN.		THAN
PANOCHE FORMATION	MORENO FORMATION	UPPER CRETACEOUS	MORENO FORMATION	UPPER CRETACEOUS	MORENO FORMATION	UPPER CRETACEOUS	C	MAASTRICHTIAN	MORENO FORMATION	C	PANOCHE GP.	LOCO FORMATION
PANOCHE FORMATION	MORENO FORMATION	UPPER CRETACEOUS	MORENO FORMATION	UPPER CRETACEOUS	MORENO FORMATION	UPPER CRETACEOUS	C	MAASTRICHTIAN	MORENO FORMATION	C	PANOCHE GP.	LOCO FORMATION
PANOCHE FORMATION	MORENO FORMATION	UPPER CRETACEOUS	MORENO FORMATION	UPPER CRETACEOUS	MORENO FORMATION	UPPER CRETACEOUS	C	MAASTRICHTIAN	MORENO FORMATION	C	PANOCHE GP.	LOCO FORMATION
PANOCHE FORMATION	MORENO FORMATION	UPPER CRETACEOUS	MORENO FORMATION	UPPER CRETACEOUS	MORENO FORMATION	UPPER CRETACEOUS	C	MAASTRICHTIAN	MORENO FORMATION	C	PANOCHE GP.	LOCO FORMATION
PANOCHE FORMATION	MORENO FORMATION	UPPER CRETACEOUS	MORENO FORMATION	UPPER CRETACEOUS	MORENO FORMATION	UPPER CRETACEOUS	C	MAASTRICHTIAN	MORENO FORMATION	C	PANOCHE GP.	LOCO FORMATION
PANOCHE FORMATION	MORENO FORMATION	UPPER CRETACEOUS	MORENO FORMATION	UPPER CRETACEOUS	MORENO FORMATION	UPPER CRETACEOUS	C	MAASTRICHTIAN	MORENO FORMATION	C	PANOCHE GP.	LOCO FORMATION
PANOCHE FORMATION	MORENO FORMATION	UPPER CRETACEOUS	MORENO FORMATION	UPPER CRETACEOUS	MORENO FORMATION	UPPER CRETACEOUS	C	MAASTRICHTIAN	MORENO FORMATION	C	PANOCHE GP.	LOCO FORMATION
PANOCHE FORMATION	MORENO FORMATION	UPPER CRETACEOUS	MORENO FORMATION	UPPER CRETACEOUS	MORENO FORMATION	UPPER CRETACEOUS	C	MAASTRICHTIAN	MORENO FORMATION	C	PANOCHE GP.	LOCO FORMATION
PANOCHE FORMATION	MORENO FORMATION	UPPER CRETACEOUS	MORENO FORMATION	UPPER CRETACEOUS	MORENO FORMATION	UPPER CRETACEOUS	C	MAASTRICHTIAN	MORENO FORMATION	C	PANOCHE GP.	LOCO FORMATION
PANOCHE FORMATION	MORENO FORMATION	UPPER CRETACEOUS	MORENO FORMATION	UPPER CRETACEOUS	MORENO FORMATION	UPPER CRETACEOUS	C	MAASTRICHTIAN	MORENO FORMATION	C	PANOCHE GP.	LOCO FORMATION
PANOCHE FORMATION	MORENO FORMATION	UPPER CRETACEOUS	MORENO FORMATION	UPPER CRETACEOUS	MORENO FORMATION	UPPER CRETACEOUS	C	MAASTRICHTIAN	MORENO FORMATION	C	PANOCHE GP.	LOCO FORMATION
PANOCHE FORMATION	MORENO FORMATION	UPPER CRETACEOUS	MORENO FORMATION	UPPER CRETACEOUS	MORENO FORMATION	UPPER CRETACEOUS	C	MAASTRICHTIAN	MORENO FORMATION	C	PANOCHE GP.	LOCO FORMATION
PANOCHE FORMATION	MORENO FORMATION	UPPER CRETACEOUS	MORENO FORMATION	UPPER CRETACEOUS	MORENO FORMATION	UPPER CRETACEOUS	C	MAASTRICHTIAN	MORENO FORMATION	C	PANOCHE GP.	LOCO FORMATION
PANOCHE FORMATION	MORENO FORMATION	UPPER CRETACEOUS	MORENO FORMATION	UPPER CRETACEOUS	MORENO FORMATION	UPPER CRETACEOUS	C	MAASTRICHTIAN	MORENO FORMATION	C	PANOCHE GP.	LOCO FORMATION
PANOCHE FORMATION	MORENO FORMATION	UPPER CRETACEOUS	MORENO FORMATION	UPPER CRETACEOUS	MORENO FORMATION	UPPER CRETACEOUS	C	MAASTRICHTIAN	MORENO FORMATION	C	PANOCHE GP.	LOCO FORMATION
PANOCHE FORMATION	MORENO FORMATION	UPPER CRETACEOUS	MORENO FORMATION	UPPER CRETACEOUS	MORENO FORMATION	UPPER CRETACEOUS	C	MAASTRICHTIAN	MORENO FORMATION	C	PANOCHE GP.	LOCO FORMATION
PANOCHE FORMATION	MORENO FORMATION	UPPER CRETACEOUS	MORENO FORMATION	UPPER CRETACEOUS	MORENO FORMATION	UPPER CRETACEOUS	C	MAASTRICHTIAN	MORENO FORMATION	C	PANOCHE GP.	LOCO FORMATION
PANOCHE FORMATION	MORENO FORMATION	UPPER CRETACEOUS	MORENO FORMATION	UPPER CRETACEOUS	MORENO FORMATION	UPPER CRETACEOUS	C	MAASTRICHTIAN	MORENO FORMATION	C	PANOCHE GP.	LOCO FORMATION
PANOCHE FORMATION	MORENO FORMATION	UPPER CRETACEOUS	MORENO FORMATION	UPPER CRETACEOUS	MORENO FORMATION	UPPER CRETACEOUS	C	MAASTRICHTIAN	MORENO FORMATION	C	PANOCHE GP.	LOCO FORMATION
PANOCHE FORMATION	MORENO FORMATION	UPPER CRETACEOUS	MORENO FORMATION	UPPER CRETACEOUS	MORENO FORMATION	UPPER CRETACEOUS	C	MAASTRICHTIAN	MORENO FORMATION	C	PANOCHE GP.	LOCO FORMATION
PANOCHE FORMATION	MORENO FORMATION	UPPER CRETACEOUS	MORENO FORMATION	UPPER CRETACEOUS	MORENO FORMATION	UPPER CRETACEOUS	C	MAASTRICHTIAN	MORENO FORMATION	C	PANOCHE GP.	LOCO FORMATION
PANOCHE FORMATION	MORENO FORMATION	UPPER CRETACEOUS	MORENO FORMATION	UPPER CRETACEOUS	MORENO FORMATION	UPPER CRETACEOUS	C	MAASTRICHTIAN	MORENO FORMATION	C	PANOCHE GP.	LOCO FORMATION
PANOCHE FORMATION	MORENO FORMATION	UPPER CRETACEOUS	MORENO FORMATION	UPPER CRETACEOUS	MORENO FORMATION	UPPER CRETACEOUS	C	MAASTRICHTIAN	MORENO FORMATION	C	PANOCHE GP.	LOCO FORMATION
PANOCHE FORMATION	MORENO FORMATION	UPPER CRETACEOUS	MORENO FORMATION	UPPER CRETACEOUS	MORENO FORMATION	UPPER CRETACEOUS	C	MAASTRICHTIAN	MORENO FORMATION	C	PANOCHE GP.	LOCO FORMATION
PANOCHE FORMATION	MORENO FORMATION	UPPER CRETACEOUS	MORENO FORMATION	UPPER CRETACEOUS	MORENO FORMATION	UPPER CRETACEOUS	C	MAASTRICHTIAN	MORENO FORMATION	C	PANOCHE GP.	LOCO FORMATION
PANOCHE FORMATION	MORENO FORMATION	UPPER CRETACEOUS	MORENO FORMATION	UPPER CRETACEOUS	MORENO FORMATION	UPPER CRETACEOUS	C	MAASTRICHTIAN	MORENO FORMATION	C	PANOCHE GP.	LOCO FORMATION
PANOCHE FORMATION	MORENO FORMATION	UPPER CRETACEOUS	MORENO FORMATION	UPPER CRETACEOUS	MORENO FORMATION	UPPER CRETACEOUS	C	MAASTRICHTIAN	MORENO FORMATION	C	PANOCHE GP.	LOCO FORMATION
PANOCHE FORMATION	MORENO FORMATION	UPPER CRETACEOUS	MORENO FORMATION	UPPER CRETACEOUS	MORENO FORMATION	UPPER CRETACEOUS	C	MAASTRICHTIAN	MORENO FORMATION	C	PANOCHE GP.	LOCO FORMATION
PANOCHE FORMATION	MORENO FORMATION	UPPER CRETACEOUS	MORENO FORMATION	UPPER CRETACEOUS	MORENO FORMATION	UPPER CRETACEOUS	C	MAASTRICHTIAN	MORENO FORMATION	C	PANOCHE GP.	LOCO FORMATION
PANOCHE FORMATION	MORENO FORMATION	UPPER CRETACEOUS	MORENO FORMATION	UPPER CRETACEOUS	MORENO FORMATION	UPPER CRETACEOUS	C	MAASTRICHTIAN	MORENO FORMATION	C	PANOCHE GP.	LOCO FORMATION
PANOCHE FORMATION	MORENO FORMATION	UPPER CRETACEOUS	MORENO FORMATION	UPPER CRETACEOUS	MORENO FORMATION	UPPER CRETACEOUS	C	MAASTRICHTIAN	MORENO FORMATION	C	PANOCHE GP.	LOCO FORMATION
PANOCHE FORMATION	MORENO FORMATION	UPPER CRETACEOUS	MORENO FORMATION	UPPER CRETACEOUS	MORENO FORMATION	UPPER CRETACEOUS	C	MAASTRICHTIAN	MORENO FORMATION	C	PANOCHE GP.	LOCO FORMATION
PANOCHE FORMATION	MORENO FORMATION	UPPER CRETACEOUS	MORENO FORMATION	UPPER CRETACEOUS	MORENO FORMATION	UPPER CRETACEOUS	C	MAASTRICHTIAN	MORENO FORMATION	C	PANOCHE GP.	LOCO FORMATION
PANOCHE FORMATION	MORENO FORMATION	UPPER CRETACEOUS	MORENO FORMATION	UPPER CRETACEOUS	MORENO FORMATION	UPPER CRETACEOUS	C	MAASTRICHTIAN	MORENO FORMATION	C	PANOCHE GP.	LOCO FORMATION
PANOCHE FORMATION	MORENO FORMATION	UPPER CRETACEOUS	MORENO FORMATION	UPPER CRETACEOUS	MORENO FORMATION	UPPER CRETACEOUS	C	MAASTRICHTIAN	MORENO FORMATION	C	PANOCHE GP.	LOCO FORMATION
PANOCHE FORMATION	MORENO FORMATION	UPPER CRETACEOUS	MORENO FORMATION	UPPER CRETACEOUS	MORENO FORMATION	UPPER CRETACEOUS	C	MAASTRICHTIAN	MORENO FORMATION	C	PANOCHE GP.	LOCO FORMATION
PANOCHE FORMATION	MORENO FORMATION	UPPER CRETACEOUS	MORENO FORMATION	UPPER CRETACEOUS	MORENO FORMATION	UPPER CRETACEOUS	C	MAASTRICHTIAN	MORENO FORMATION	C	PANOCHE GP.	LOCO FORMATION
PANOCHE FORMATION	MORENO FORMATION	UPPER CRETACEOUS	MORENO FORMATION	UPPER CRETACEOUS	MORENO FORMATION	UPPER CRETACEOUS	C	MAASTRICHTIAN	MORENO FORMATION	C	PANOCHE GP.	LOCO FORMATION
PANOCHE FORMATION	MORENO FORMATION	UPPER CRETACEOUS	MORENO FORMATION	UPPER CRETACEOUS	MORENO FORMATION	UPPER CRETACEOUS	C	MAASTRICHTIAN	MORENO FORMATION	C	PANOCHE GP.	LOCO FORMATION
PANOCHE FORMATION	MORENO FORMATION	UPPER CRETACEOUS	MORENO FORMATION	UPPER CRETACEOUS	MORENO FORMATION	UPPER CRETACEOUS	C	MAASTRICHTIAN	MORENO FORMATION	C	PANOCHE GP.	LOCO FORMATION
PANOCHE FORMATION	MORENO FORMATION	UPPER CRETACEOUS	MORENO FORMATION	UPPER CRETACEOUS	MORENO FORMATION	UPPER CRETACEOUS	C	MAASTRICHTIAN	MORENO FORMATION	C	PANOCHE GP.	LOCO FORMATION
PANOCHE FORMATION	MORENO FORMATION	UPPER CRETACEOUS	MORENO FORMATION	UPPER CRETACEOUS	MORENO FORMATION	UPPER CRETACEOUS	C	MAASTRICHTIAN	MORENO FORMATION	C	PANOCHE GP.	LOCO FORMATION
PANOCHE FORMATION	MORENO FORMATION	UPPER CRETACEOUS	MORENO FORMATION	UPPER CRETACEOUS	MORENO FORMATION	UPPER CRETACEOUS	C	MAASTRICHTIAN	MORENO FORMATION	C	PANOCHE GP.	LOCO FORMATION
PANOCHE FORMATION	MORENO FORMATION	UPPER CRETACEOUS	MORENO FORMATION	UPPER CRETACEOUS	MORENO FORMATION	UPPER CRETACEOUS	C	MAASTRICHTIAN	MORENO FORMATION	C	PANOCHE GP.	LOCO FORMATION
PANOCHE FORMATION	MORENO FORMATION	UPPER CRETACEOUS	MORENO FORMATION	UPPER CRETACEOUS	MORENO FORMATION	UPPER CRETACEOUS	C	MAASTRICHTIAN	MORENO FORMATION	C	PANOCHE GP.	LOCO FORMATION
PANOCHE FORMATION	MORENO FORMATION	UPPER CRETACEOUS	MORENO FORMATION	UPPER CRETACEOUS	MORENO FORMATION	UPPER CRETACEOUS	C	MAASTRICHTIAN	MORENO FORMATION	C	PANOCHE GP.	LOCO FORMATION
PANOCHE FORMATION	MORENO FORMATION	UPPER CRETACEOUS	MORENO FORMATION	UPPER CRETACEOUS	MORENO FORMATION	UPPER CRETACEOUS	C	MAASTRICHTIAN	MORENO FORMATION	C	PANOCHE GP.	LOCO FORMATION
PANOCHE FORMATION	MORENO FORMATION	UPPER CRETACEOUS	MORENO FORMATION	UPPER CRETACEOUS	MORENO FORMATION	UPPER CRETACEOUS	C	MAASTRICHTIAN	MORENO FORMATION	C	PANOCHE GP.	LOCO FORMATION
PANOCHE FORMATION												

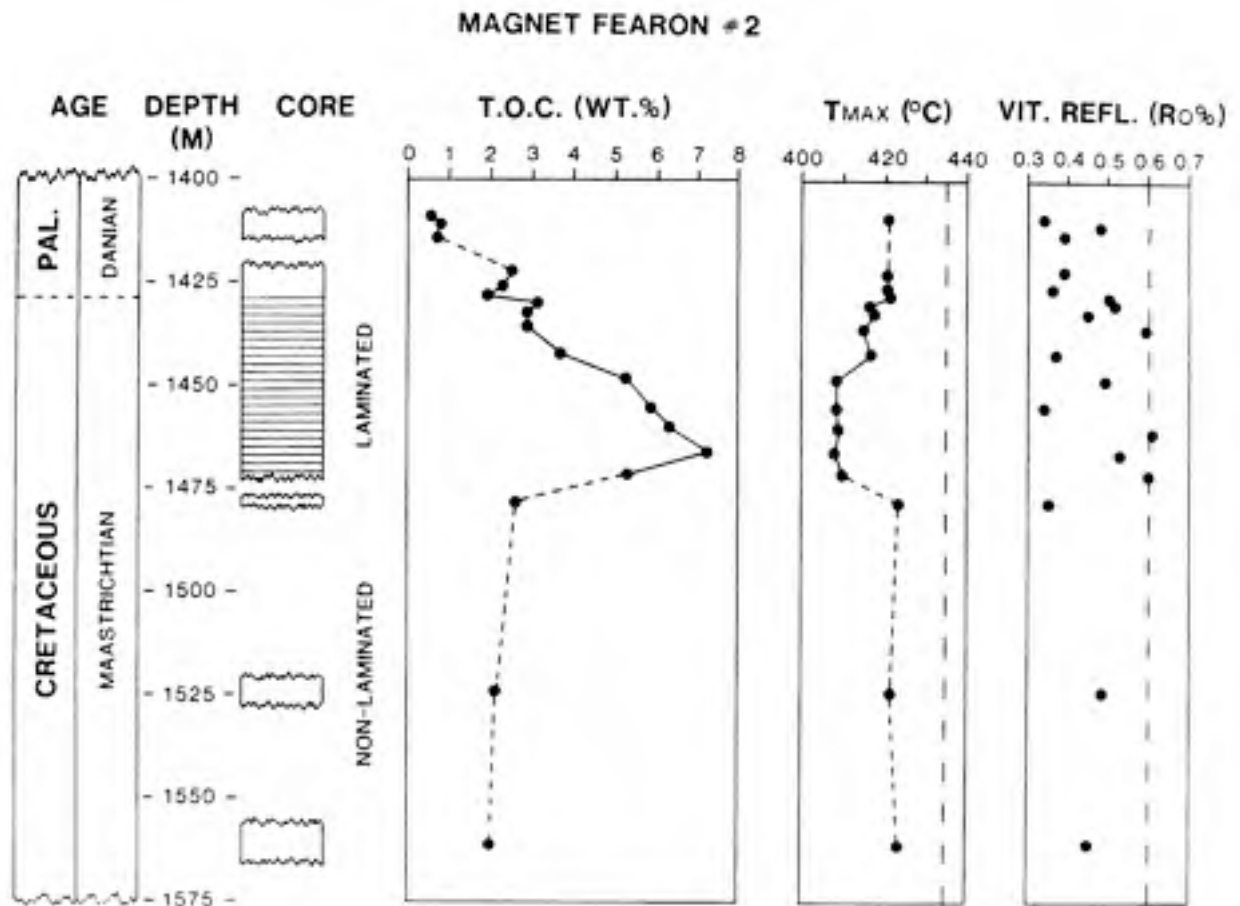


Figure 42. Core coverage and age correlation for the Moreno Formation section penetrated by the Magnet Fearon #2 well, with TOC, Rock-Eval T_{max} , and vitrinite reflectance data from analyses of core samples. The dashed lines in the T_{max} and vitrinite reflectance plots are generally-accepted values corresponding to the onset of oil generation in rocks containing conventional Type II kerogens.

McGuire, 1988

Moreno Fm. Silica Diagenesis and Organic Quality

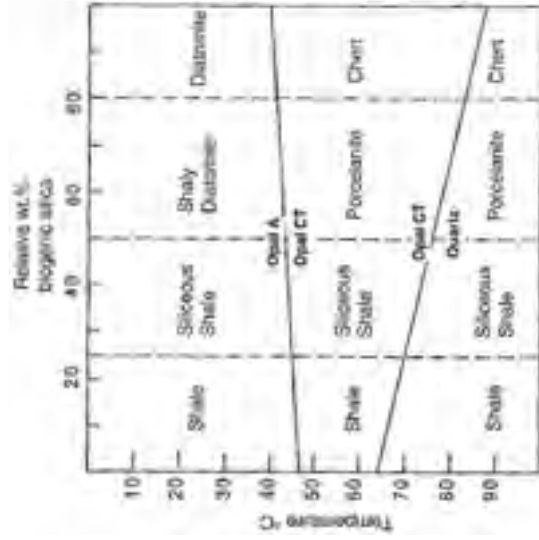


Figure 8—Diagram illustrating silica diagenesis as it relates Monterey siliceous rock types to percent biogenic silica and thermal history (Isaacs, 1982; Behl and Garrison, 1998; A. Carpenter, 1996, personal communication).

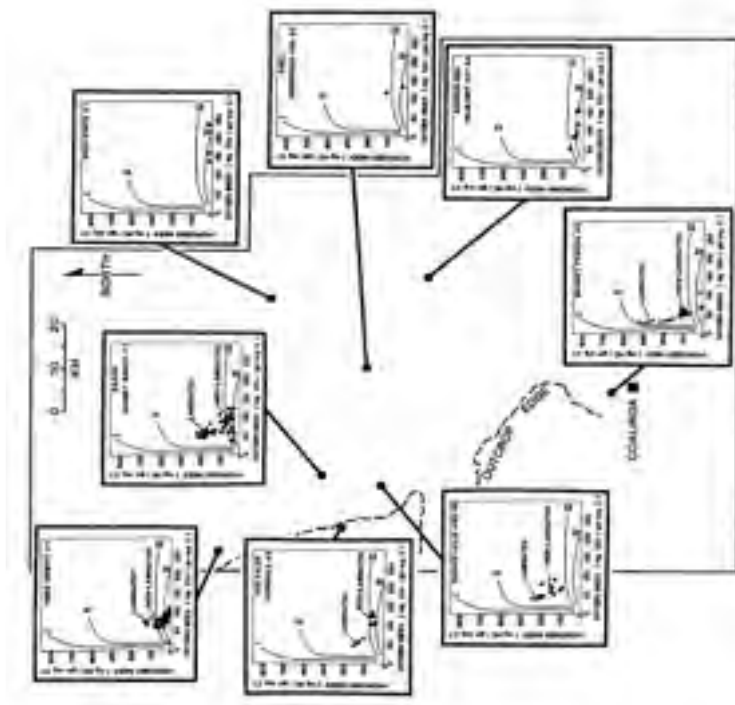
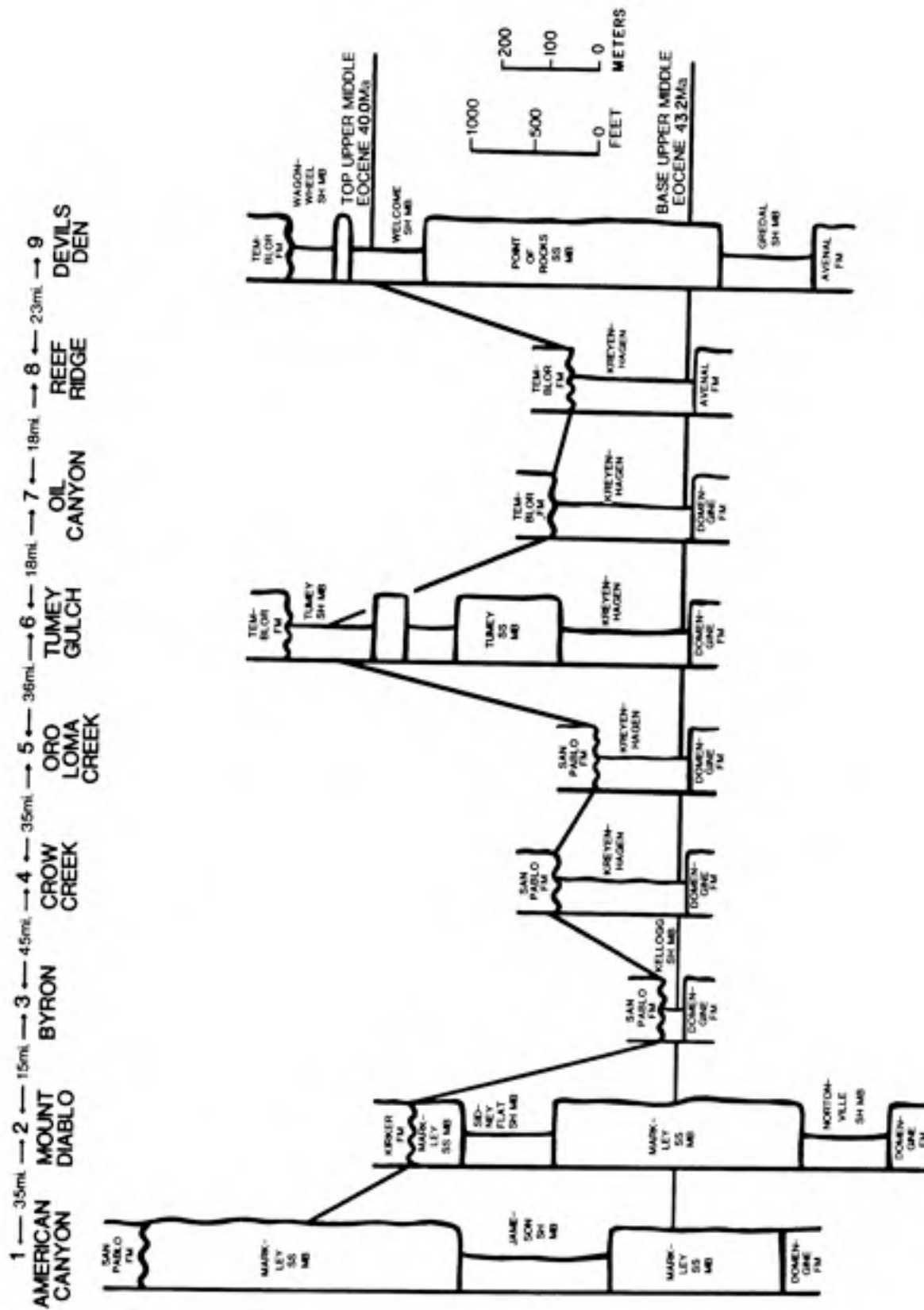


Figure 50. Rock-Eval pyrolysis data for Moreno Formation core samples from right wells in the central San Joaquin basin, plotted on modified van Krevelen diagrams. The positions of the wells within the basin are shown on the same basin map as Figure 25-30 (Chapter 2). The data point out the presence of laminated sediments containing relatively hydrogen-rich organic matter in the western portions of the study area, whereas the eastern portions of the area are characterized by non-laminated sediments containing only lightly oxidized organic matter.

McGuire, 1988



R. Milam, Stanford PhD

EXXON CHENEY RANCH NO. 1
section 29, T14S, R13E

sample	Tmax	S1	S2	S3	PI	S2/S3	PC	TOC	HI	OI
3521	389	1.22	3.09	2.55	0.28	1.21	0.35	2.24	137	113
3576	414	0.91	7.86	3.15	0.1	2.49	0.73	2.91	270	108
3624	409	0.72	3.38	2.07	0.18	1.63	0.34	1.69	200	122
3723	421	0.76	5.67	2.32	0.12	2.44	0.53	2.07	273	112
3826	423	0.82	7.73	2.54	0.1	3.04	0.71	2.5	309	101
4068	407	0.81	7.18	3.89	0.1	1.84	0.66	3.3	217	117
4278	410	0.78	10.46	3.56	0.07	2.93	0.93	3.88	269	91
4316	413	0.53	9.97	4.09	0.05	2.43	0.87	3.15	318	129
4387	423	0.23	2.4	2.02	0.09	1.18	0.21	1.55	154	130
4413	422	0.41	7.71	1.9	0.05	4.05	0.67	2.34	329	81

CHEVRON JACALITOS NO. 67
section 17, T21S, R15E

sample	Tmax	S1	S2	S3	PI	S2/S3	PC	TOC	HI	OI
3995	410	0.33	1.99	1.08	0.14	1.84	0.19	1.29	154	83
4013	421	0.58	7.73	1.48	0.07	5.22	0.69	2.23	346	66
4031	412	0.29	1.69	1.14	0.15	1.48	0.16	1.35	125	84
4549	414	0.85	25.89	4.98	0.03	5.19	2.22	5.49	471	90
4594	414	0.98	27.87	3.52	0.03	7.91	2.4	5.44	512	64
4610	412	0.43	11.98	3.32	0.03	3.6	1.03	3.48	344	95
4646	415	0.89	20.16	2.92	0.04	6.9	1.75	3.84	525	76
4705	419	0.69	12.34	2.47	0.05	4.99	1.08	3.28	376	75
4748	429	0.37	3.29	1.18	0.1	2.78	0.3	1.46	225	80
4785	416	0.08	0.25	0.45	0.25	0.55	0.02	0.25	100	180

MOBIL WILLIAMSON NO. 33
section T26S, R20E

sample	Tmax	S1	S2	S3	PI	S2/S3	PC	TOC	HI	OI
8325	432	1.4	14.25	0.74	0.03	19.25	1.3	2.65	537	27
8612	430	1.71	24.99	1.52	0.06	16.44	2.22	4.98	501	30
8997	434	0.81	9.24	0.71	0.08	13.01	0.83	2.09	442	33
9017	437	0.59	2.39	0.59	0.2	4.05	0.24	1.03	232	57
9057	435	0.76	6.54	0.84	0.1	7.78	0.6	1.74	375	48
9077	437	1.46	7.7	0.76	0.16	10.13	0.76	1.96	392	38
9195	432	0.22	1.85	1.04	0.11	1.77	0.17	1.57	117	66
9537	437	0.34	2.2	0.54	0.13	4.07	0.21	1.04	211	51
9540	435	0.55	8.61	0.73	0.06	11.79	0.76	2.2	391	33
9646	440	0.23	2.59	0.62	0.08	4.17	0.23	1.03	251	60

R. Milam, Stanford PhD

Kreyenhagen Fm. Silica Diagenesis and Organic Quality

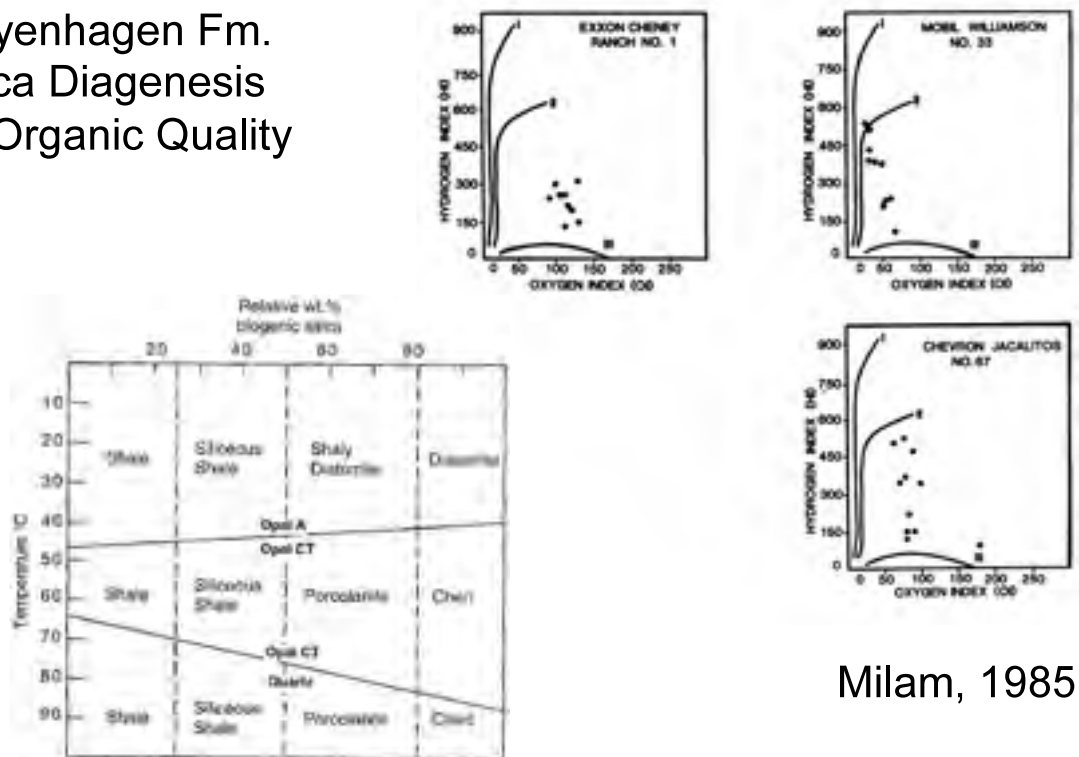


Figure 8—Diagram illustrating silica diagenesis as it relates Monterey siliceous rock types to percent biogenic silica and thermal history (Isaacs, 1982; Behl and Garrison, 1994; A. Carpenter, 1996, personal communication).

Milam, 1985

A

KREYENHAGEN
FIELD

KETTLEMAN
NORTH DOME
FIELD

TULARE LAKE
FIELD

GETTY OIL CO.
KREYENHAGEN 14
SEC. 24, T2S-16E

McGILLIOW OIL CO.
STANDARD 1
SEC. 21, T2S-16E

AMBA
034
W. 21, T2S-16E

TIGER OIL CO.
KREYENHAGEN
SEC. 21, T2S-16E

GRANT BAKING OIL CO.
JAN-2
SEC. 21, T2S-16E

AMERICAN PACIFIC OIL
UNIVERSITY WESTLAKE 1
SEC. 21, T2S-16E

SALPER LAND CO. HILLARD-SUMNER
JAN-2
SEC. 17, T2S-16E

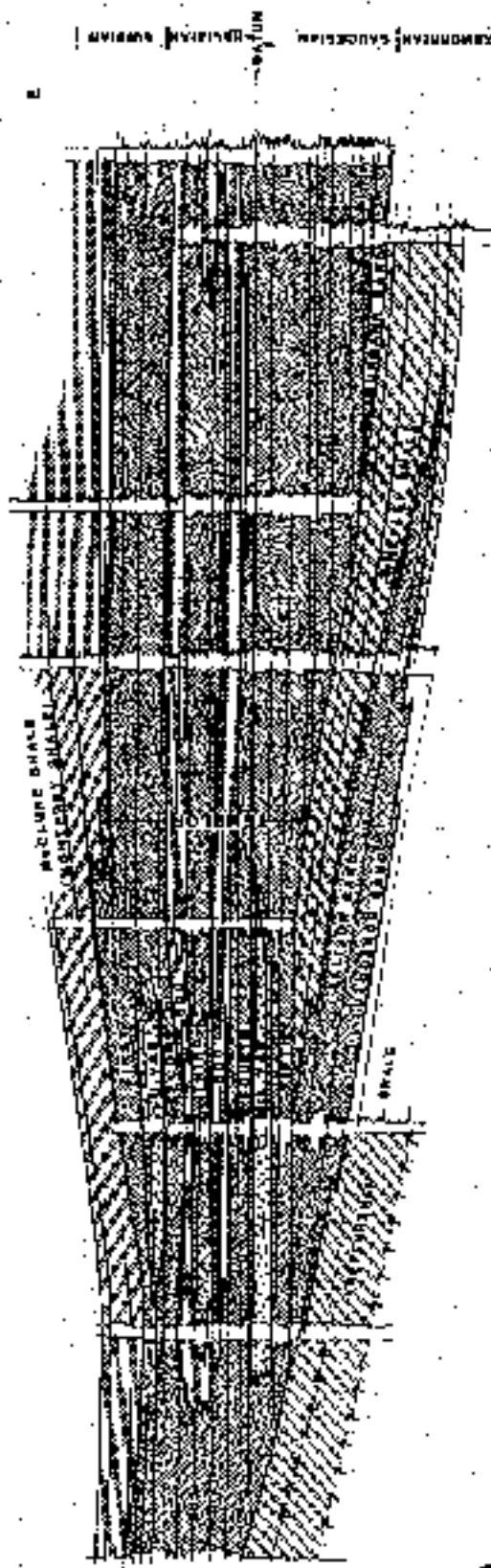
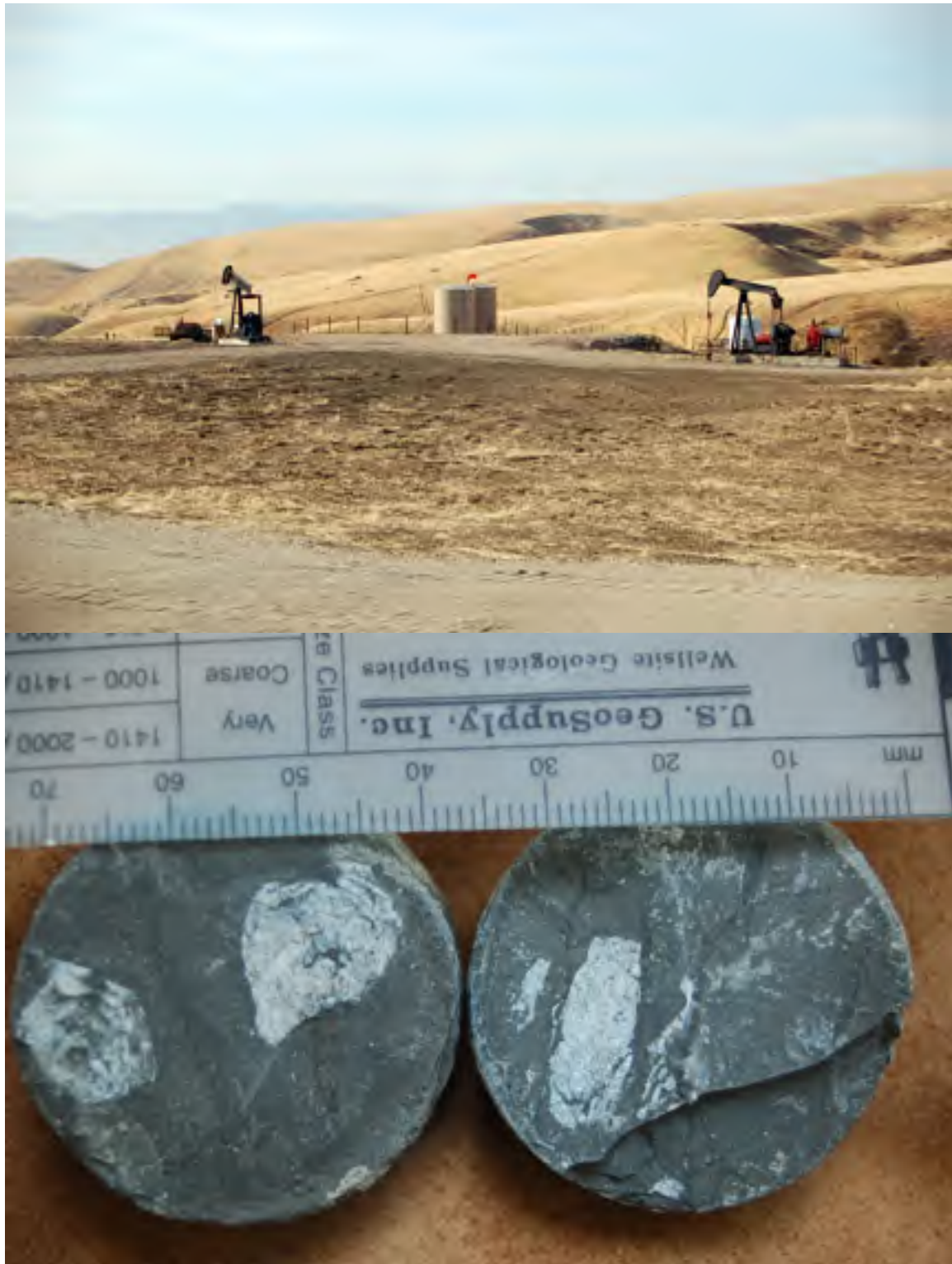


Figure 10. Stratigraphic section A-A' from Kreyenhagen to Tulare Lake Fields. The line of the section is included on the base map (Figure 1). The stratigraphic datum is the top of the Kettleman North Dome Field "Q" Point in well 314-28J. The regional Kreyenhagen-Saucasian erosional hiatus is evident as well as some of the environmental relationships along the west side of the study area. Most of the maps and interpretations in this article are based upon similar sections by Kuespert [1981].

**Stop 3, 4, and 5 in Oil
Canyon:
Moreno, Kreyenhagen and
Temblor Formations,
and
Temblor Brea Deposit**



CA = Coalinga anticline
OC = Oil Canyon
KF = Kreyenhagen Fm.
CF = Coalinga field



Top: Pump-jacks at re-vitalized Oil City field spudding in Moreno Fm.
Bottom: Thin-shelled low-oxygen molluscs, Moreno Fm.



Top: Syn-form in fractured Kreyenhagen Fm. with oil at road level, Oil Canyon
Bottom: Kreyenhagen Fm. shale with oil lining bedding planes and fractures, Oil Canyon.



Top: Sandstone injectite cutting Kreyenhagen Fm., ca 100 m east of Oil Canyon.
Bottom: Oil-saturated Lower Variegated Mbr., Temblor Fm., just east of Oil Canyon.



Top: Disharmonious deformation of Temblor Fm. sandstone (left) and Kreyenhagen Fm. mudstone (left) along Oil Canyon viewed to the west.
Bottom: Brea near Oil Canyon, Coalinga Anticline.

**Stop 6 on
Coalinga anticline:
Temblor Formation on
Cartwheel Ridge**

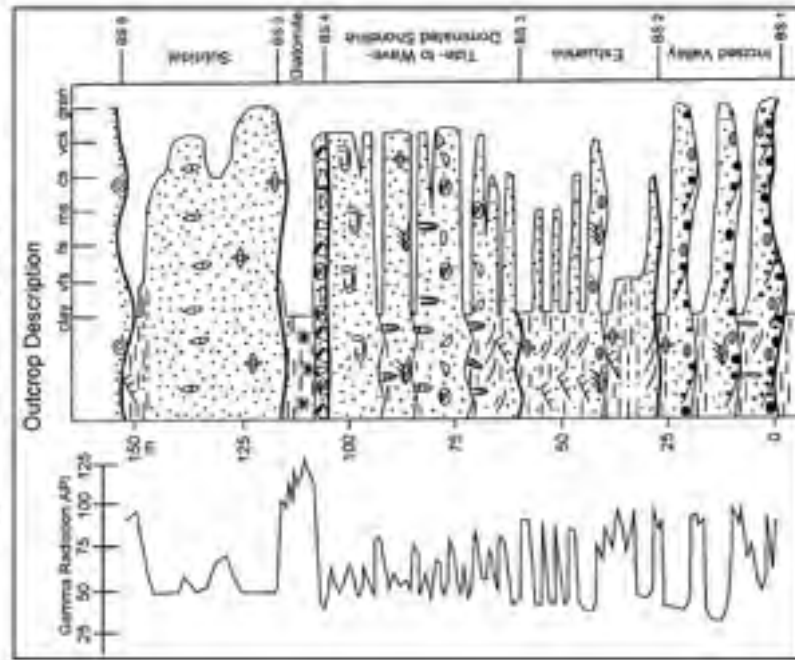
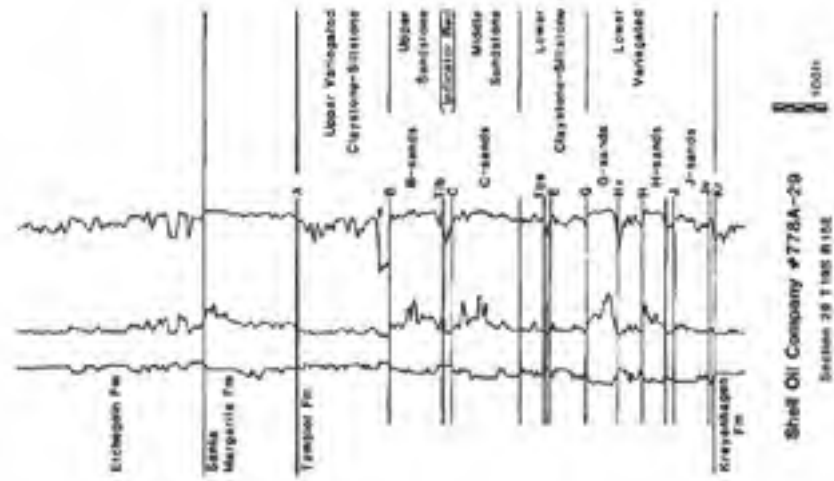


Fig. 5. Lithology description for Carradine Ridge. (a) Lithology (see Fig. 2 for location; Fig. 8 for legend). The Carradine Ridge is present below 6 m and the Salsburg Formation occurs above 157 m. v/s=very fine sand, fs=fine sand, ms=medium sand, cs=coarse sand, vcs=very coarse sand, grn=gravel, 85.1=bedding surface.



Shell Oil Company #778A-29
Section 29 T 18S R 10E
100m

Bate, 1985

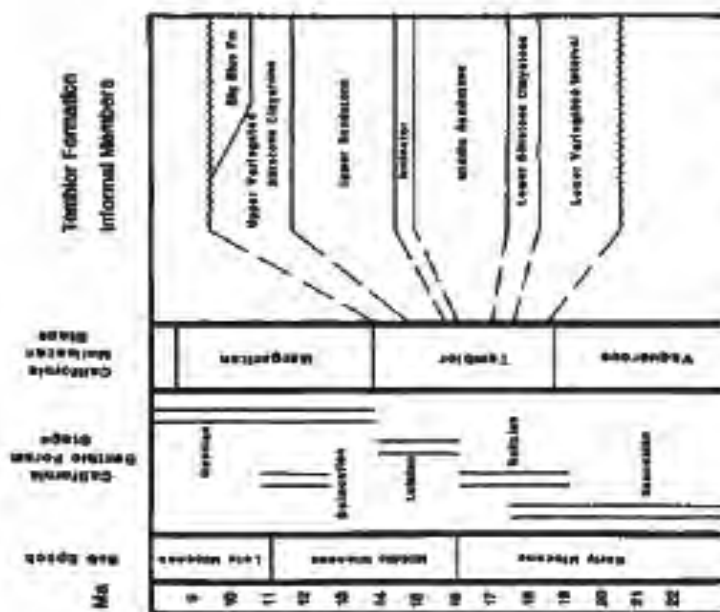


Figure 2. Informal members of the Temblor Formation on Coalinga anticline, and stratigraphic position of the Big Blue Formation, with biochronology of Poore and others (1981).

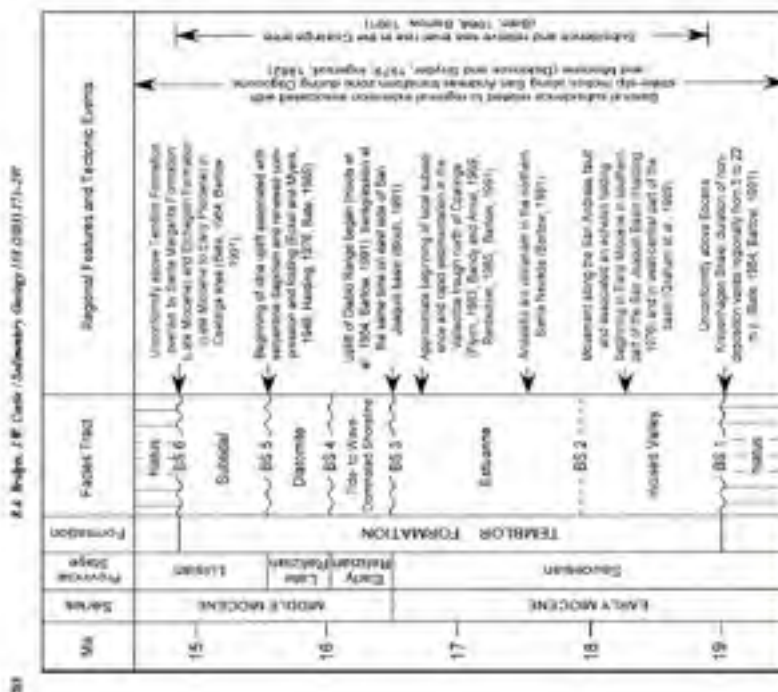
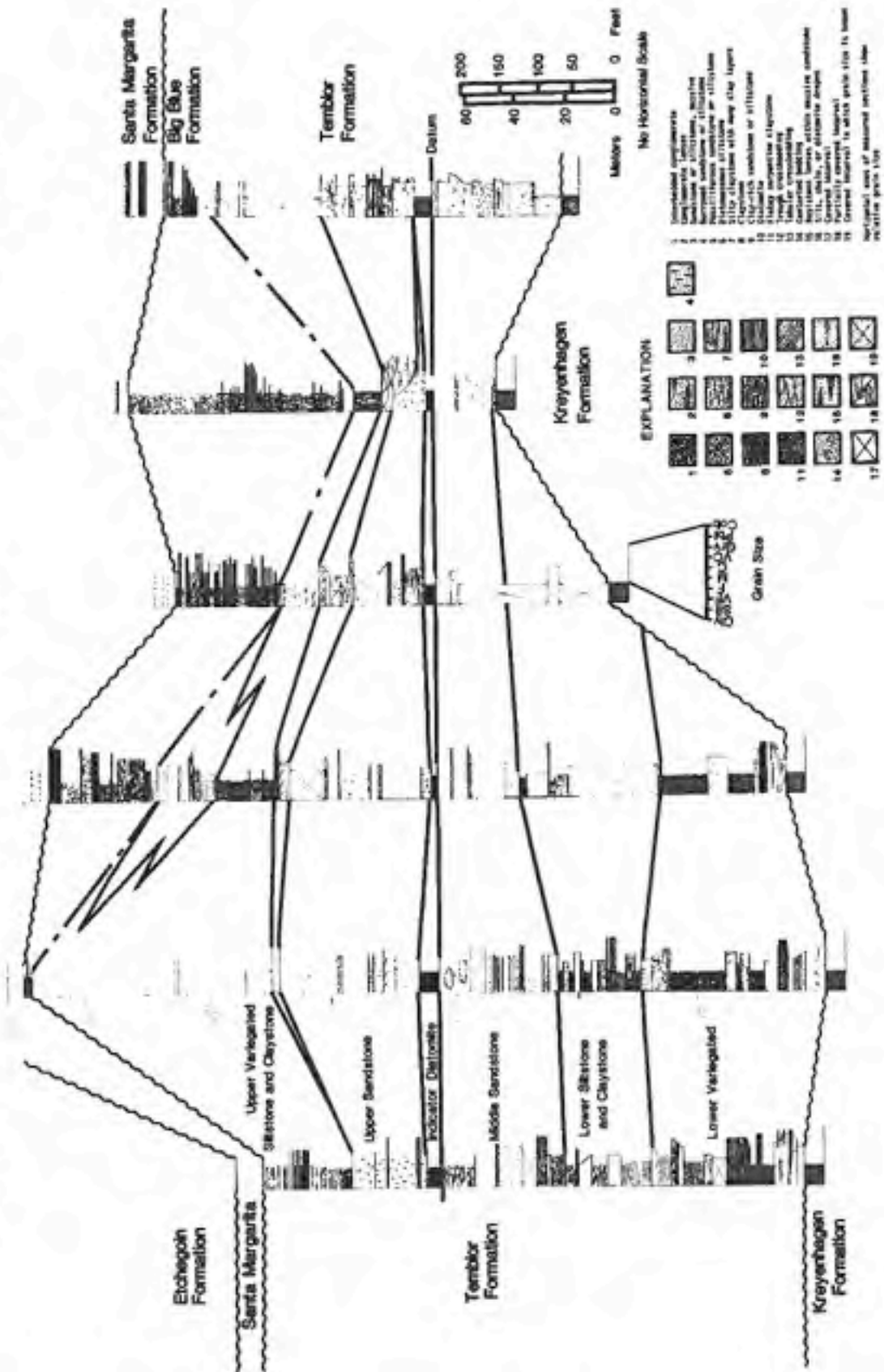


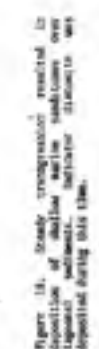
Fig. 18. Correlation of Temblor Formation facies tracts and bounding surfaces related to regional tectonic and sedimentary events. Provided figure was from Klomparens (1981) and Burrell (1981). BS = bounding surface.

S CARTWHEEL HILL 2021 SKUNK NORTH DOMENGINE DOMENGINE N
RIDGE FIELD CREEK RANCH





Top: Lower Variegated Mbr, Temblor Fm. disconformably overlying Kreyenhagen Fm.
Bottom: Oyster reef in estuarine facies of the middle Temblor Fm., Cartwheel Ridge.



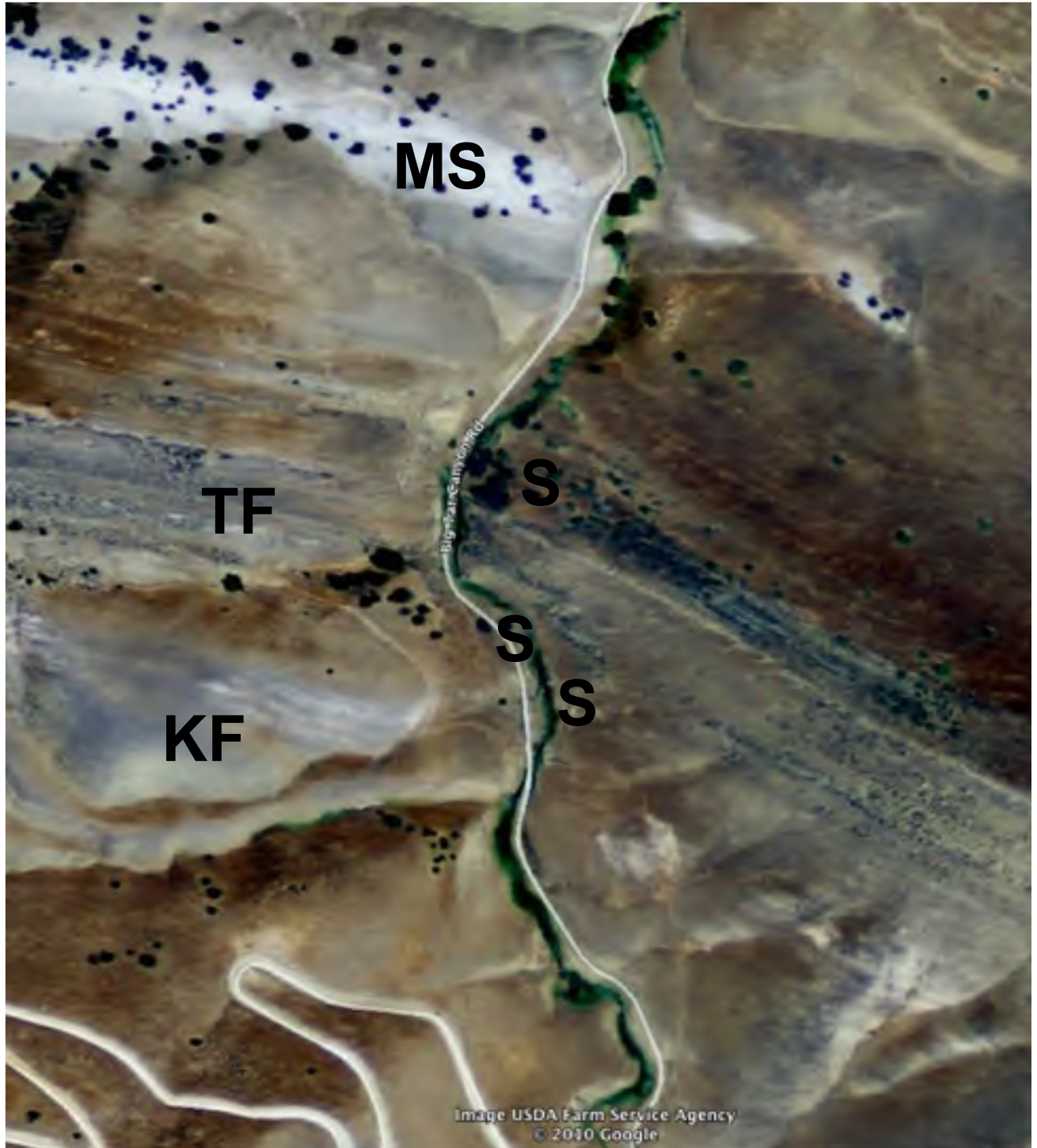
Stop 8 in Big Tar Canyon

**McLure Shale Member,
Temblor and
Kreyenhagen Formations
with active oil seep**

**Reef Ridge:
Temblor Formation and
McLure Shale**



BTC = Big Tar Canyon (road) EF = Etchegoin Formation
MS = McLure Shale Member of Monterey Fm. TF = Temblor Formation
KF = Kreyenhagen Formation



BTC = Big Tar Canyon EF = Etchegoin Formation
 MS = McLure Shale Member of Monterey Fm. TF = Temblor Formation
 KF = Kreyenhagen Formation



Active seep of Kreyenhagen-sourced oil near the top of the Kreyenhagen Fm. along Big Tar Canyon Road. Kreyenhagen is thermally immature at this location.



Top: Ridge-forming Temblor Fm. (left), overlain by gray McLure Shale Member of Monterey Fm. (center) and low hills of Etchegoin Fm. Shot from Reef Ridge. Avenal in distance.

Bottom: Ridge of Temblor Fm. (right), grassy Kreyenhagen Fm. (center), Domengine Fm. (left).



Top: *Turritella coquina* of a 'reef' bed exposed on Reef Ridge north of Big Tar Canyon.
 Bottom: View south from Big Tar Canyon to McLure McLure Shale Member of Monterey Fm.



McLure Shale Member of Monterey Fm. exposed along Big Tar Canyon Road. Section includes mudstone and porcelanite, the latter occurring as the prominently outcropping bundles of beds.

Oil tanks 1.2 mi. down Big Tar Canyon Road.

The oil tanks on the left are part of the Union Oil Tar Canyon Pump Station which services a pipeline running roughly northwest-southeast across Kettleman Plain.

Cattleguard and manmade concrete dip in road 1 mi. further at foot of Kreyenhagen Hills.

This is the approximate location of the unconformable contact between the Quaternary valley fill and the underlying 3000 feet of nonmarine sandstones, siltstones and conglomerates known as the Plio-Pleistocene Tulare Formation. Tulare Formation conglomerates hold up the first low hills.

Old water tank on right side of road 0.7 mi. past cattleguard and concrete dip.

Just beyond this is the approximate position of the conformable contact between the Tulare Formation and the underlying upper Pliocene San Joaquin Formation. The San Joaquin Formation consists of about 2200 feet of soft, sparsely fossiliferous siltstones and clay shales deposited under marine, brackish and lacustrine conditions. Thin and discontinuous bearing beds in the upper part of the formation mark some of the brackish water phases (Adgeoke, 1969). A 50 foot thick pebble conglomerate/pebbly sandstone interval (the Sascayo Conglomerate Member of Adgeoke, 1969) marks the base of the San Joaquin formation.

Sign on right 0.4 mi. further: "Jerry Sagasser ranch headquarters, 4 miles".

The dirt road branching off to the right from here leads to the Jerry Sagasser Ranch. Two excellent exposures of the Tumbler Formation occur on this property, in Baby King Creek and Garza Creek canyons.

0.3 miles past J. Sagasser ranch road - Big Tar Canyon Road makes a sharp jog to the right and then to the left. Road enters small alluviated flat.

This is the approximate location of the conformable contact between the San Joaquin Formation and the underlying Blue Sandstone Member of the lower to middle Pliocene Etchegoin Formation. The 1700 foot thick Blue Sandstone Member takes its name from the lenticular masses of coarse-grained, cross-bedded, blue sandstone, up to 500 feet thick, which are interbedded with the semifriable sandstones, siltstones, claystones, and minor conglomerates characteristic of the marine Etchegoin Formation.

Near end of flat 0.9 mi. further on, road makes a gradual turn to the right, passes an intersection with another paved road and then crosses Big Tar Creek for the first time.

This marks the approximate location of the contact between the Blue Sandstone Member and Basal Brown Member of the Etchegoin Formation. The 3500 foot thick Basal Brown Member contains less sandstone and more claystone and siltstone than the Blue Sandstone Member.



Figure 2-5. Map showing Reef Ridge stops 2-2 through 2-7 of the field trip.

Continue 0.5 mi. Just past the remains of an abandoned ranch road (right side of road).

This is the approximate position of the conformable contact between the Basal Brown Member of the Etchegoin formation and the underlying Reef Ridge Shale of the Monterey Formation.

We will now drive 0.7 mi. through the section to the base of the Tumbler Formation. We will be examining the Tumbler Formation and Monterey Formation exposed here for the duration of the trip (Fig. 2-5).



Figure 2-6. Kreyenhagen Formation (Miocene)/Tumbler Formation (Miocene) unconformable contact in Big Tar Canyon.

STOP 2-2. KREYENHAGEN FM./TEMBLER FM. CONTACT

In the ditch on the north side of the road is an active oil seep, one of many in Big Tar Canyon (there is another in the creek bottom across the road). This seep produces 10 gallons of fluid (25% oil) per day (Hodgson, 1930). It is also home to the sorely mistreated Petroleum Fly (*Petrolia petraea*), whose larvae inhabit the petroliferous nether reaches of a dark and dangerous seep micro-world where sticks and sampling apparatuses of the maliciously curious strike with little warning.

The oil fly's much-maligned home lies near the base of the Tumbler Formation. Follow the abandoned road just above the seep for about 50 yards to the roadcut exposure of the Miocene/Eocene unconformity.

The brittle brown-to-purplish-grey siliceous sandstones in the left half of the outcrop (Fig. 2-6) represent the Eocene Kreyenhagen Formation. The lower Tertiary sequence in Big Tar Canyon is made up of the upper Eocene Kreyenhagen Formation and the underlying middle Eocene Avenal Sandstone. The Kreyenhagen Formation consists of 950-1250 feet of siliceous shales which were deposited in marine waters of bathyal depths (Bobbie, 1973). The Avenal Sandstone, which we will not see here, consists of 300-500 feet of fossiliferous shallow-marine sandstone. It conformably underlies the Kreyenhagen Shale and unconformably overlies the Upper Cretaceous Panoche Formation.

The friable, fine-grained, silty, unfossiliferous, massive light-colored sandstones of the right half of the outcrop (Fig. 2-6) represent the basal Tumbler Formation. A thin pebble layer at the base of the sandstone marks the unconformity. As innocuous as it may appear, this unconformity represents all of the Diogeneans

and most, if not all, of the early Miocene. There is no early Miocene "Vaqueros" molluscan fauna in the basal Tumbler Formation on Keef Ridge. However, some workers have correlated portions of this unfossiliferous and poorly exposed interval with the Vaqueros Formation (e.g., Bromlette, 1934; Goudkoff, 1934; Woodring, and others, 1940).

In Big Tar Canyon the Tumbler Formation is just over 700 feet thick (Fig. 2-7). It thickens by several hundred feet northwestward towards Baby King and Garza Creeks, and also down-dip into the subsurface. The formation consists mostly of heavily bioturbated, massively bedded, fine-to-medium-grained "dirty" sandstones with interbedded intervals of sandy siltstone; thin-bedded siltstone, shale and fine sandstone; and coarse-grained sandstone which may be cross-bedded to planar laminated and conglomeratic. Sandy coquina beds, such as the "reefs", are common and pebbly horizons are not infrequent.

Macrofossils are abundant in the Tumbler Formation. The most common are *Turritella oggiana* (gastropod), *Scaphiopsis andersoni* (pelecypod), *Vanuxemella* (*Scutella*) *verrilli* (echinoid), and fragmented *Salinus gregarius* (barnacle). Several species, including *Crepidula rostralis* and *Cancellaria deliana* (gastropods), and *Palaemonetes wassatales* (pelecypod) are restricted to the "Tumbler Stage" and indicate a middle Miocene age for the Tumbler Formation (Adegoke, 1969; Addicott, 1970; Addicott, 1972).

Faunal and sedimentary characteristics indicate deposition of the Tumbler Formation sands primarily on a shallow marine shelf well above storm wave base. Brief periods when tidal processes were dominant, however, are indicated by several thin intervals within the Tumbler Formation (Cooley, this volume).

The following descriptions highlight interesting features in the Big Tar Canyon section of the Tumbler Formation.

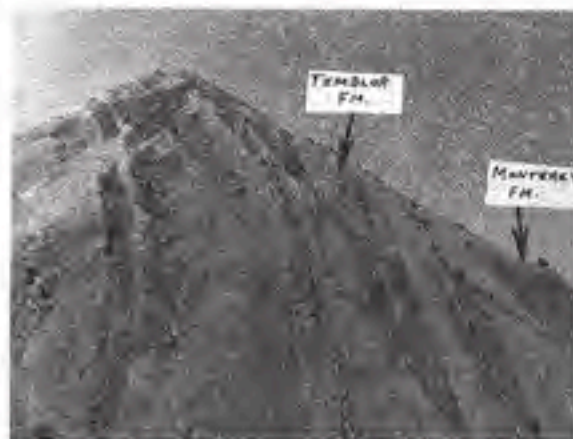


Figure 2-7. Tumbler Formation exposed on northwest side of Big Tar Canyon.

Return to Big Tar Canyon Road and walk upsection to the point at which several prominent sandstone ledges are exposed all the way down to road level.



Figure 2-8. "Reef bed" exposure on southeast side of Big Tar Canyon Road.

STOP 2-3. "REEF" BEDS

The most striking features of the Tealor formation on Reef Ridge are the "reef" beds. These form prominent weathering-resistant ledges (Fig. 2-8) which crest the ridge. The beds consist of sandy bioclastic limestone, the framework of which is a dense network of molluscan molds and shell fragments. Most of the beds are massive, but some are planar-laminated or show isolated cross-beds. The beds are conglomeratic and occasionally contain mammal bones and cobbles. The "reef" beds are 1-6 feet thick and alternate with finer-grained sparsely fossiliferous gray sandstones which are massive, planar laminated, or cross-bedded.

The beds are tabular to lenticular and can be laterally discontinuous. On the northwest side of the road, the two lowest beds overlap and pinch out beneath a large sandstone lens (Fig. 2-9). The uppermost bed is tabular and continuous, except for a slight downward swelling near the top of the slope.

"Reef" bed sedimentary structures suggest that these are high energy storm-lag deposits. The beds were probably sourced by tidal channels which lay not far to the west of Reef Ridge (Cooley, this volume).



Figure 2-9. Tabular and lentic sandstone bodies within the "Reef Beds". Northwest side of Big Tar Canyon Road.

A cowpath just above the creek on the south side of the road leads from the "reef" bed ledges to a gully. We will walk along this gully to the next prominent ledge which marks the beginning of our Stop 2-4.

STOP 2-4. "BUTTON-BEARING" SANDSTONES

The ledge-forming sandstone consists of moderately-sorted, medium-to-coarse-grained, planar laminated to cross-bedded, fossiliferous calcareous sandstone. The laminae and cross beds are armored with highly comminuted "button" sand dollars of the species *Yagueronella* (*Scutella*) *merriami*. The cross-bedding in this ledge is tabular in sets up to 14 inches thick. Cross-bedding directions suggest dominantly westerly paleocurrents, with minor bidirectionality. Across the road this unit is not cross-bedded, but rather shows well-developed, discontinuous linear horizons of "button" armoring. A few tens of yards farther on the bed is replaced - except for a thin interval at the top - by a massive, unfossiliferous, well-sorted, yellowish-brown, medium-grained sandstone. The whole "button-bearing" bed, however, reappears about 150 yards beyond that.

The "button-bearing" unit's coarse-grained character, bioclastic content, current lamination, and cross-bedding suggest it was deposited by strong currents in shallow water. Since the unit is laterally correlative with open-shelf tidal deposits, it too was probably of tidal origin (Cooley, this volume). The lateral discontinuity of all but the uppermost beds may indicate filling of troughs or shallow depressions on the sea floor.

Continue upsection along the gully to the next fossiliferous ledge, which represents Stop 2-5.

STOP 2-5. BARNACLE BEDS

A barnacle-bearing bed of fine-to-medium-grained calcareous grey sandstone occurs stratigraphically below the fossiliferous ledge. The unabraded barnacles (*Balanus armatus*) occur with shell debris in 7 or 8 discrete layers 4-14 inches apart. Clusters of 2 to 6 barnacles, cemented at their bases to large shell fragments, occur in some of the layers (Fig. 2-10). Some of these clusters are in life position. Thus, the sand was deposited in less than 12 meters (39.3 feet) of water, the maximum depth of occurrence of similar barnacles on the west coast today (L. Phillips, pers. comm., 1982).

The barnacles are large enough to indicate more than a year's *in situ* growth before death (L. Phillips, pers. comm., 1982). The thin shelly layers which the barnacles colonized probably represent multi-year intervals of nondeposition. The interbedded sparsely fossiliferous sandstones probably represent sudden influxes of sediment which smothered and buried the barnacles. This episodic sedimentation was probably storm-related. Normal fair-weather tidal or wave-induced currents kept the sea floor swept clean of sand, allowing the barnacles to grow. Severe turbulence associated with big storms periodically buried those colonies which grew between the storms.

The resistant ledge underlying the barnacle bed consists of a medium-grained sandy coquina which contains abraded shells of a large peccot, as well as gastropods (including *Turritella* sp.), oysters, and barnacles. The bed is tabular and can be traced northwestward several miles to Baby King and Garza Creeks with little change in character. Its geometry, lateral continuity, lack of internal sedimentary structures, and the diverse fauna of abraded fossils, suggest a storm origin for this bed.



Figure 2-10. Barnacle clusters in growth position cemented to large shell fragments along discrete horizons within a massive sandstone.

We will continue walking along the gully almost to the creek, where several thin sandstone beds are visible.

STOP 6. TEBLOR FM./MONTEREY FM. CONTACT

Thick far-sorted conglomerates mark the basal Monterey formation in Garza Creek and Baby King Creek canyons to the northwest (Cosley, this volume). The lateral equivalents exposed in Big Tar Canyon vary along strike from thin pebble conglomerates to fine-to-medium-grained sandstones which contain only a few pebbles. Conglomerates include andesitic porphyry, greenstone, sandstone, and chert clasts. The lithic sandstone matrix also contains skeletal fragments of barnacles, oysters and peccots. Many small oil seeps are associated here with this basal unit and the beds are often tar-stained. The resistant sandstones are interbedded with brown nonresistant siltstones and fine-grained sandstones (Fig. 2-11).



Figure 2-11. Basal sandstones of the Monterey formation exposed on the southeast side of Big Tar Canyon.

What does this unconformity represent? Teblor Formation sedimentation began roughly at the same time as did the present episode of wrench fault tectonism (e.g., Harding, 1975, Fig. 2). Loomis and Ginzler (1982) state that a major northward-progressing regional uplift in the San Joaquin Valley occurred at 15-13 mybp (see also Graham and others, this volume) when the Mendocino Fracture Zone was subducted under the area. They calculated maximum total uplift during this time as 500 meters. Inception of uplift followed by subduction of an unstable triple junction (which, however it's done, must give the overlying crust one big bellyache) would explain the apparent general shallowing of Teblor formation depositional environments upwards, at a time when global sea level was rising (Vail and Mitchum, 1980).

The time following this tectonically active period was marked by a complete change in sedimentation style - from shoaling clastics to deeper water, fine-grained, biogenic sediments. The transition is often gradational (Graham and others, this volume), yet is marked in some places by basal sandstones and conglomerates.

Mapping the Teablor Formation/Monterey Formation contact, Cooley (this volume) noted that a thick basal conglomerate occurs in Baby King and Garza Creeks, but it thins laterally to sandstones and thin pebbles conglomerates interbedded with shales as you see here. At the north and south ends of the Reef Ridge structure, the section is truncated and overlain with angular discordance by the Monterey Formation. It would appear that the Teablor Formation at Reef Ridge represents part of a mid-Miocene trough fill (Cooley, this volume).

At some point during Miocene uplift stages/early post-uplift time, subaerial exposure to the west of Reef Ridge caused a pulse of gravels to be funneled into the Reef Ridge trough. The rim of the trough show only a minor disconformity, without thick conglomerates as in the center, yet no truncation of section as at the extreme ends. We are standing near the southern rim of the trough here in Big Tar Canyon.

These shoal water sandstones and conglomerates appear to have been the final phase of trough filling, for the overlying Monterey Formation siliceous rocks show no expression of the troughs. Instead clay shales and fine-grained sandstones of probably shelf depths grade rapidly into siliceous sedimentary rocks with bathyal benthic foraminiferal faunas (Dibblee, 1972; Bandy and Arnal, 1969).

The initial post-uplift subsidence seems to have been rapid. The Big Tar Canyon section, dated by paleontologic data provided by Gulf Oil Co. and summarized by Bandy and Arnal (1969) indicate a Luizian age for the upper Teablor Formation and a probable lower Mohnian age for the basal Monterey Formation (an age date that way comes from higher in the section than the basal sandstones).

What caused this rapid subsidence? Who knows? Arm-waving possibilities:

Eustatic sea level rise. A drop in global sea level at 13 mybp was followed by a rise that lasted until 11 mybp (Vail and Mitchum, 1983). This period of rising sea level could explain the initiation of Monterey Formation deposition, thus eliminating the need for a tectonic subsidence mechanism. While the timing probably fits for the Reef Ridge section, a eustatic sea level rise at 13 mybp will not explain the generally older Teablor Formation/Monterey Formation further south in the Teablor Range. Instead, post-uplift subsidence appears to have progressed northward, just as did the uplift itself.

Thermal decay after a heating event (i.e., cooling and contraction). Subsidence caused by thermal decay is generally a "hotspot"-related phenomenon (e.g., Detrick and Crough, 1978). Therefore, this idea assumes that passage of the Mendocino Fracture Zone created a thermal instability, as suggested by sequentially younger volcanic centers developed from south to north along the San Andreas system (Dickinson and Snyder, 1979; Graham and Peabody, 1981).

Basin extension as the Mendocino Fracture Zone translated northward with propagation of the San Andreas fault (for explanation of the geometry of this situation, see Ingersoll, in press). Add to

this the possible existence of a "slab window" (Dickinson and Snyder, 1979) which would perhaps increase crustal depression.

Isostatic compensation. Uplifts at triple junctions appear to be isostatically compensated by a directly underlying lithospheric mass (Crough, 1979). In this case, the compensating mass under the Mendocino Fracture Zone would have been moved northward by the San Andreas fault. The uplifted overlying plate, now uncompensated, would subside.

This event is only one of several such shoaling/deepening events recorded in San Joaquin Valley stratigraphy (another being the Kreyenhagen Formation/Teablor Formation contact we looked at earlier). Whatever the big-picture reason for the change in style of Miocene sedimentation, it was followed by a relatively quiescent period in which the basin filled in with little subsidence beyond that produced by load-imposed subsidence (Bandy and Arnal, 1969; Loomis, pers. comm., 1982). The period of Monterey Formation deposition corresponds to a period of increased strike-slip movement along the San Andreas fault (Harding, 1976). Wrench fault-related drag folds grew along the fault, and deformation propagated increasingly eastward with time (Harding, 1976). An interplay of wrench fault tectonism and eustatic sea level change seems to have been the primary control on sedimentation patterns from middle Miocene to the present. Indeed, the next shoaling event in the section, that of the elastic-rich Reef Ridge Member/Elchegoin Formation, is apparently the reflection in the San Joaquin basin of a global sea level fall which occurred at roughly 6.5 mybp (Vail and Mitchum, 1980; Keller and Barrois, 1981).

Continue along the gully to the road; walk up the road to the Molure Member outcrop to your left (Fig. 2-12).



Figure 2-12. Exposure of Monterey Formation on northwest side of side of Big Tar Canyon. Resistant beds which are dotted with trees are dominantly porcelanites.

STOP 2-7. MOLURE MEMBER

The section at Stop 2-7 grades from clay shales and siltstones above the sandstones of Stop 2-5 to increasingly more siliceous shales (fig. 2-13). A porcelanitic zone 22 meters (72 feet) thick probably marks the lower to mid-Muhlenberg electric log high-resistivity zone of maximum transgression (Graham and others, this volume) - roughly equivalent to the tar-bleeding Antelope Shale we examined yesterday at Chico Martinez Creek.

The siliceous part of the Molure Member here is very much like that in the Polonio Pass area, although thinner. It consists of nonlaminated siliceous shales and porcelanites containing abundant quartz silt and recrystallized white peloids. There is probably much less clay here than in the Pyramid Hills Road section, since the weathering color here is brown rather than blue-green. Above this outcrop, the section is progressively less siliceous, grading from porcelanites to siliceous shales to clay shales. The Reef Ridge Member is a poorly defined unit here, simply representing the transition from biogenic siliceous sedimentation to the sandstone/shale sequence of the Etchegoin formation. The Monterey formation on Reef Ridge appears to represent a thin symmetrical transgression/regression event. The transgression was due to post-uplift subsidence of the basin, and regression was due to passive infilling of the basin, augmented by a eustatic drop in sea level, as already discussed. (See also Graham, and others, this volume.)

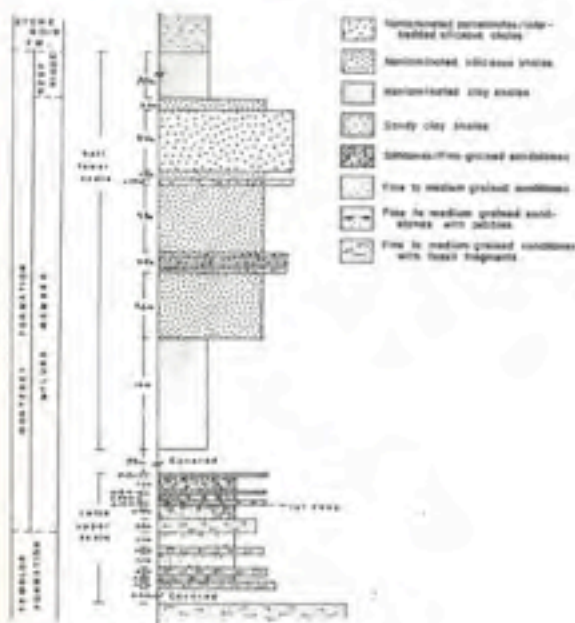


Figure 2-13. Measured section of the Monterey Formation in Big Tar Canyon.

Biogenic silica in the porcelanite zone is opal-CT. In the Sarza Creek section, there is an opal-CT/quartz boundary in the lower siliceous shales; this has not been verified for the Big Tar Canyon section, but probably occurs in roughly the same part of the section. Therefore, this section may have seen sufficient burial (a maximum of 10,000', corresponding to 212°F) to just enter the hydrocarbon generative window. However, kerogen is not abundant in these rocks. Their total organic carbon values are generally much less than 1 wt %. Furthermore the nonlaminated nature of the sediment suggests that its associated organic matter was probably subjected to oxidation and/or biodegradation post-depositionally. Therefore, the Monterey formation here, although somewhat more organic-rich than at the Pyramid Hills Stop, is still not a likely source for high-grade oil. In general, the shelf facies of the Monterey formation is probably a poor source rock, whereas several lithotypes within the basinal facies - especially the mat-laminated lithotype - are undoubtedly major hydrocarbon sources within the basin.

END OF DAY TWO

Troops disperse.



REFERENCES CITED

- Addicott, W.O., 1970. Miocene gastropods and biostratigraphy of the Kern River area, California: U.S. Geol. Surv. Prof. Paper, n. 642, 174 p.
- Addicott, W.O., 1972. Provincial Middle and Late Tertiary Molluscan stages, Tumbler Range, California: Pacific Coast Miocene Biostratigraphic Symposium, Pacific Sect. SEPM Proc., p. 1-26.
- Addicott, W.O., 1973. Oligocene molluscan biostratigraphy and paleontology of the lower part of the type Tumbler formation, California: U.S. Geol. Surv. Prof. Paper, n. 791, p. 1-48.
- Adegoke, O.S., 1969. Stratigraphy and paleontology of the marine Neogene formations of the Coalinga region, California: Calif. Univ. Pub. Geol. Sci., v. 80, 241 p.
- Bandy, O.L. and Arnal, R.E., 1969. Middle Tertiary basin development, San Joaquin Valley, California: Geol. Soc. Amer. Bull., v. 80, p. 783-820.
- Berthel, K.W. von, 1976. Coccolithen, Flugschaub und Gehalt an organischen Substanzen in Oberjura-Plattenschiefer Bayerns und SE Frankreichs: Eclogae Geol. Helv., v. 69, n. 3, p. 627-639.

**4th Annual Stanford BPSM
Industrial Affiliates Meeting
November 5, 2011**

8:30 am	Steve Graham Introduction
8:50 am	Tapan Mukerji: Spatial uncertainty modeling, new course, and benchmark model
9:30 am	Tess Menotti: 3D strike-slip basin modeling in the Salinas Basin, California
10:00 am	Danica Dralus: Kinetics of the opal-CT to quartz phase transition determined by hydrous pyrolysis experiments
10:30 am	Break to examine lunch menu on next page
10:45 am	Blair Burgreen: Key controls on petroleum systems in a forearc basin: A case study of the East Coast Basin using 2D basin and petroleum system modeling
11:15 am	Yao Tong: Introduction to basin and petroleum system analysis for characterizing gas shale reservoir rocks in the Piceance Basin, Colorado
11:30 am	Lunch in Farmhouse Room in Harris Ranch Restaurant
1:00 pm	Allegra Hosford Scheirer and Les Magoon: Review of BPSM
1:20 pm	Meng He: Two-dimensional burial history model and geochemistry shed light on petroleum systems and mixed oil in the Vallecitos area, San Joaquin basin, California
1:50 pm	Keisha Durant: Basin and petroleum system modeling on the Sur and northern offshore Santa Maria area, offshore central California
2:20 pm	David Zinniker: New techniques for recognizing (and determining the source of) high-maturity hydrocarbons in California petroleum provinces
2:50 pm	Break
3:05 pm	Tess Menotti: Petroleum geology of Mongolia
3:30 pm	Ken Peters: Gas shale: the key to success is better geology, technology, and petroleum system modeling
4:00 pm	Group Discussion
5:00 pm	Adjourn

NOTES

HARRIS RANCH RESTAURANT

TOUR GROUP LUNCH MENU

Lunch Entrées include two freshly baked Harris Ranch chocolate chip cookies
Choice of coffee, tea or soda.

ENTRÉE SALADS

All Salads are served with a freshly baked cheese roll and whipped butter.

Chicken Caesar Salad

Crisp romaine lettuce leaves tossed with our Caesar dressing, croutons, and grated parmesan cheese, topped with pepper Dijon chicken.

Horseradish Flank Steak

Caesar Salad

Romaine lettuce tossed in creamy horseradish dressing with marinated Flank Steak, avocado, cherry tomatoes, roasted garlic, and Bleu cheese topped with shaved red onion.

HOT ENTREES

Beef Stew

Tender chunks of Harris Ranch Beef braised in a rich broth with farm fresh vegetables. Served in a sourdough bread bowl. Accompanied by freshly baked rolls and whipped butter.

Harris Ranch Pot Roast

Our award-winning tender slow roasted beef brisket, roasted garlic mashed potatoes and gravy with farm fresh vegetables. Served with freshly baked rolls and whipped butter.

HARRIS RANCH FAVORITES

Ranch Burger

Jack or cheddar cheese, lettuce, tomatoes, red onion, pickles, and our special dressing. Served with our signature wedge cut fries and a dill pickle spear.

BBLT Panini

Roasted Tri-Tip, bacon, lettuce, tomatoes, cheese and horseradish cream pressed between crusty Italian Bread. Served with our signature wedge cut fries and a dill pickle spear.

Fresh Chicken Salad Sandwich

Diced chicken, grapes, celery, shallots and toasted almonds in a honey Dijon dressing with fresh tarragon and basil on a croissant with lettuce and tomato. Served with our signature wedge cut fries and a dill pickle spear.

*Menus and pricing are subject to change.

The East Coast Basin is a petroliferous forearc basin located both onshore and offshore of the North Island, New Zealand (Fig. 1), and has been intermittently explored since the late 19th century. The basin's history is very complex with significant lateral variations in its development related to the tectonic configuration along the convergent margin. Differences in the subduction rate and angle at the Hikurangi trench, rate of accretion, and character of the subducting crust manifest themselves as three distinct basin segments: a northern segment with a minor accretionary wedge studded by plateau and seamount collisional scars and major slope slumping, a central segment with a wide and emergent accretionary wedge, and a southern segment with a minor accretionary wedge merging into a strike-slip boundary.

These lateral variations in basin configuration directly impact the development of the petroleum system through the burial and uplift history, heat flow, structural character, and seal properties. Basin and petroleum system modeling of 2D transects through each basin segment provides a means to better understand how variations in the forearc configuration affect petroleum system development, and to define which parameters most strongly influence hydrocarbon prospectivity.

Although the East Coast Basin is a challenging area to explore due to stratigraphic and structural complexity, the tectonic history has provided a key sequence of events for petroleum system development. The prospective source rocks were deposited during a late Cretaceous-Oligocene passive margin phase and include the Waipawa Black Shale (TOC=3.6%; HI=245 mg HC/g TOC; 17 m thick) and possibly the Whangai Formation (TOC=0.56%; HI=159 mg HC/g TOC; 400 m thick). Sand-rich turbidites and shelfal marine formations were deposited

during the Miocene – present active margin phase and are typically enclosed by mudstone seals. Imbricate thrust faulting and folding due to the compressional regime created syn-depositional structural traps, thickened the overburden, and possibly created new pathways for fluid migration. However, the basin is synchronously undergoing a period of cooling due to cold slab subduction that may offset the thermal effects of the structurally thickened overburden. Timing, geometries, and shale-gouge ratios of faults are also of particular importance for hydrocarbon migration as a 100-200m layer of low permeability smectitic mudstone lies between the source and reservoir formations, possibly preventing any migration prior to Neogene tectonism.

2D Basin and petroleum system modeling will address (1) the impact of laterally variable model parameters (i.e. heat flow, subsidence rate, migration pathways) on petroleum system development and how this relates to spatial variations in the forearc configuration and development, (2) the effect of thrust faulting on migration and maturation of the Waipawa and Whangai source rocks, (3) the significance of the smectitic mudstone layer on the timing of migration, and (4) possible heat flow scenarios in a basin with a passive to convergent margin tectonic history.

Preliminary 1D modeling reveals the wide range in petroleum system development across the East Coast Basin based exclusively on burial history. Potential source rocks in the Central Hawke's Bay and Gisborne regions have undergone the deepest burial and therefore the highest degree of kerogen transformation, while potential source rocks in the inland Southern Hawke's Bay region are the least generative. Maturation of the Waipawa Black Shale begins at 35 Ma in the Central Hawke Bay region during the passive margin setting,

however the critical moment occurs for most areas between 14 Ma – present day during the active margin setting. While 1D modeling has revealed lateral differences in the East Coast Basin petroleum system

development due to burial history, additional complexities need to be considered to better constrain and understand petroleum system evolution.

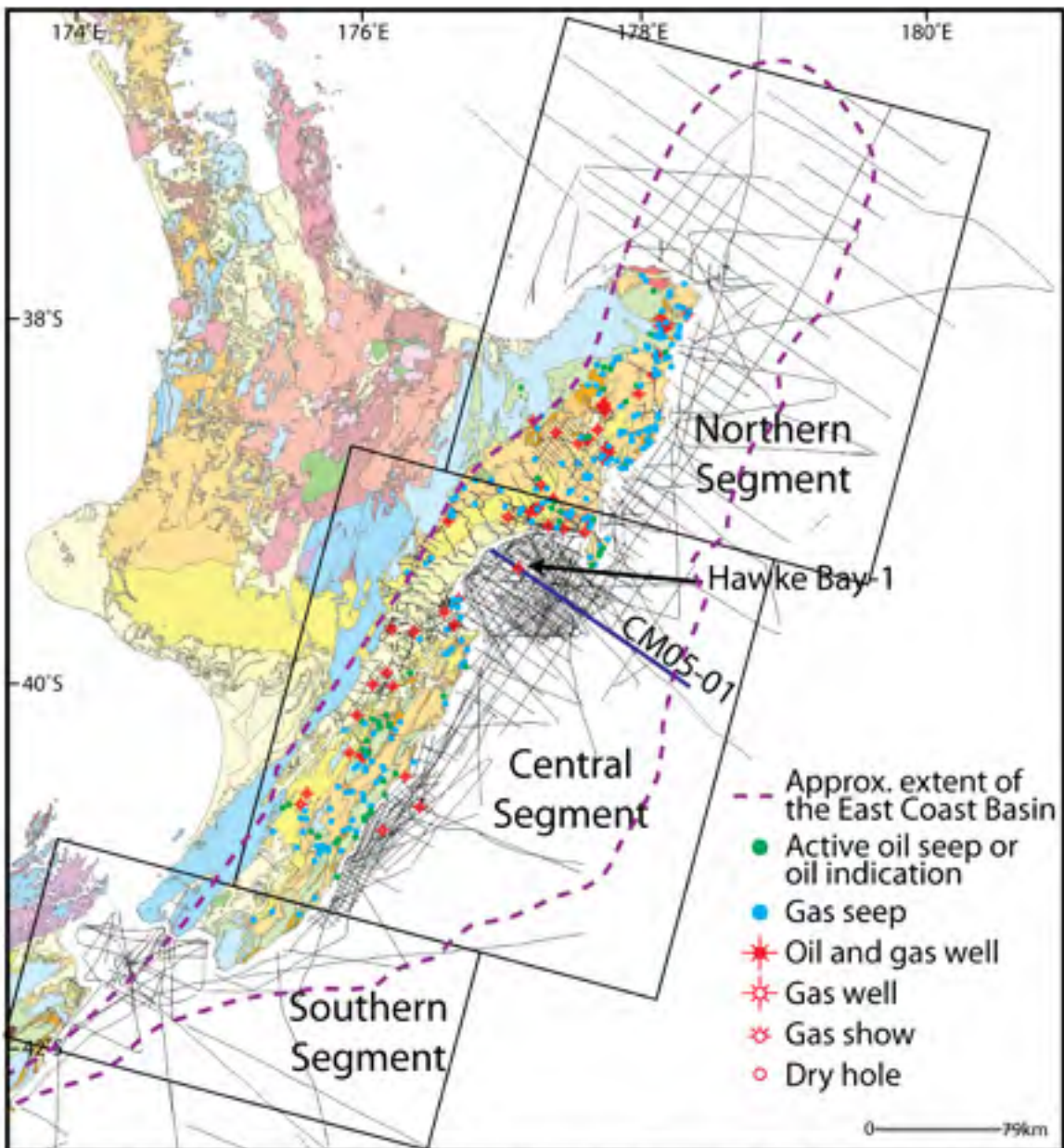


Figure 1. The East Coast Basin is located on the eastern margin of the North Island, New Zealand. Seismic surveys, numerous onshore wells, and 3 offshore wells provide a modest data set for basin and petroleum system modeling. Gas and oil seeps are present throughout the onshore region, although many uncertainties exist regarding the development of the petroleum system. This study will first assess the Hawke Bay Region through 2D modeling of the CM05-01 seismic line, which is constrained by the offshore Hawke Bay-1 well. (Geologic map, seismic data map, and well locations from the GNS PDQ Map Database; Oil and gas seeps from Francis et al. (2004); Basin segments based on Lewis and Pettinga (1993))

Diatomite comprises primarily amorphous opal (opal-A) from the deposition of marine diatoms. Its largely disconnected pore structure gives it a high porosity but very low permeability. During burial, diatomite undergoes a diagenetic conversion, first to microcrystalline opal (opal-CT) and ultimately to quartz. While porosity decreases during this transformation, permeability temporarily increases as migrating fluids create flow paths. The evolution of permeability can lead to the formation of diagenetic traps for petroleum even if no structural traps are present; examples include the Rose and North Shafter fields in the San Joaquin Basin. Silica phase changes at depth can be difficult to identify using seismic data, so geochemical predictions of the locations of these phase changes are a valuable tool in exploration.

Zero-order kinetic parameters describing the opal-CT to quartz phase transition were calculated by Ernst and Calvert (1969) based on their hydrothermal experiments using Monterey Formation opal-CT and distilled water. The phase transition requires the dissolution of opal-CT and

precipitation of quartz, two processes whose rates depend on the chemistry of the saturating fluid. In this study, we conducted hydrous pyrolysis experiments similar to those of Ernst and Calvert but with conditions that more closely reflect those found in nature. We used a weathered Monterey Formation porcelainite from Lompoc, California, saturated with a buffered aqueous solution that maintained a pH between 7.0 and 8.2. Pyrolysis was limited to temperatures below the critical point of water to ensure liquid water was always present.

Under our experimental conditions, the reaction rate of the opal-CT to quartz phase transition showed a greater dependence on temperature than the Ernst and Calvert data, resulting in faster transitions at laboratory temperatures and slower expected transitions at basin temperatures. These new reaction rates were incorporated into a dynamic basin model along the SJ-6 seismic line of the San Joaquin Basin to estimate the depth of the opal-CT to quartz transition. The result was a transition 1500 ft deeper than predicted by the previous kinetic data.

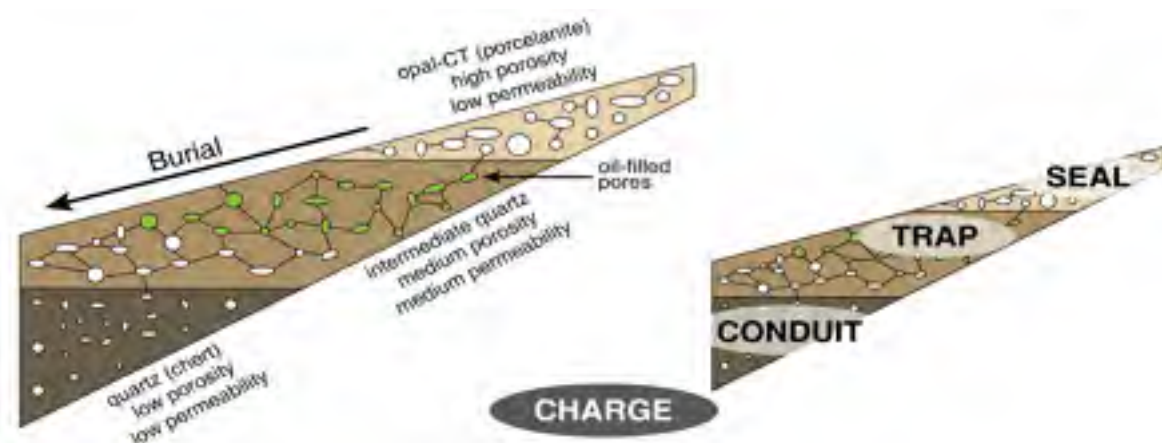


Figure 1: (left) Cartoon of a single siliceous layer undergoing transformation from opal-CT to quartz during burial; relative physical properties are indicated. (right) Evolving physical properties can lead to a single depositional layer playing multiple roles in a petroleum system.

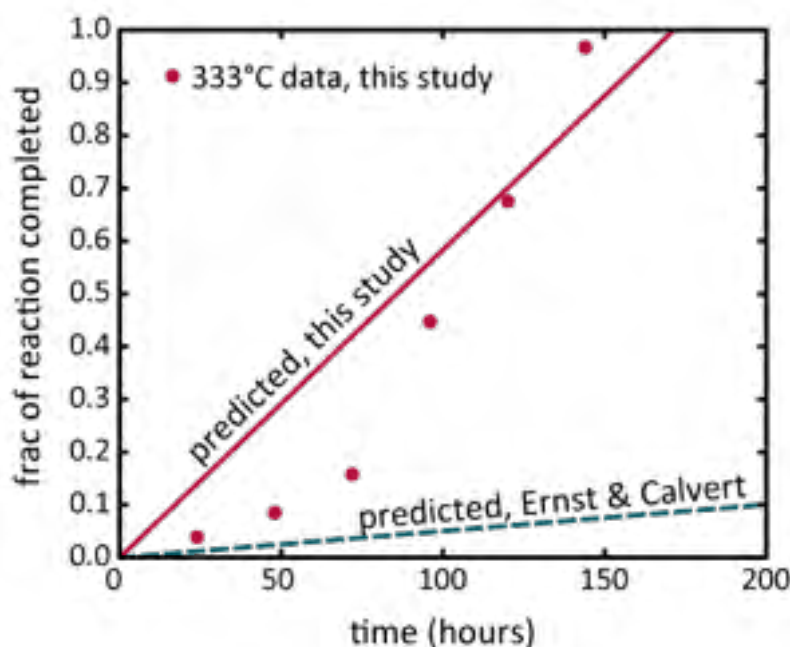


Figure 2: Example comparing the reaction progress of our experiments with those of Ernst and Calvert. Data collected in this study are shown as points. The solid line shows the predicted progress based on derived kinetic parameters; the dashed line shows the prediction of Ernst and Calvert. At this (high) temperature, opal-CT has fully transformed to quartz while the Ernst and Calvert kinetics predict less than 10% transformation.

DURANT, K.A., Scheirer, A.H., Peters, K.E., Graham, S.A., and Magoon, L.B., *Basin and petroleum system modeling of the Sur and northern offshore Santa Maria areas, offshore Central California*

The Sur basin (also called the Partington basin) is an undrilled, asymmetrical basin offshore central California. It is the northwestern extension of the offshore Santa Maria basin, and therefore shares similar stratigraphy and tectonic history. Although some successful petroleum discoveries have occurred in the southern offshore Santa Maria area, the Sur basin and northern offshore Santa Maria areas have never been commercially explored. Peters and others (2008) collected tarball and seep samples from the central California coast and suggested that some may have originated from seeps within the Sur and northern offshore Santa Maria areas. In this study, we used three-dimensional (3D) basin and petroleum system modeling to evaluate whether a mobile petroleum charge exists in

these areas. A 3D geologic model of the Sur and northern Santa Maria areas was constructed by converting travel time isopach maps to depth via well data available in the nearby southern offshore Santa Maria area. Because Type IIS kerogen generated significant amounts of heavy sulfur-rich crude oil in the southern offshore Santa Maria area, Type IIS kerogen kinetics was used to simulate petroleum generation from the Miocene Monterey Formation in the 3D basin model. The Monterey Formation was split into the lower calcareous-siliceous, the carbonaceous marl and the clayey-siliceous members. Other stratigraphic inputs for the model included the Lower Foxen, the Upper Foxen, the Lower Sisquoc and the Upper Foxen Formations. The model results suggest that the Miocene Monterey

Formation source rock is thermally mature and generated volumetrically significant accumulations of low-maturity petroleum in minor anticlines sealed by the mudstone of the Sisquoc Formation or by the clayey-

siliceous member of the Monterey Formation. The model results also suggest the potential for unconventional shale oil opportunities.



Figure 1: Map shows location and geological setting of the Sur basin and the offshore Santa Maria basin modified after McClellan et al. (1991) and Sorlien et al. (1995). Study area is outlined by red dashed line. Faults are solid red lines. Basin outlines are solid blue lines.

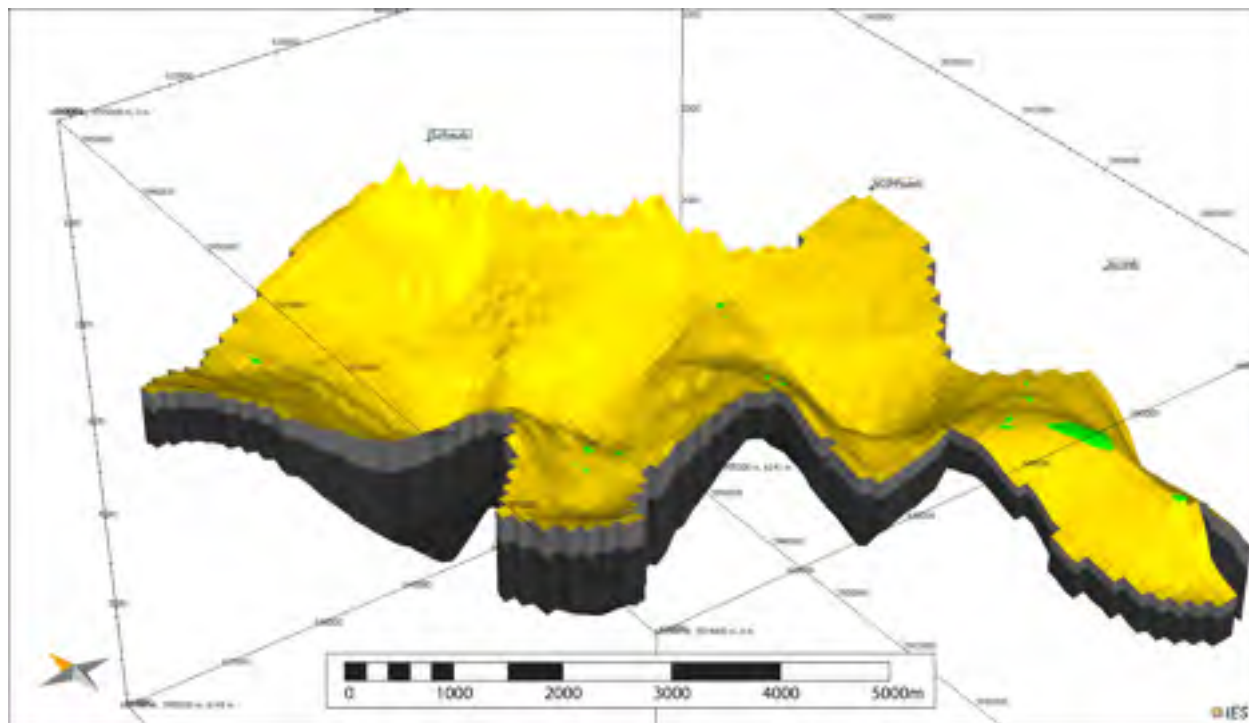


Figure 2: Shows accumulations (green) predicted in the 3-D model within the Sur and northern offshore Santa Maria Areas. The model predicts 31 accumulations containing approximately 29 million barrels of oil (MMbbl).

HE, M., *Two-dimensional burial history model and geochemistry shed light on petroleum systems and mixed oil in the Vallecitos area, San Joaquin Basin, California*

The Vallecitos Syncline is a westerly structural extension of the San Joaquin basin. Dispersed oil accumulations in the Vallecitos area make oil and gas exploration challenging. Our earlier 1D model indicated that there could be two active source rocks in the syncline: Eocene Kreyenhagen Formation and Cretaceous Moreno Formation.

Biomarker analysis was conducted on 23 oil samples from the syncline. Source-related biomarkers show two genetic groups, which may originate from two different source rocks. Diamondoid analyses for those samples indicate mixtures of oil-window maturity and high maturity oils. A deep, high-maturity source was strongly suggested based on the geochemical features of the samples.

A 2D line along a published cross-section through the deepest part of the syncline was selected to conduct thermal history, basin evolution, and migration analyses. Stratigraphic evidence and modeling suggest that several recent episodes of erosion are required due to folding that removed significant overburden. Thick (~2km) overburden rock in the syncline pushed shallow Eocene Kreyenhagen source rock into the oil window around 14 Ma. In contrast, the Cretaceous Moreno source rock reached extremely high maturity (dry gas window) at same time.

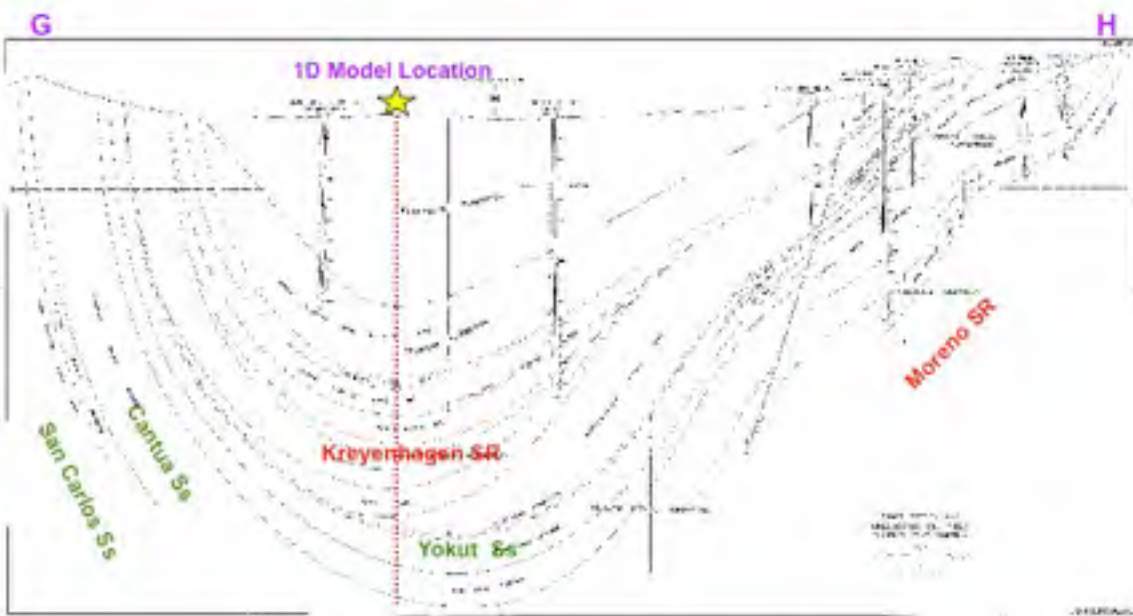
Results suggest that in the Vallecitos Syncline the bottom and the top of the Cretaceous Moreno Formation reached thermal maturity at 37 Ma and 18 Ma,

respectively. The synclinal Eocene Kreyenhagen Formation became thermally mature at 14 Ma. The 2D model results indicate that the Kreyenhagen Formation has a maximum transformation ratio (TR) of 50% at its base, whereas the Moreno Formation has TR~100%. These results are supported by biomarker and diamondoid geochemistry, which indicate that the Kreyenhagen oils contain a high-maturity component that could originate from the Moreno Formation. The results are consistent with our earlier 1D burial history model in the Vallecitos Syncline. Compound-specific

isotope analysis (CSIA) and quantitative extended diamondoid analysis (QEDA) were employed to confirm correlations and determine oil mixtures.

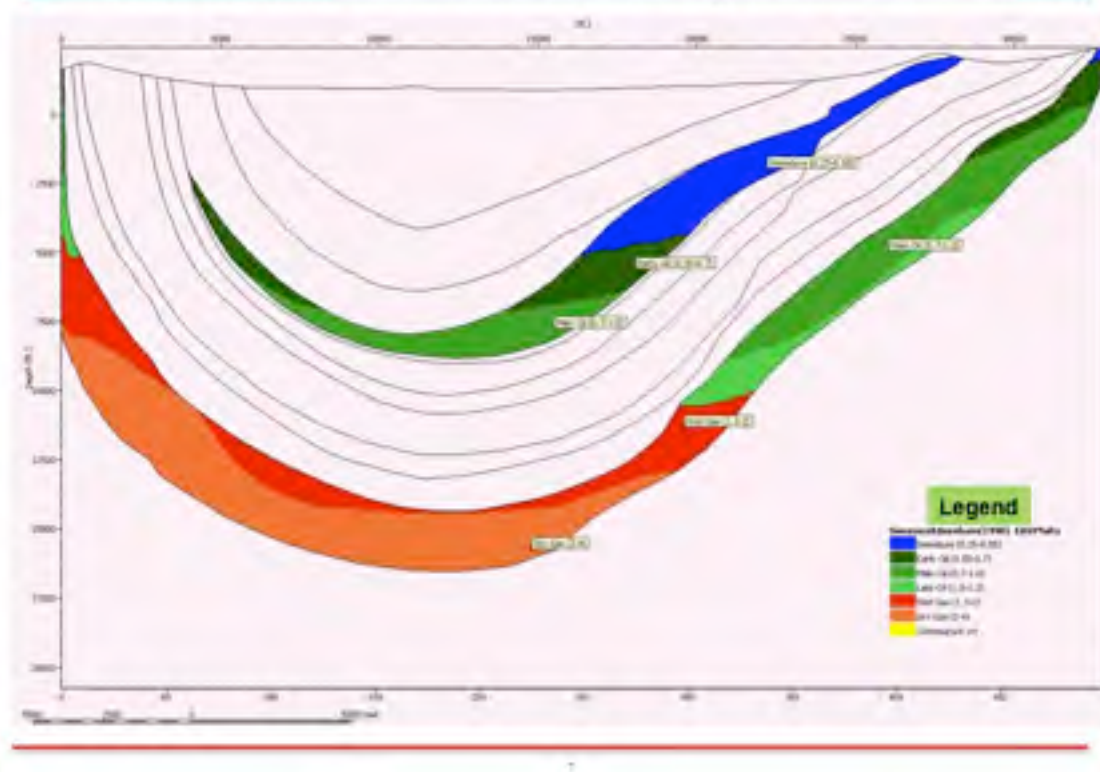
Migration analysis on our 2D profile indicates hydrocarbon loss on both flanks of the cross-section. Effective traps are absent in the cross-section and most of the generated hydrocarbons probably migrated out of the model along strike or perpendicular to it. A future 3D model could better explain the main migration pathways, if additional structural data become available.

Cross-section GH in Vallecitos Syncline



California State Division of Oil and Gas, 1982

2D Model results: simulated Ro value (combination model)



MEMOTTI, T. and Graham, S.A., *3D strike-slip basin modeling in the Salinas Basin, California*

The Salinas Basin, California contains a petroleum system that boasts a giant oil field that has been producing heavy oil for the past half-century. Yet despite its relatively long-standing history as a steady source of oil production, many aspects of the basin's geologic and petroleum system history are still poorly understood. The Salinas Basin offers an opportunity to explore modern basin modeling techniques in a strike-slip setting, while addressing outstanding, unresolved geologic questions. This project combines the techniques of basin modeling and oil geochemistry in order to improve our understanding of the Salinas Basin as a petroleum province. A primary

goal of this project is to develop 3D basin and petroleum system models of the Salinas Basin to ascertain the impact of strike-slip displacement on oil field distribution. These basin models will be constrained by plausible migration scenarios as suggested by oil properties including the relative biomarker abundances of the oils from five Salinas Basin oil fields.

The Salinas Basin is a Cenozoic transpressional basin in the Coast Ranges of central California. Miocene displacement along the San Andreas fault system resulted in rapid subsidence of localized basins along the paleo-coast, including the Salinas Basin. The appreciable tectonic subsidence of these

silled basins coincided with flourishing marine biological productivity, ultimately yielding thick biosiliceous deposits. Accumulation of over 3.5 km of the siliceous upper member of the Monterey Formation, as well as a calcareous lower member in the Hames Valley depocenter serves as the overburden and source rock of the Salinas Basin petroleum system. The Monterey Formation source rock in the Hames Valley depocenter demonstrates both good organic richness (TOC 2-8%) and is within early oil window levels of thermal maturation (R_o 0.5-0.8%). The Hames Valley depocenter is thus an oil-prone pod of active source rock, which has sourced the half-billion barrel San Ardo oil field ~9 km NE of the depocenter. The majority of production of the heavy (9-23° API) oil in the Salinas Basin occurs in shallow, shelfal upper Miocene sandstones at San Ardo field; however there are six, much smaller accumulations (<1 mmbbl each) aligned sublinearly to the NNW of San Ardo oil field. This field distribution spans a lateral distance of 50 km. A trend towards increasing oil quality is apparent from south (9-13° API) to north (17-23° API), with the San Ardo oils demonstrating the lowest API gravity. This project aims to provide an explanation for the bimodal field size distribution through basin and petroleum system modeling in conjunction with oil geochemical analyses.

The Neogene strike-slip faulting of the Salinas Basin complicates 3D basin model construction, but also necessitates a 3D model approach in order to capture the role of lateral translation along strike-slip faults in forming the present-day field distribution. Beginning in the late Miocene, the primary depocenter was dissected by the

Reliz-Rinconada fault, a NNW-SSE trending strike-slip fault related to the San Andreas fault system. The western side of the depocenter now resides in the Arroyo Seco ravine, ~40 km north of its eastern counterpart in Hames Valley. While the Arroyo Seco depocenter does not reach the magnitude of burial seen in the Hames Valley depocenter to the southeast (over 2.5 km burial in Arroyo Seco as compared to 3.5 km in Hames Valley), thermal maturity profiles from exploratory wells indicate potential for oil generation from this secondary source.

Our approach for modeling the Salinas Basin involves construction of 3D numerical basin models in PetroMod® software (version 11, sp4; Fig. 1). The preliminary models are simplified representations of the Salinas Basin, using general characteristics of the basin based on publically-available subsurface (well log) and outcrop data as framework. 1D burial history models in the basin depocenters allow calibration of thermal history. Currently, there is no standardized technique for 3D basin and petroleum system modeling with strike-slip faults, however this is a crucial component to understanding the Salinas Basin petroleum province since the Reliz-Rinconada fault splits the main depocenter. Thus, this project aims to develop a method for implementation of lateral fault motion in 3D models to test the role of strike-slip faulting on hydrocarbon distributions in the basin. Preliminary synthetic models have successfully demonstrated plausible hydrocarbon generation-expulsion-migration histories that result in multiple accumulation distribution possibilities.

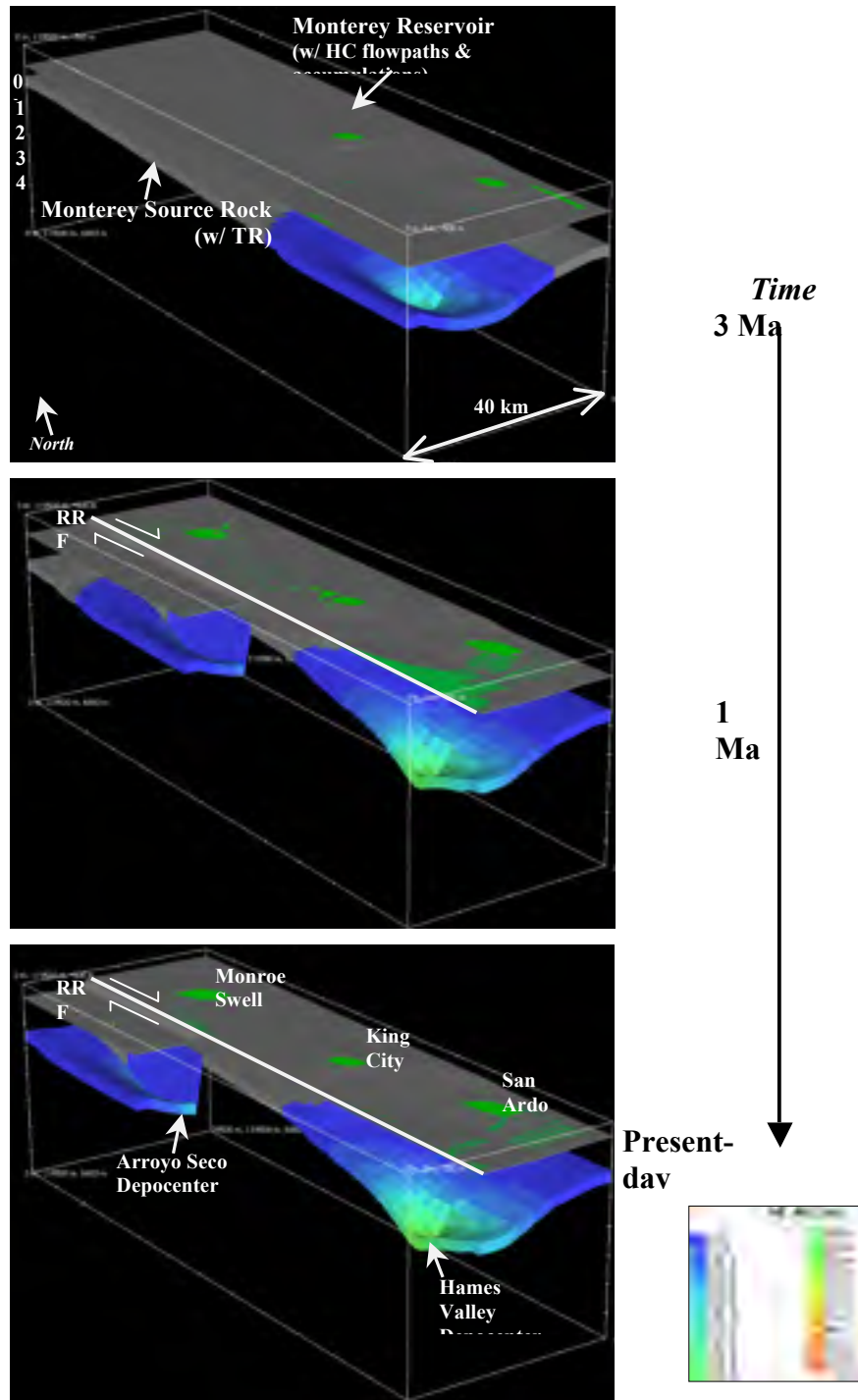


Fig. 1 - Preliminary 3D basin and petroleum system models using simplified Salinas Basin geology highlight the potential role of the Reliz-Rinconada strike-slip fault (RRF) on hydrocarbon migration. The source rock level of the Monterey Formation is overlain with transformation ratio (TR), indicating the Salinas Basin depocenter is actively generating during strike-slip fault displacement in this model. There is potential for hydrocarbon migration from both western and eastern pods of active source rock, with the western pod (Arroyo Seco) contributing primarily to the northernmost accumulation (Monroe Swell field). Potential carrier beds (fractured Monterey Formation and sandstone Vaqueros Formation) are not shown. (Vertical exaggeration: 5X.)

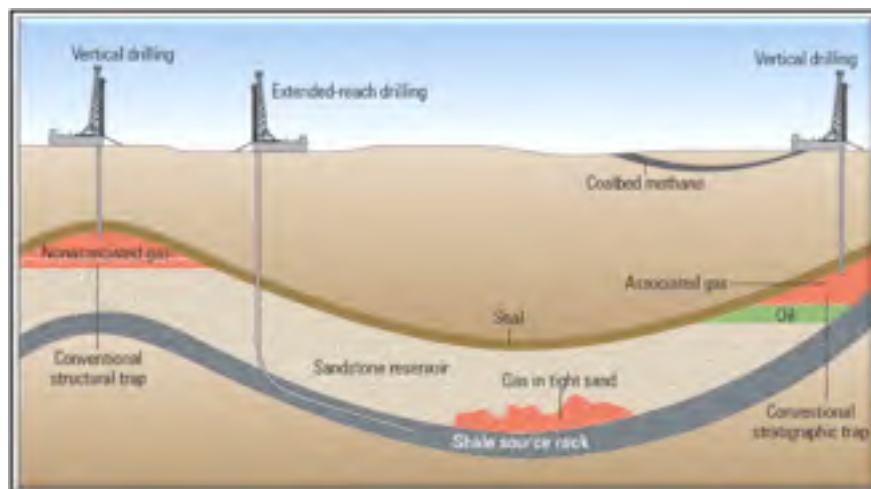
PETERS, K.E., *Gas Shale: the Key to Success is Better Geology, Technology, and Petroleum System Modeling*

Gas shale plays rely on finding areas where low porosity, low permeability (“tight”) source rocks can be exploited as “unconventional” reservoirs. Practical use of directional drilling and stimulated horizontal wells beginning in the 1980s has led to hydrocarbon gas production rates that far exceed those of many vertical wells. Some estimate that North America contains the equivalent of more than nine times the conventional oil reserves of Saudi Arabia as unconventional gas. As a consequence, the petroleum industry is undergoing a dramatic revitalization and there is growing demand for talented young geoscientists. Economic exploitation of shale gas plays requires an understanding of both geology and technology. Technical innovations made shale gas commercial in the first place and technology now enables the reduction in costs necessary for its survival. This lecture describes three simple rules that are being used to insure the success of gas shale plays:

- Understand the geology and geochemistry of the play (e.g., thermal maturity, vertical heterogeneity, fracture problems)

- Understand how to apply cost effective technology to exploit the play (e.g., microseismic events along wellbore help define the extent of fractures)
- Leverage models to understand how to bring the right technology to each play (e.g., aim for areas showing high stress based on three-dimensional models)

The aim of the Basin and Petroleum System Modeling (BPSM) program at Stanford University is to train the next generation of petroleum system modelers. Petroleum system modeling provides an integrated framework to estimate resource richness early in the life of unconventional plays. Models and logging-while-drilling (LWD) technology can optimize well placement. Integration of core, log, and seismic data can be used to construct models that define sweet spots within the play at the appraisal and early development phase. Interpretation of microseismic data in models can optimize perforation strategy and fracture design to reduce completion costs while improving production.



TONG, Y., *Introduction to basin and petroleum system analysis study for characterizing shale gas reservoir rocks in the Piceance Basin, Colorado*

The high price of conventional oil and the associated concern about security of US hydrocarbon supplies have focused attention on expanded use of unconventional sources of oil and gas. Gas shales and tight gas represent an enormous potential among unconventional resources.

Our study area, Piceance Basin, is a geologic structural basin in northwestern Colorado, in the United States. The Williams Fork Formation and other tight gas sandstones in

the Piceance Basin contain up to 322 tcf of in-place hydrocarbon gas, which represents one of the largest gas resources in the Rocky Mountain region (Johnson et al., 1987). Gas production from the Mesaverde Group in the Piceance Basin increased from less than 200 MMCFGD in the year 2000 to more than 1 BCFD in 2008 (Cumella and Scheevel, 2008). Figure 1 from Leibovitz (2010) shows locations of major gas and oil fields in the Piceance Basin.

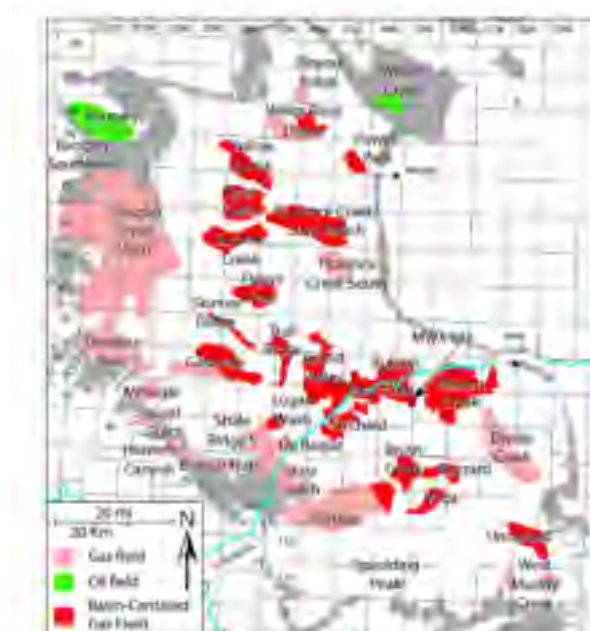


Figure 1: Map of major oil and gas accumulations in the Piceance Basin (from Leibovitz, 2010). Outcrop distribution of the Williams Fork Formation is shown in grey.

Although Piceance Basin began produce from 1931 and 38 fields have been discovered and produce petroleum since then, there are still many interesting aspects remain unexplored. One of our study goals is to better understand the generation, evolution of Piceance Basin and to achieve a better geophysical and geochemical characterization of shale gas resources. We believe that quantitative assessment of the dynamic source-rock thermal maturity, hydrocarbon generation, and migration

pathways in this basin are critical factors for efficient exploitation of this resource.

In this project, we will first build initial 1-D basin models calibrate with the results of 1-D modeling built by Zhang et al. (2008). Then, both 2-D and 3-D models will be built based on available sequence stratigraphic studies and interpretations of 2-D seismic data. After complete the 3D-BPSM of the Piceance Basin, we can provide the following information:

1. Temperature history,

2. Maturation history
3. Pressure/overpressure history
4. Location and timing of hydrocarbon generation.
5. Hydrocarbon composition
6. Hydrocarbon expelled from the source rock
7. Hydrocarbon migration through the carrier rock
8. Hydrocarbon accumulation and loss

The dynamic model will also help us address several questions which are not clear now. Such as: How should we explain both the basin centered gas accumulations (BCGA) and the conventional fields in this basin? Why gas saturation decreases from East to West, this is due to lack of overburden on

Cameo coal or lack of Cameo coal in the West?

Another important aspect of this project would be assessment of uncertainties. We know that Basin and Petroleum System Modeling covers large spatial and temporal intervals. Many of the input parameters are highly uncertain. We will focus on both parameters uncertainty and spatial uncertainty quantification. We will start with probabilistic approaches based on Monte Carlo simulations or experimental design to first give an assessment of parameter uncertainty. The other advanced methods such as Multi-Point Statistics (MPS), distance and kernel-based method will be applied to address the spatial uncertainty.

ZINNIKER, D., *New techniques for recognizing (and determining the source of) high-maturity hydrocarbons in California*

Deep petroleum systems are little understood components of California's sedimentary basins. Condensates, high API gravity admixtures to black oils, and thermogenic gas represent new and difficult plays for exploration. Our work is aimed at recognizing these systems, their source rocks, their thermal history and migration. It involves surveying extensive sample libraries for the occurrence of cracked oil with abundant ultra-stable markers and mapping out their contribution to known reservoirs.

Previous work in California on less stable molecular markers (i.e. biomarkers) was successful at sourcing less mature components but was largely blind to high-maturity contributions to reservoirs.

Ultra-stable components (diamondoids, light hydrocarbons, simple aromatics, and select biomarkers) can be fingerprinted and correlated with specific petroleum source rocks using ratios of structures, isomers, and isotopes. These

components give us the best chance of correlating petroleum source rocks and less mature oil samples with their thermally cracked counterparts.

Preliminary work quantifying select persistent ultra-stable markers in petroleum seep samples shows promise for identifying cracked components where evaporation and biodegradation has removed more commonly utilized light hydrocarbons, aromatics, and diamondoids. This has the potential to increase the reach of ultra-stable marker analysis to more accessible and geographically distributed samples.

The almost universal occurrence of stacked source rocks and high-relief structures in sedimentary basins makes the occurrence of high-maturity hydrocarbons (as condensates or admixtures to mixed oils) the rule rather than the exception. However, the identification of these components (and unraveling of aspects of their thermal history and migration) allows high-maturity

petroleum systems to be more successfully modeled and targeted for exploration.

A growing database of more than 100 petroleum samples from the San Joaquin, Salinas, Santa Barbara, Los Angeles, and the Eel River basin is being collected. High maturity contributions have already been recognized in many San Joaquin, Santa Barbara, and Eel River fields as part of this work. Fingerprinting of ultra-stable markers indicates deep cracked sources from the

Cretaceous, Eocene, and Miocene are each important in California basins. Most deep contributions are found as mixtures with black oils where they dominate the distribution of ultra-stable markers but contribute little to the distribution of biomarkers. Understanding unique independent fingerprints related to both biomarkers and to ultra-stable markers provides us with a fuller view of petroleum systems in California.

POST SCRIPT

geoexp.com

GEOSCIENCE EXPLAINED Petroleum Systems: Following Oil Through Time



History of Oil:
80 Years of Discovery

TECHNOLOGY
Integrating the Toolbox
EXPLORATION
What Next for the Russian Arctic?

Following the Oil Through Time



Tom Lorenson

THOMAS SMITH

Four-D petroleum system modelling allows an explorationist to understand the movement of hydrocarbons from an active source rock to a fluid's final destination in the basin, ultimately helping to reduce exploration risk.

Leslie B. Magoon doing what he has done much of his career, sampling oil from a seep, in this case the McKittrick oil seep about 50 km west of Bakersfield, California. Les has a MS degree in geology from the University of Oregon in Eugene. He worked for Shell Oil Company for 8 years and then became a research geologist with the US Geological Survey, where he developed the petroleum system concept.

Knowing where and when hydrocarbons are generated and where they finally end up seems so basic, yet it took years for the concept of the petroleum system to become an accepted practice. Now, using fast computers and innovative software, all exploration data including wells, seismic lines, geochemical data on the source rock and known hydrocarbons can be incorporated into petroleum system models. This concept provides the geoscientist with a new understanding of how a basin's rocks and fluids change over time, helping to reduce hydrocarbon exploration risks.

Leslie B. Magoon, Emeritus Scientist, US Geological Survey, Menlo Park, California, has spent most of his career "mapping fluids, collecting and analysing oil and gas samples". He first presented his work on the petroleum system concept as a brochure and poster in 1986. This was after an earlier paper on the subject was rejected by three prominent petroleum geologists, possibly not understanding his approach, who said "we already do this". With ever increasing computer power over the past decade, his original concept is now being applied to present and future petroleum provinces around the world.

What it Really Means

"Nature's distribution of hydrocarbon fluids is the petroleum system," says Les. "Deposition of sedimentary rock into a basin provides the setting and once a hydrocarbon fluid network forms, it can then be modelled as a petroleum system."

To really understand the definition of a petroleum system, it is important to break it down. Les explains, "The essential elements of a petroleum system are the source rock, reservoir rock, seal rock, and overburden rock. The two processes that are key to understanding a petroleum system are the trap formation and the generation-migration-accumulation of hydrocarbons. These essential elements along with the processes control the distribution of petroleum in the lithosphere."

"Genetically related hydrocarbons give the explorationist an idea about the correlation between the source rock and the petroleum occurrences. This can range from just having a source in the same geographic location (very speculative correlation) to a positive

petroleum-source rock correlation (known correlation). As for shows, seeps and accumulations, any amount of oil or gas is proof of a petroleum system. Finally, we use the term active source rock to denote when that actually occurs, not what stage of maturity the source rock may be at today."

"The definition and a breakdown of some of these elements are needed to visualise the concept," continues Les. "We also had to refine and extend some vocabulary and create a series of graphic diagrams as a folio sheet. It is important for geoscientists to understand that generation-migration-accumulation need to be modelled at the time it happens, which we call the critical moment."

Development of the Concept

Like all science and most new concepts, the petroleum system was developed over a period of time. A foundation of principles in geology dating back to the 17th century and much more recent 20th century developments in organic geochemistry are two key disciplines

Petroleum System:

As defined from AAPG Memoir 60

The essential elements and processes as well as all genetically related hydrocarbons that occur in petroleum shows, seeps, and accumulations whose provenance is a single pod of active source rock.

Also called hydrocarbon system and oil and gas system.

necessary to formulate the petroleum system concept. Discoveries in the geosciences over the last 50 years have greatly added to our knowledge about the earth and the dynamics of the earth's systems.

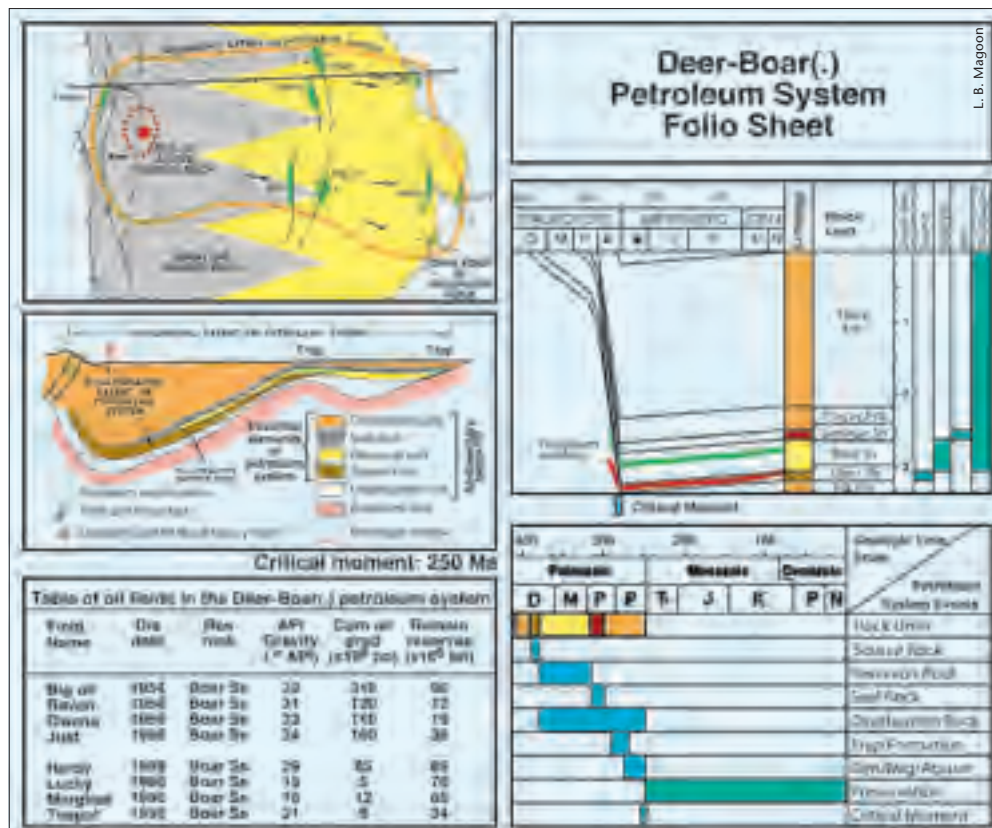
It was near the beginning of this recent period of scientific discovery (1966) that Les Magoon was hired by Shell Oil Company to study source rocks in the Santa Barbara Channel, California. This was the beginning of a chain of events and experiences that would eventually lead to the concept of the petroleum system.

"When I was working for Shell, we would do source and migration studies," explains Les. "The explorationists for Shell would say to me, 'We already know there is oil here, why do we need to do more basin analysis?' This was when I started to realise that we needed a better way to look at both the geology or the rocks and the geochemistry or the fluids."

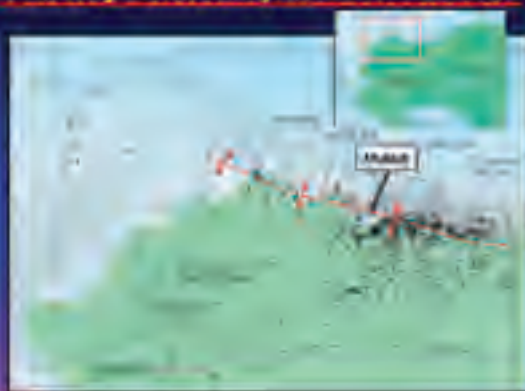
"While I was attending the AAPG Annual Meeting in Denver, Colorado in 1972, I listened to presentations by Wally Dow," says Les. "He and Jack Williams at Amoco Research presented papers on the geochemistry of oil they collected in the Williston Basin. They were able to correlate crude oils to specific source rocks, which were key ingredients in their concept of oil systems."

Les went on to work for the US Geological Survey in 1974, concentrating on oil and gas

An example of a typical folio sheet showing the petroleum system map, cross section, table of oil fields, burial history chart, and events chart. "The concept provides a new understanding of independent variables – rock, fluid, time – needed to assess risk relative to petroleum prospects."

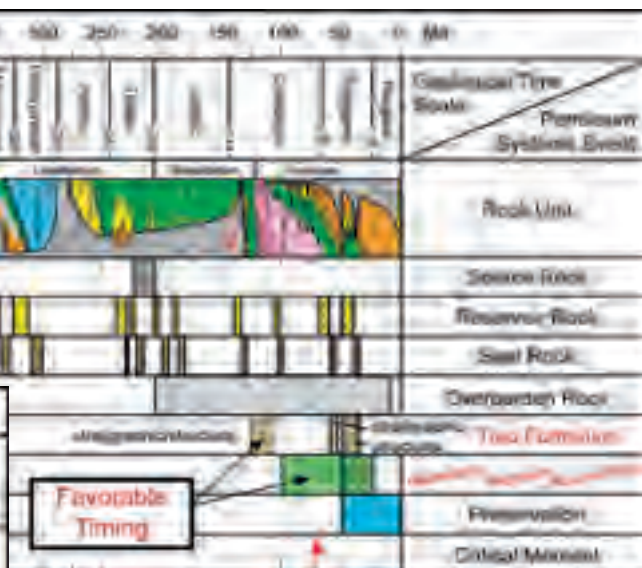
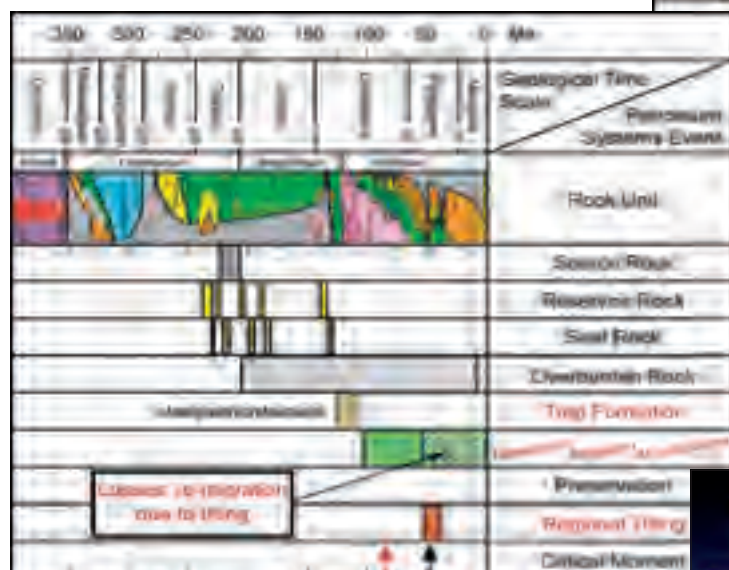


The Mukluk Prospect Lies In a Play Fairway Defined by the Barrow Arch



Location map showing the Mukluk prospect along the same play fairway as the Prudhoe Bay Field. The structure as identified on seismic is 32 km long and 14 km wide.

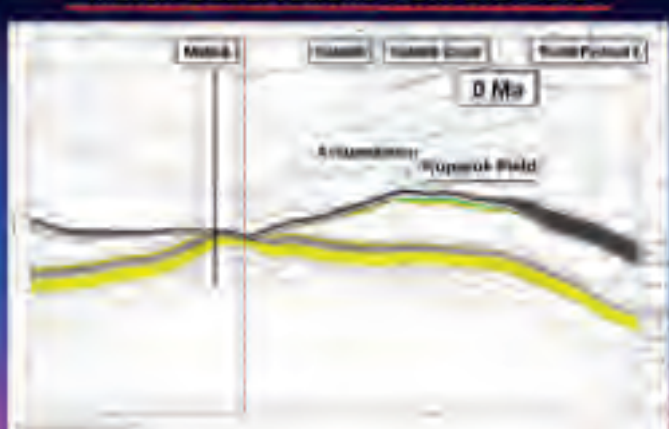
Images: Ken Peters, 2011 AAPG Pacific Section



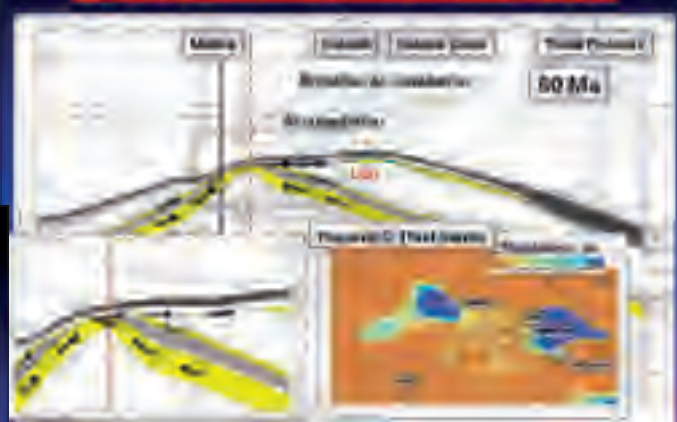
Trap formation at Prudhoe Bay preceded generation of hydrocarbons in this petroleum system, which resulted in the accumulation of hydrocarbons. The hatched pattern indicates the estimated time of eastward tilting in the Tertiary due to deposition to the east of Prudhoe Bay. The Prudhoe Bay Field tilted as well but oil was preserved because of effective seal rocks across the reservoir.

In the case of the Mukluk prospect, the critical moment is moved to about 67 Ma when regional tilting occurred. Structure formation was still favourable for accumulation until tilting, as evidenced by the oil-stained drill cuttings through the reservoirs. Once tilted, oil underwent secondary migration into the traps near the Kuparuk Field.

Accumulations Predicted by the Model Match Observations from the Field



Tilting -60 Ma Caused Remigration Along Kuparuk C Thief Sands Above the LCU



Present-day cross section showing that Mukluk oil migrated into the Kuparuk Field matching the model predictions.

The importance of looking at prospects through time is clearly demonstrated in this cross section. After tilting of the Mukluk structure, Kuparuk 'C' sands acted as carrier beds allowing oil to migrate south-east.

resource assessment. He quickly found that geology and geochemistry are trumped largely by statistics. By 1982, this led him to start developing a concept to help rank prospective areas.

"At first, the petroleum system concept was not well received," says Les. "It met early resistance, but others would comment 'this is important, pursue it'. I essentially started over and presented it as a series of poster sessions. The first was in 1987 at another AAPG Annual Meeting. Wally and I then organised a half-day session on the petroleum system for the 1991 AAPG Annual Meeting."

The 1991 session was the big turning point for the concept. Three years later Magoon and Dow published AAPG Memoir 60, *The Petroleum System – From Source to Trap*. The memoir, designated a classic by AAPG, is now out of print but can be purchased on CD.

A Powerful Tool

"Using static snapshots like fairway maps fails to account for the timing of petroleum system events," says Ken Peters, consulting professor at Stanford University. "Basin and petroleum system modelling software allows us to quantify the petroleum system concept. It can explain why traps are barren or filled with

hydrocarbons and is a powerful tool in assessing exploration risk."

An example from Alaska's prolific North Slope will help to demonstrate how petroleum system modelling, through the use of event charts, can be used as a prediction tool. The prospect was named Mukluk and, prior to drilling, expectations ran high. The prospect was right on trend with the Prudhoe Bay Field along the Barrow Arch Fairway. The entire structure was leased in 1982 with the total high bids exceeding US\$1.5 billion. At that time, a consortium of companies

headed by BP touted that it contained more than 1.5 Bb of recoverable oil (any connection to the bidding?). In 1983, the consortium built a gravel island and drilled a \$120 million well; still the most expensive dry hole ever drilled.

So What Happened?

"Our models indicate that oil accumulated in the Mukluk prospect, Prudhoe Bay, and other structures along the Barrow Arch, starting about 97 Ma," says Ken Peters. "Overburden Brookian deposition (Cretaceous and Tertiary in age) occurred



L. B. Magoon

Since 1986, Les has devoted much of his time developing and promoting the concept of the petroleum system. He and W. G. Dow, as co-editors, received the R. H. Dott, Sr. Memorial Award for AAPG Memoir 60, *The Petroleum System – From Source to Trap*.

For Gravity and Magnetic Data Globally Count on Fugro— Mapping Geology to the Basement...



...And beyond with the most comprehensive non-exclusive airborne, land and marine potential fields geophysical database, including AeroMagnetic, Land Gravity, Marine Gravity and Bathymetry data around the world. Interpretation includes:

- Basement architecture
- Tectonic elements
- Structural/geologic fabric
- Salt mapping
- Depth to basement
- ArcGIS deliverables



Fugro Gravity & Magnetic Services

For personal assistance & consultation,
please contact fgmsdata@fugro.com
or 713-369-6123.

www.fugro-gravmag.com

from the south-west to north-east across the North Slope. These episodes of uplift and burial caused eastward tilting along the Barrow Arch starting at 67 Ma. Another key to our modelling was the mapping of sandstone bodies deposited on the Lower Cretaceous Unconformity. The sands served as thief zones for the re-migration of hydrocarbons."

"When modeling a basin or prospect, it is important to visualise what is actually happening through time," says Ken. "Cross sections through the Mukluk High show present-day closure as well as one drawn at 75 Ma. However, the 41, 55, and 60 Ma sections show that petroleum migrated up dip along sands (Kuparuk 'C') deposited above the Lower Cretaceous Unconformity to the south-

east, towards the present-day location of the Kuparuk Field. At Prudhoe Bay, the Ivishak Formation reservoir sandstone is in superposition with shale across the Lower Cretaceous Unconformity (LCU) that trapped the oil. Had this thief sand been present, Prudhoe oil could have ended up somewhere else as well."

Reality

Donovan Krouskop, State of Alaska geophysicist, says, "The data around Mukluk was good quality and it's offshore enough that permafrost/velocity issues are not a problem. The vertical resolution of the data is the limiting factor. They (BP's geoscientists) could not see separate top and bottom reflectors of the Kuparuk sand, but would have seen an amplitude

anomaly at the LCU level. I do not think that would have been enough to affect the decision to drill."

Les Magoon agrees, saying, "Mukluk would have been drilled regardless of the timing because the prospect was so large. Exploration is full of risk and some prospects just beg to be drilled because one cannot be sure any evaluation is correct (until drilled)."

These two geoscientists have pointed out that a weakness in the petroleum system concept is the inability to actually predict volumes and the secondary processes that act over geologic time. The current state of art for 4D petroleum system modelling is that it is a great tool to better understand subsurface hydrocarbon generation, migration and accumulation. Using this approach, geoscientists can better predict the pod of active source rock and the timing of petroleum generation, thermal maturity, and migration pathways to possible traps, as has been pointed out in this article.

Ken Peters addresses the concept's shortcomings this way, "Current 4D petroleum system modelling is limited in predicting volumes, compositions, and secondary processes. As seen in the Mukluk example, we can predict these things very accurately after the fact. We are hoping to address these questions with our industrial affiliates Basin and Petroleum System Modelling (BPSM) programme at Stanford University through long-term research."

Ken concludes, "Computerised 4D modelling considers the relative timing of petroleum system events, processes and dynamics of associated fluids to better assess whether past conditions were suitable to fill reservoirs and survive to the present day. Understanding the total process through time could have a major impact on economies throughout the world."

Author's Note: I first met Les Magoon during the summer of 1980 working on the Alaska Peninsula. Under his guidance, we examined petroleum seeps, source rocks, and potential reservoir rocks in an effort to understand the overall petroleum potential of the Shelikof Strait prior to a Federal OCS lease sale. After this work, I was certainly not surprised by his future publications on petroleum system and the overall acceptance of the concept. ■

Basin and Petroleum System Modelling

Through their Basin and Petroleum System Modelling (BPSM) programme, Stanford University has the only formal university curriculum in the world offering graduate students visualisation and quantification of the geohistory of sedimentary basins and petroleum system. The programme is designed to train the next generation of basin and petroleum system modellers, devise the quantitative tools that, in combination with assessment methodology, can be used to rigorously evaluate geologic risk in various exploration settings, and to conduct basic and applied energy-focused research. Schlumberger has donated the PetroMod modelling software to the BPSM programme and technical support is being provided by their Aachen Technology Center.

Modelling of the subsurface through time (4D) has emerged over the last decade as a major research focus of the petroleum industry. Four-D petroleum system modelling has grown because it better quantifies the generation, migration and entrapment of resources. The BPSM group was started in 2008 by a group of experienced geoscientists recognising the need, from both the industry and academia, for graduates with expertise in this field.



L. A. Cicero
Stanford News Service

Stanford University in Palo Alto, California, is a leading research and teaching institution.